UNIVERSITY OF NAPLES FEDERICO II

PH.D. PROGRAM IN

CLINICAL AND EXPERIMENTAL MEDICINE

CURRICULUM IN TRANSLATIONAL MEDICAL SCIENCES

XXXV Cycle

(Years 2019-2022)

Chairman: Prof. Francesco Beguinot

PH.D. THESIS

HYPOMETHYLATION OF THE P53-TARGET ZMAT3 IS ASSOCIATED WITH SENESCENCE OF SUBCUTANEOUS ADIPOCYTE PRECURSOR CELLS IN INDIVIDUALS WITH A FAMILY HISTORY OF TYPE 2 DIABETES

TUTOR

Prof. Francesco Beguinot

PH.D. STUDENT

Dr. Pasqualina Florese

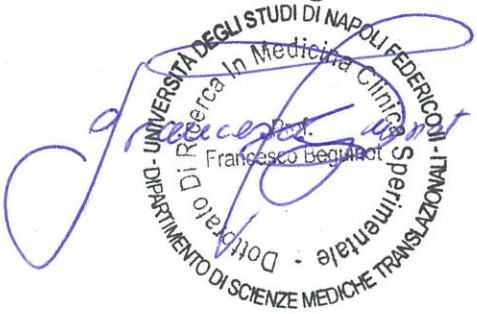

TABLE OF CONTENT

	Page
ABSTRACT	**1**
1. INTRODUCTION: molecular basis of ageing in Type 2 Diabetes	**2**
1.1 Type 2 Diabetes	**3**
1.2 AT and pathophysiological processes in age-related AT dysfunction	**5**
1.2.1 APC function decline	**9**
1.2.2 Chronic sterile inflammation	**10**
1.2.3 Cellular senescence	**11**
1.3 Linking AT senescence to chronic metabolic diseases	**14**
1.3.1 Obesity	**14**
1.3.2 Type 2 Diabetes	**16**
1.4 Family History of Diabetes: an important risk factor to develop T2D	**18**
1.5 Epigenetics	**19**
1.5.1 DNA methylation	**20**
1.5.2 DNA methylation during ageing and senescence	**22**
1.6 *ZMAT3* as candidate epi-gene for senescence in APCs	**25**
2. EXPERIMENTAL PROCEDURES	**26**
2.1 Study participants	**26**
2.2 Isolation and culture of APC	**26**
2.3 Adipogenic differentiation of APC	**27**
2.4 Flow cytometry analysis	**27**
2.5 Primer sequences	**28**
2.6 Bisulphite sequencing	**28**

2.7 RNA isolation and qPCR **28**

2.8 Western Blot **28**

2.9 Construction and functional analysis of luciferase reporter vectors **29**

2.10 Construction and transfection of *ZMAT3* expression vector **30**

2.10.1 Construction and transfection of *TP53* expression vector **30**

2.11 Multiplex SASP protein analysis **30**

2.12 Chromatin immunoprecipitation (ChIP) **30**

2.13 Senescence induction **31**

2.14 RNA interfering **31**

2.15 PFTα treatment **31**

2.16 Senolytic treatment **32**

2.17 SAT bioptical samples **32**

2.18 Statistical analysis **33**

3. RESULTS **36**

3.1 Senescence phenotyping in APCs from FDRs of T2D subjects **36**

3.2 The role of *ZMAT3* in premature senescence of FDR APCs **41**

3.3 Functional analysis of the *ZMAT3* intronic region **41**

3.4 Senescence induction by *ZMAT3* overexpression in human APCs **47**

3.5 Adipocyte differentiation of *ZMAT3* overexpressing APCs **57**

3.6 Effects of senolytics treatment on *ZMAT3* DNA methylation profile and adipocyte differentiation in FDR APCs **60**

3.7 Age-, senescence- and T2D-associated *ZMAT3* expression in SAT **64**

4. DISCUSSION & CONLUSION **69**

5. REFERENCES **75**

6. LIST OF PUBBLICATIONS **104**

ABSTRACT

Senescence of adipose precursor cells (APCs) impairs adipogenesis, contributes to the age-related subcutaneous adipose tissue (SAT) dysfunction, and increases risk of type 2 diabetes (T2D). First-degree relatives of T2D individuals (FDRs) feature restricted adipogenesis, reflecting the detrimental effects of APC senescence earlier in life and rendering FDRs more vulnerable to T2D. Epigenetics may contribute to these abnormalities but the underlying mechanisms remain unclear. In previous methylome comparison in APCs from FDRs and individuals with no diabetes familiarity (CTRLs), ZMAT3 emerged as one of the top-ranked senescence-related genes featuring hypomethylation in FDRs and associated with T2D risk. Here, we investigated whether and how DNA methylation changes at ZMAT3 promote early APC senescence. APCs from FDR individuals revealed increases in multiple senescence markers compared to CTRLs. Senescence in these cells was accompanied by ZMAT3 hypomethylation, which caused ZMAT3 upregulation. Demethylation at this gene in CTRL APCs led to increased ZMAT3 expression and premature senescence, which were reverted by ZMAT3 siRNA. Furthermore, ZMAT3 overexpression in APCs determined senescence and activation of the p53/p21 pathway, as observed in FDR APCs. Adipogenesis was also inhibited in ZMAT3-overexpressing APCs. In FDR APCs, rescue of ZMAT3 methylation through senolytic exposure simultaneously downregulated ZMAT3 expression and improved adipogenesis. Interestingly, in human SAT, ageing and T2D were associated with significantly increased expression of both ZMAT3 and the P53 senescence marker. Thus, DNA hypomethylation causes ZMAT3 upregulation in FDR APCs accompanied by acquisition of the senescence phenotype and impaired adipogenesis, which may contribute to FDRs predisposition for T2D.

1. Introduction: molecular basis of ageing in Type 2 Diabetes

Healthcare and sanitation advancements have significantly increased human life expectancy (Shuling et al., 2020). Over the last 200 years, the average age at death has steadily increased by about 2.5 years per decade. However, ageing is a well-known risk factor for the development of a variety of chronic diseases, also known as Non-Communicable Diseases, such as cardiovascular disease, stroke, cancer, osteoarthritis, dementia, and type 2 diabetes (T2D). As a result, the pressure on the world health system increases. In fact, chronic diseases impose a high burden on the elderly population in terms of health and economics due to the long duration of these diseases, the decrease in the quality of life and the costs for treatment (Sierra et al., 2015). Interestingly, ageing and chronic diseases may share common pathophysiological pathways which include: *i.* decline in progenitor cell function; *ii.* cellular senescence; *iii.* chronic sterile inflammation; and, *iv.* dysfunctions of the macromolecular and cell organelles (*e.g.*, genomic instability, shortening of telomeres, epigenetic changes, loss of the nuclear lamina interactions, and mitochondrial dysfunction). Any fundamental ageing process that is triggered is likely to have an impact on the others (Tchkonia et al., 2018) and may impact on the tissue specifically involved in the development of chronic metabolic diseases, *e.g.* adipose tissue (AT) in patients with obesity and T2D (Sierra et al., 2015; Tchkonia et al., 2018; Lancet., 2012; Stout et al., 2017; Burton et al., 2018). As such, ageing and age-related diseases (ARDs) may be consdered as alternative trajectories of the same process that occur place at different rates, based on interactions between genetic, epigenetic and environmental factors, and lifestyle throughout the lifespan (Franceschi et al., 2018). T2D has generated considerable interest among ARDs. T2D phenotypes like impaired glucose intolerance and postprandial hyperglycemia are associated with aand are common in the elderly. T2D and obesity, on the other hand, may appear in young people, such as First-Degree Relatives of T2 patients, replicating the mechanisms of accelerated ageing. In this scenario, I will discuss the causal link between age-related AT dysfunctions that contribute to T2D onset, with a focus on the impact of cellular senescence and DNA methylation, as well as the therapeutic strategies used to specifically target senescent cells (SNCs).

1.1 Type 2 Diabetes

Diabetes mellitus is a major public health problem that has serious consequences for human life and health-care costs worldwide (Onyango et al., 2018). According to the International Diabetes Federation (IDF), in 2019, diabetes caused 4.2 million deaths and affected 463 million adults aged 20 to 79, a number that is expected to rise to 700 million by 2045 (Galicia-Garcia et al.,2020), making it a worldwide epidemic (fig.1). According to the World Health Organization (WHO), diabetes mellitus is defined as a chronic and metabolic disease identified by elevated blood glucose levels, which over time causes damage to the heart, vasculature, eyes, kidneys, and nerves. Over 90% of diabetes mellitus patients have type 2 diabetes (T2D), which is characterized by insufficient insulin secretion by pancreatic islet cells, tissue insulin resistance (IR), and an insufficient compensatory insulin secretory response, all of which lead to hyperglycemia (American Diabetes Association 2022).

The global rise in obesity, sedentary lifestyles, high calorie diets, and population ageing are the primary causes of T2D (Galicia-Garcia et al., 2020). These modifiable risks are coupled with non-modifiable risk factors (ethnicity, family history, and genetic predisposition) that provide a strong genetic basis for T2D (Chatterjee et al.,2017). However, some familial aggregations and many of the environmental exposure effects, connected to T2D, are not due to genetic variation. They could be the result of epigenetic processes, namely heritable alterations in gene expression that occur in the absence of changes in the original DNA sequence (Drong et al., 2012). As a result, epigenetics identifies a biological link between environmental factors and the development of T2D (Ling et al., 2009). Indeed, the mother's nutritional intake and lifestyle affect fetal development in the uterus, increasing the fetus's risk of developing T2D later in life (Russel et al., 2010). Furthermore, early life exposures such as nutrition and other factor produce long-term changes that can contribute to T2D and cardiovascular disease (Drong et al., 20212).

The main pathophysiological processes of T2D development are alterations of the feedback loops between insulin action, insulin secretion, and the ability of insulin-sensitive tissues to respond to insulin, which result in abnormally high blood glucose levels (Stumvoll et al., 2015). Insulin resistance (IR) refers to a decrease in the metabolic response of insulin-responsive cells to insulin or, at a systemic level, an impaired/lower response to circulating insulin by blood glucose levels. There are three broad categories of IR and insulin-deficient conditions: *i.* diminished insulin secretion by β-cells; *ii.* insulin antagonists in the plasma, due either to counter-regulatory hormones or non-hormonal bodies that impair insulin receptors or signalling; and *iii.* impaired insulin response in target tissues. There are three main extra-pancreatic insulin-sensitive organs that play major roles in the last process: adipose tissue (AT), skeletal muscle, and liver (Stumvoll et al., 2015). A defective action of insulin in these tissues

often precedes the development of systemic IR, thus progressively leading T2DM. In this scenario, adipose tissue (AT) plays a crucial role. Insulin acts on the AT by stimulating glucose uptake and triglyceride synthesis and inducing FFA and glycerol uptake from circulation, while suppressing triglyceride hydrolysis (Gastaldelli et al., 2017). An impaired response to insulin stimulation by AT leads to inadequate suppression of lipolysis, impaired glucose uptake, enhanced FFA release into plasma, adipokine deregulation, and secretion of pro-inflammatory mediators (Goyal et al., 2021). The resulting chronic inflammatory state plays an important role in the pathogenesis of systemic IR and T2D (Spinelli et al., 2020).

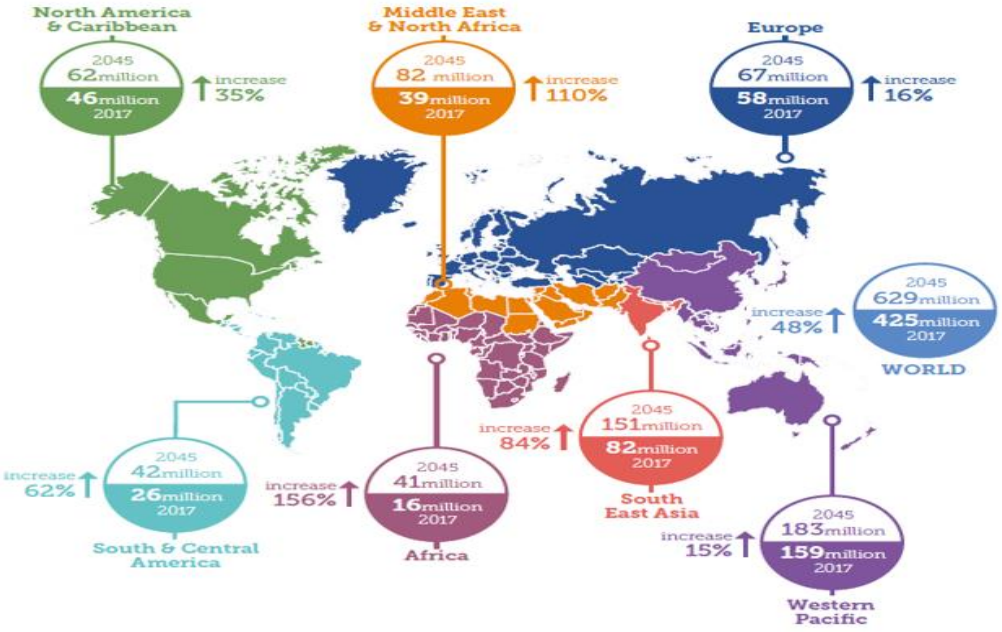

FIGURE 1. Diabetes cases worldwide (2017) and increase in diabetes cases by 2045: The International Diabetes Federation Atlas (IDF Atlas 2017) figure provides a worrying indication of the future impact of diabetes on the global development.

1.2 AT and pathophysiological processes in age-related AT dysfunction

Adipose tissue (AT) is a large and dynamic endocrine, immune, and regenerative organ that plays a crucial role in controlling systemic metabolic homeostasis and inflammation. AT is also involved in maintaining whole-body insulin sensitivity and energy levels (Palmer et al., 2010). AT has historically been classified into two types, white adipose tissue (WAT) and brown adipose tissue (BAT) (Geoffrey 2018). The white and brown adipocytes comprising these depots exhibit physiological differences, which give rise to specialized tissue functions. WAT is critical for energy storage, endocrine communication, and insulin sensitivity, and identifies the largest AT volume in most mammals, including humans. WAT is the predominant type of fat in the human body. It can be found beneath the skin (subcutaneous adipose tissue - SAT), around internal organs (visceral adipose tissue - VAT), and in the central cavity of bones (bone marrow fat), as well as cushioning various parts of the body. In contrast, BAT is mainly present in mammals postnatally and during hibernation. BAT is located primarily in the upper back, above the clavicles, around the vertebrae, and in the mediastinum. The primary function of BAT is to generate heat through non-shivering thermogenesis, which is especially important in preventing hypothermia in new-borns (Allison et al., 2020).

AT regulates metabolic homeostasis by producing hormones, cytokines, growth factors, and other peptides. These effector molecules, termed adipokines, exert their effects in endocrine, paracrine, and autocrine manners (Choe et al., 2016). They participate in a wide range of physiological processes and molecular pathways, including glucose and lipid metabolism, cell proliferation signalling, cytokine signal transduction, and inflammation. Under physiological conditions, anti-inflammatory cytokines maintain insulin sensitivity in AT. On the other hand, the increased secretion of pro-inflammatory cytokines (*e.g.*, TNF-α, Interleukin-8 (IL-8), IL-6, IL-1β, and monocyte chemotactic protein-1 (MCP1) leads to low-grade chronic inflammation and IR, which are commonly associated with ageing and obesity, as well as an increased risk for cardiovascular disease and T2D (Chawla et al., 2011; Huh et al., 2014; Smith et al., 2016).

Throughout early life, by controlling adipocyte progenitor cell (APC) differentiation and fat cell turnover, AT can efficiently respond to a wide range of changes in energy supply and regional microenvironment. The capacity to cause this compensatory response differs by local fat distribution (Stout et al., 2017). Molecular, cellular, physiological, and anatomical differences between SAT and VAT highlight the specificity of each fat depot and its characteristic function (Tchkonia et al., 2013). Due to the large replicative and adipogenic capacity of APCs and the decreased lipolytic activity and lower insulin sensitivity of adipocytes in SAT compared to those in VAT, subcutaneous fat can expand by increasing adipocyte cell size (hypertrophy) and number (hyperplasia), while visceral fat typically

expands by increasing adipocyte cell size (Tchkonia et al., 2005). Once this storage capacity is exceeded and the ability to develop new adipocytes is compromised, SAT becomes hypertrophic, inflamed, and dysfunctional, and surplus lipids accumulate in other AT depots (*i.e.*, VAT or peri/epicardial fat) and in ectopic locations (*i.e.*, liver and skeletal muscle). These events lead to local and systemic inflammation and IR, which in turn contribute to the onset of T2D (Longo et al., 2019). SAT adipocyte hypertrophy commonly occurs in elderly individuals, obese patients and FDRs, and has been shown to represent an independent predictor for IR and T2D risk (Hammarstedt et al., 2018; Goodpaster et al., 2005; Goodpaster et al., 2003).

Many studies have described the dynamics of age-related changes in fat mass and regional distribution (Kyle et al., 2001; Kyle et al., 2001; Kuk et al., 2009). Redistribution of fat from subcutaneous to intra-abdominal visceral depots occurs primarily in men and women throughout middle age and is independent of changes in total adiposity, body weight, or waist circumference (Palmer et al., 2016; Tchkonia et al., 2010; Kuk et al., 2009. In elderly individuals' fat is stored outside of these AT depots and accumulates in muscle, liver, and other ectopic sites (Palmer et al., 2016; Stout et al., 2014; Goodpaster et al., 2005; Goodpaster et al., 2003; Kyle et al., 2001; Kyle et a., 2001; Kuk et al., 2009). As a consequence, adipocyte hypertrophy, inflammation, and fibrosis arise in SAT during the early stages of ageing before glucose tolerance is impaired and local IR progressively develops. Altogether, these metabolic disturbances contribute to the development of T2D and other ADRs (Stout et al., 2017). In support of the pathophysiological significance of these age-related AT dysfunction, clinical studies in humans, including nonobese individuals, have clearly demonstrated that treatments affecting fat mass, such as calorie restriction (CR), exercise, and bariatric surgery, have beneficial effects on energy metabolism and metabolic risk factors for T2D, CVD and cancer. This evidence indicates that the cascade of molecular and cellular events underlying age-related AT damage starts in SAT and is caused by the reduced function of resident APCs, increased inflammation, and accumulation of SNCs (Palmer et al., 2016; Tchkonia et al., 2010; Stout et al., 2014). Telomere length (TL) erosion is known to represent a significant marker of ageing and senescence, both at the cellular and tissue levels (López-Otín et al., 2013). Interestingly, age-related TL shortening mainly occurs in SAT compared to VAT and is due to shorter telomeres in the stromal vascular fraction (SVF) cells which include APCs. This evidence supports the concept that ageing of APCs is linked to compromised SAT hyperplastic/healthy expansion (Lakowa et al., 2015; Schipper et al., 2008). Several studies indicate that age reduces the replicative and adipogenic capacity of SAT APCs (Burton et al., 2018; Fajas et al., 2003; Cinti., 2002; Caso., 2013; Sepe et al., 2011). Accordingly, APCs SAT of healthy elderly subjects (age>60) display decreased proliferation and differentiation ability compared to APCs isolated from young individuals (age 18-30). The age-related declining function of APCs is associated with an increase in plasma levels

of the inflammatory marker soluble tumour necrosis factor receptor 2 and increased AT secretion of the pro-inflammatory cytokine tumour necrosis factor-α (TNF-α) (Caso., 2013). These findings support the notion that, during ageing, the progressive impairment in adipogenesis is related to a pro-inflammatory condition of SAT, which, in turn, contributes to limiting insulin sensitivity in the tissue (Fig.2).

The causes of APC ageing are multifactorial and include genetic features of APCs and epigenetic factors. The AT microenvironment can also play a role (Tchkonia et al., 2010). Indeed, growing evidence underlines a causal role for AT inflammation in this scenario (Tchkonia et al., 2010; Stout et al., 2014; Sepe et al., 2011). High levels of pro-inflammatory cytokines and chemokines are found in both the fat tissue and blood of elderly. This condition, known as inflammageing, is a high-risk factor for many ARDs, multi-morbidity, and frailty (Ferrucci et al., 2018). AT is a major source of TNF-α, Interleukin-8 (IL-8), IL-6, IL-1β and monocyte chemotactic protein-1 (MCP-1) in serum from elderly and insulin-resistant individuals (Tchkonia et al., 2010; Stout et al., 2014; Caso et al., 2013; Ferrucci et al., 2018). The secretion of these pro-inflammatory factors positively correlates with the size of mature adipocytes and is a predictor of T2D in these same subjects (Hammarstedt et al., 2018; Spranger et al., 2003). The evidence that the age-related IL-6 increase is up to 10-fold higher in SAT than in VAT indicates that inflammation associated with age is more severe in subcutaneous than in visceral fat Tchkonia et al., 2010). The prevalent cell types responsible for age-related inflammatory changes in SAT are APCs and AT macrophages (ATMs) (Sepe et al., 2011; Tchkonia et al., 2007; Skurk et al., 2007; Martinez et al., 2009). The cross-talk between APCs, adipocytes, and ATMs creates self-perpetuating processes that maintain a pro-inflammatory milieu in SAT and drive chronic systemic inflammation, leading to metabolic dysfunction (Sepe et al., 2011). The underlying mechanisms of age-related inflammation are still far from being fully understood. Nevertheless, growing evidence from animal and human studies suggests a causal role of cellular senescence. Most SNCs feature a senescence-associated secretory phenotype (SASP) which is characterized by an increased secretion of pro-inflammatory factors. The SASP is a dynamic and complex phenotype composed of a wide range of cytokines, chemokines, proteases, and growth factors, which vary with cell type and cell microenvironment. Thus, SNCs are a major contributor to the age-related pro-inflammatory AT secretion profile (Freund et al., 2010).

SAT is a crucial site for the accumulation of senescent cells during ageing. Indeed, age-related TL shortening occurs primarily in SVF cells isolated from SAT (Freund et al., 2010), also supporting the concept that APCs are among the more senescent-susceptible human progenitor cells (Tchkonia et al., 2010). Senescent APCs operate both in a cell-autonomous manner to enhance evolution toward senescence and to restrain adipogenic and lipogenic functions and in a non-cell-autonomous manner by

paracrine mechanisms. When secreted, SASP factors suppress adipocyte differentiation in neighbouring non-senescent APCs, cause inflammation of adjacent healthy cells and propagate senescence, inducing local and systemic detrimental effects even with low numbers of SNCs (Tchkonia et al., 2018; Trabucco et al., 2016; Xu et al., 2015; Xu et al., 2015; Nelson et al., 2012; da Silva et al., 2019). Consistently, transplanting a small number of senescent murine or human APCs (i.e., 0.5-1 million) into middle-aged mice is sufficient to cause disability within two months, accelerate the onset of ARDs, and reduce survival (Xu et al., 2018). Similar findings were drawn from preclinical studies in mice (*e.g.*, aged mice, progeroid mice, and diet-induced obese mice), and from human clinical trials (*e.g.*, diabetic kidney disease individuals). Indeed, removing just 30 % of SNCs using either genetic or pharmacological strategies (i.e., senolytics and SASP inhibitors) was effective in preventing, alleviating or reversing age-related AT dysfunction, inflammation, and IR (Xu et al., 2018; Roos et al., 2016; Farr et al., 2017; Lewis-McDougall et al., 2019; Schafer et al., 2016; Palmer et al., 2019; Ogrodnik et al., 2019; Fuhrmann-Stroissnigg et al., 2017; Schafer et al., 2017; Hickson et al., 2020). These findings underline the crucial role of senescent APCs in driving ageing phenotypes and strongly support the selective targeting of these cells as a novel way of alleviating chronic metabolic disorders and increasing the duration of human health.

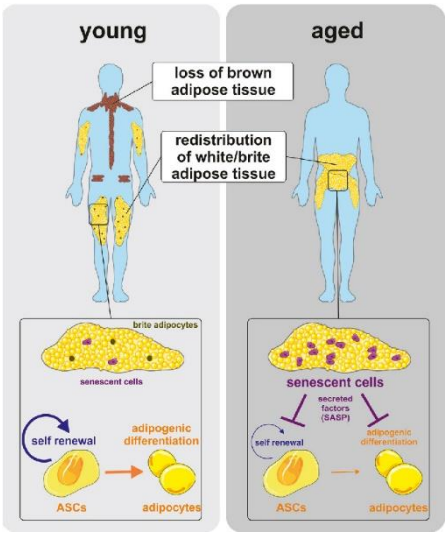

FIGURE 2. Panoramic of pathophysiological processes in age-related AT dysfunction: Accumulating senescent cells in the adipose depots leads to change functionality of the adipose organ with age. This is consistent with the possibility that senescent fat cells and preadipocytes could be the main sources of the increased fat tissue inflammatory cytokines and chemokines liable of impaired adipogenesis in nearby fat cells, potentially contributing to age-related lipodystrophy and fat redistribution. Schosserer et al., 2017

1.2.1 APC function decline

APCs are among the most abundant progenitor pools in the body (Tchkonia et al., 2010). They are mainly resident in fat depots, although a small pool of circulating APCs exists (Crossno et al., 2006). The primary role of APCs is to differentiate into mature, lipid-storing and insulin-responsive adipocytes. APC differentiation, also known as adipogenesis, is a tightly regulated process involving several transcription factors that work in concert to underpin the acquisition and maintenance of the fat cell phenotype (Rosen et al., 2005). Although SAT and VAT adipocytes are likely to differentiate from APCs with distinct characteristics, they share similar transcriptional programs (Stout et al., 2014; Tchkonia et al., 2002). Peroxisome proliferator-activated receptor gamma (PPARγ) is a critical regulator of adipocyte differentiation (Fajas et al., 1999). PPARγ is a ligand-dependent transcription factor that induces gene expression by binding to PPARγ responsive elements (PPRE) following dimerization with retinoid X receptors (RXR) (Lefterova et al., 2008). PPARγ directly controls the expression of genes involved in adipocyte lipid uptake, transport and metabolism, insulin signalling, and adipokine production (Lehrke et al., 2005). The CCAAT/enhancer-binding protein (C/EBP) is a transcription factor family member which regulate PPARγ expression. PPARγ binds a ligand, heterodimerises with retinoid X receptors (RXR) and then induces C/EBPα (Wu et al., 1996; Hamm et al., 2001), which in turn further enhances PPARγ expression levels (Clarke et al., 1997). Thus, a positive feedback loop that supports and maintains lipid accumulation and terminal differentiation is created by PPARγ and C/EBPα (Rosen et al., 2002). Indeed, both PPARγ and C/EBPα have essential roles in initiating differentiation programs and controlling the expression of genes needed to acquire and sustain adipocyte phenotypes (Madsen et al., 2014, Longo et al., 2016; Pirone et al., 2019).

APCs also have important immune and proinflammatory functions, which is another aspect of their biology. Their secretory phenotype differs from that of differentiated adipocytes and is much more similar to that of macrophages (Tchkonia et al., 2006; Kirkland et al., 1994). Indeed, APCs can transform into macrophage-like cells and express toll-like receptors (TLRs) (Charrière et al., 2003; Cousin et al., 1999). (Chung et al., 2006; Vitseva et al., 2008). TLR activation promotes intracellular signaling pathways that cause the release of inflammatory cytokines and chemokines (Poulain-Godefroy et al., 2010). While APC immunological activity is an important defence mechanism, it also predisposes WAT at risk for chronic inflammation throughout ageing and obesity. WAT inflammation impairs APC differentiation capacity, decreases adiponectin secretion (Gustafson et al., 2009, Isakson et al., 2009), and maintains the inflammatory status (Mu et al., 2018). This phenotype initiates a vicious cycle that is critical in age-related SAT dysfunctions (Stout et al.,2014). In comparison to APCs from younger donors, APCs from elderly exhibit lower levels of C/EBPα, PPARγ, and their target genes after

stimulation of adipocyte differentiation (Karagiannides et al.,2001; Schipper et al., 2008). Importantly, C/EBPα overexpression restored the adipogenic ability of APCs isolated from older individuals (Karagiannides et al.,2001). Consistently, shorter lifespans, alterations in body weight, fat depots, and glucose homeostasis are all progeroid characteristics in C/EBPα mutant mice (Karagiannides et al., 2001). Lower PPARγ expression also leads to a shorter lifespan and lipodystrophy (Argmann et al., 2009). Furthermore, anti-adipogenic regulators such as C/EBP liver inhibitory protein (C/EBP-LIP), C/EBP homologous protein (CHOP), and CUG triplet repeat-binding protein (CUGBP) are similarly altered with age in APCs, adipocytes, and intact AT (Karagiannides et al., 2001, Pirone et al., 2019).

All of these molecular and cellular abnormalities appear at different rates in SAT and VAT, and SAT appears to be mainly affected (Tchkonia et al., 2010). The differences in gene expression profile, epigenetic pattern, and exogenous microenvironment between these fat depots are responsible for their specific susceptibility to age-related changes (Tchkonia et al., 2007; Keller et al., 2016).

1.2.2 Chronic sterile inflammation

Sterile inflammation develops without external causes, and chronic sterile inflammation is a feature of ageing and is more pronounced in AT (Ferrucci et al., 2018). In fact, during ageing, the AT secretory profile shifts to a more pro-inflammatory signature in response to physical, chemical or metabolic stimuli (e.g., genomic, hypoxic, nutrient, oxidative, and endoplasmic reticulum stress) (Palmer et al., 2016; Tchkonia et al., 2010; Stout et al., 2014; Sepe et al., Ferrucci et al., 2018).

APCs predominantly secrete more pro-inflammatory cytokines and chemokines, termed adipokines, that trigger a cascade of events driving the surrounding cells to an inflammatory state. This, in turn, results in impaired adipocyte function, activation of ATMs, and recruitment of T-lymphocytes and monocytes from blood (Sepe et al., 2011; Kirkland et al., 2002). Human studies indicate that expression and secretion of TNF-α, IL-6 and MCP-1 are higher in APCs from elderly subjects than in those from younger individuals and that ATM content in healthy subjects is positively correlated with age (Kirkland et al., 2010; Stout et al., 2014; Caso et al., 2013; Ferrucci et al., 2018; Martinez et al., 2009).

ATMs can be polarized in two ways: conventionally active (M1) and alternatively activated (M2). M1 macrophages express pro-inflammatory cytokine genes (TNF-alpha, IL-6, and MCP-1), whereas M2 macrophages express anti-inflammatory cytokine genes (Fujisaka et al., 2016). While most ATMs in young AT are M2 cells, the number of ATMs increased from 5% to 50% of total cells as AT aged (Lu et al., 2021). ATMs thus play a role in age-related inflammation, impaired adipogenesis, and IR. Indeed, several studies have shown that TNFα impacts on cell size and insulin sensitivity of mature adipocytes, as well as impairing adipogenesis. TNFα inhibits adipocyte differentiation via several mechanisms,

including suppression of PPARγ and C/EBPα expression and activity, as well as activation of the adipogenesis inhibitors CHOP, CUGBP, and C/EBP-LIP. These processes are important in sustaining adipogenesis inhibition in APCs during ageing (Pararasa et al., 2015), resulting in local and systemic IR (Lu et al., 2021).

1.2.3 Cellular senescence

Cellular senescence is a terminal and stable state of growth arrest in which cells are unable to proliferate and differentiate despite optimal growth conditions and mitogenic stimuli (Di Micco et al., 2020). SNCs have both beneficial and detrimental effects on the organism. On the one hand, senescence has positive effects, particularly in the early stages of development. Senescence, on the other hand, is thought to be one of the reasons cell tissues age, and an increased burden of SNCs accelerates ageing and the onset of ARDs, leading to overall organism ageing (Mylonas and O'Loghlen et al., 2022). Cellular senescence has been identified as a response to different stressors which converge on activation of common effectors (Childs et al., 2015). According to type of stressors, cellular senescence can be classified into replicative senescence, oncogene-induced senescence, stress-induced premature senescence, or programmed senescence (Song et al., 2020). Multiple stimuli can induce cellular senescence. These include metabolic signals (*e.g.*, high levels of glucose, ceramides, certain fatty acids, hypoxia and reactive oxygen species), inflammatory factors, telomeric shortening from repeated cell replication, DNA damage response and mitochondrial dysfunction (Hernandez-Segura et al 2018). In addition to growth arrest, SNCs exhibit typical structural and molecular changes, including an enlarged and flattened morphology, increased cytosolic vacuolization, resistance to apoptosis, changes in the levels of heterochromatin and/or euchromatin, and destabilization of nuclear integrity due to the downregulation of the *Lamin B1* (*LMNB1*) gene, activation of lysosomal β-galactosidase (senescence-associated β-galactosidase [SA-β-gal]), upregulation of cell cycle inhibitors such as p53, p21 and p16, and SASP acqusition (Rufini et al., 2013) (Fig.3). The scientific community has struggled to identify universal and unequivocal markers characterizing the senescence state. The difficulty in identifying such markers reflects the complexity of the senescence phenotype and the existence of highly heterogeneous senescence programs. Currently, the only possibility resides in combining the measurement of multiple hallmarks in the same sample. Indeed, the most reliable approach to SNCs identification involves the use of a panel of different markers, including SA-β-gal, loss of LMNB1, increased levels of both cell cycle inhibitors (e.g., CDKN1A) and commonly secreted SASPs (Spinelli et al., 2020).

Among multiple mechanisms that trigger the senescence pathways, p53 activation plays a critical role (Rufini et al., 2013; Rovillain et al., 2011; Kumari et al., 2021). Recent data suggests that p53 controls

cellular senescence in response to a variety of signals, including short telomeres, DNA damage, and overexpression of tumor suppressor genes (Itahana et al., 2001). Importantly, p53 by inducing the transcription of its target the p21-encoding CDKN1A gene acts as a molecular link between pathways involved in cell senescence, inflammation, and IR in the adipose tissue. Indeed, *Minamino et al.* demonstrated the key role of the p53/p21 pathway in the induction of premature senescence in the AT in both of obese and insulin-resistant mice and in that of T2D patients (Minamino et al., 2009;).

SAPS acquisition is one of the most important characteristics of SNCs (Song et al., 2020). The SASP phenotype is highly heterogeneous and controlled at multiple levels (Faget et al., 2019). It is primarily regulated at the transcriptional level by nuclear factor-kB (NF-kB), which mainly\ induces the production of pro-inflammatory cytokines and chemokines (Faget et al., 2019). Trascriptional regulation of SASP factors is also controlled by Janus kinase (JAK), p38, and other MAP kinases upstream (McHugh et al., 2018; Hernandez-Segura et al., 2018). At post-transcriptional level, SASP is mainly regulated by a rapamycin (mTOR) signaling network (Hernandez-Segura et al., 2018). SASP exerts many activities, each with tissue and context-specific effects. SASP acquisition is important for the age-related limited hyperplastic expansion and storage capacity of SAT (Tchkonia et al., 2018; Tchkonia et al., 2013). Indeed, among the SASP components released by SAT-resident senescent APCs, IL-6, TNF-α, interferon-γ (IFN-γ), and activin A can directly impair adipocyte differentiation and insulin sensitivity (Xu et al., 2015). JAK inhibition has recently been proposed as a way to restore defective adipogenesis caused by SNCs, preserving fat mass and metabolic function in the elderly. Indeed, JAK inhibition suppresses SASP factors, including IL6, TNFα and activin A, in senescent APCs, leading to reduced lipotoxicity and increased insulin sensitivity (Xu et al., 2015). Thus, SASP inhibitors attenuate deleterious and systemic effects of SASP without killing SNCs. However, removing already formed and persistent SNCs might decrease the spread of senescence and reduce tissue dysfunction. The clearance of senescent cells is promoted by 'senolytics', small molecules, peptides, and antibodies that selectively eliminate SNCs (Khosla et al., 2020).

Senolytics were discovered as a result of a hypothesis-driven, mechanism-based approach (Robbins et al., 2020). This research revealed that SNCs have increased the expression of anti-apoptotic pathways (SCAPs), which protect them from their proapoptotic SASP (Zhu et al., 2015b), making them resistant to apoptosis (Khosla et al., 2020). Thus, SCAPs have been identified as senolytic targets as a result. Indeed, inhibiting the SCAPs with senolytic agents causes apoptosis in SNCs but not in non-senescent cells (Kirkland et al., 2017). Senolytics must be administered intermittently because the establishment of the senescent phenotype is a slow and dynamic process. This "hit-and-run" therapeutic method is based on SCAPs redundancy and has long-term effects (Kirkland et al., 2020). Interestingly,

intermittent administration of the senolytic combination Dasatinib (a Src/tyrosine kinase inhibitor - D) plus Quercetin (a natural flavonoid that binds to BCL-2 and modulates transcription factors, cell cycle proteins, pro-and anti-apoptotic proteins, growth factors, and protein kinases - Q) selectively eliminates SNCs from mouse and human cell cultures, from ageing mice, from mice with IR and with many other chronic metabolic alterations, and from isolated AT explants from obese and diabetic human individulas (Kirkland et al., 2018; Novais et al.,2021). Furthermore, D + Q administration increases PPARγ and CEBPα expression, two key transcription factors involved in the regulation of adipogenesis and AT insulin responsiveness (Xu et al., 2017). Furthermore, D+Q administration reduces pro-inflammatory cytokine secretion in AT, as well as the complications that accompany it (Novais and colleagues, 2004). Thus, clearing cellular senescence and targeting SASP can improve APC function and help to prevent or reverse age-related metabolic diseases like T2D. More research is required, however, to develop sensitive and specific assays that track the multiple changes associated with the senescence phenotype in order to define highly precise treatment targets.

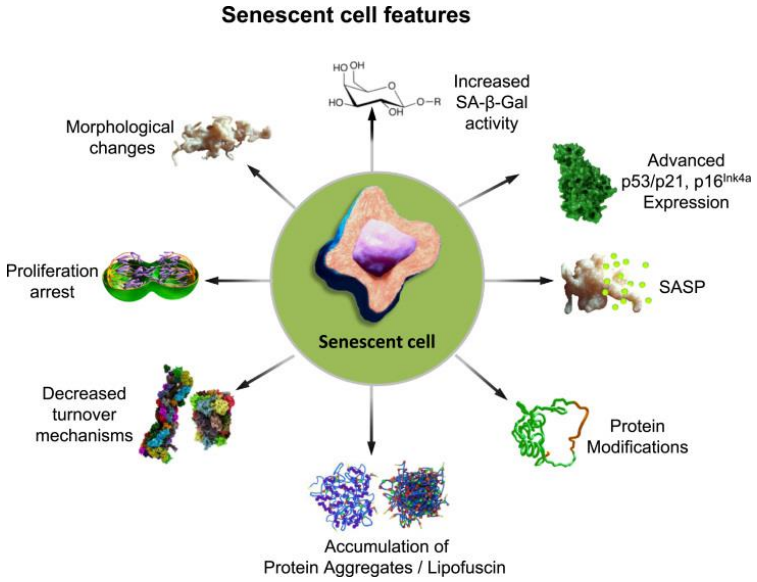

FIGURE 3. Features of senescent cells: Several markers were identified to characterize the senescent state in relation to morphology and proteostasis. During the development of senescence, cells show morphological changes by extension of their size and protein content or nuclei enlargement. Also, their lysosomes size and number increase resulting in an elevated activity of SA-β-Gal, the most widely used marker for senescence. The cells enter a proliferative arrest state, detected by cell cycle inhibitor levels such as p53/p21 and tumor suppressor p16INK4a, the latter is correlated with the formation of the SAHF. Other factors secreted during senescence are cytokines and chemokines, growth factors, proteases, fibronectin as well as ROS and RNS, altogether these are summarized as the SASP. Additionally, proteostasis changes during senescence shown by an increase in modified proteins, accumulation of protein aggregates and reduced functionality of the proteasomal and autophagy systems. Höhn et al., 2017

1.3 Linking AT senescence to chronic metabolic diseases

1.3.1 Obesity

Obesity is a major risk factor for IR and T2D. Obese people exhibit IR at a younger age compared to lean individuals, predisposing them to develop T2D (Palmer et al., 2016; Ahima., 2009). This early onset IR is attributed to AT dysfunction and low-grade chronic inflammation, similar as in ageing (Ahima et al., 2009) (Fig.4). The premature accumulation of senescent cells in AT represents a determining factor in linking obesity, ageing, AT dysfunction, and inflammation (Xu et al., 2015; Palmer et al., 2019; Muñoz-Espín et al., 2014). Indeed, selective removal of these cells from AT in obese mice alleviates the obesity-related derangement in fat tissue function and glucose homeostasis (Palmer et al., 2019). Accordingly, approaches that are successful in counteracting obesity and ageing, such as exercise and nutritional interventions, exert their health effects by targeting cellular senescence in AT (Fontana et al., 2007; Most et al., 2017; Lewis-McDougall et al., 2019; Ahima.,2009). As epigenetic factors respond adaptively to lifestyle they may be implicated independently of age in the acquisition of a senescent phenotype (Lewis-McDougall et al., 2019; Nilsson et al., 2017; Parrillo et al., 2019; Ungaro et al., 2012; Raciti et al., 2017; Parrillo et al., 2016; Desiderio et al., 2019). In the obesity setting, due to caloric overload, fat tissue is subjected to mechanical, hypoxic, oxidative, and ER stress. Once activated, the stress responses initiate a cascade of events in AT leading to senescence induction, functional decline, macrophage infiltration, and inflammation, resulting in IR (Muñoz-Espín et al., 2014; Ahima., 2009). The harmful effects of excess nutrients and the protective influence of exercise in obesity-related AT ageing have been demonstrated by the use of middle-aged mice undergoing physical exercise and/or fast-food diet (FFD) feeding. Administration of a FFD simultaneously causes adverse effects on body weight and insulin sensitivity and increases the expression of senescence markers (i.e., SA-β-gal, p53, p21, and p16) and SASP factors (i.e., IL-6, MCP-1, and PAI-1) in fat tissue. By preventing senescent cell accumulation and SASP development, physical exercise neutralizes the FFD induced detrimental effects on metabolic parameters (Schafer et al., 2016).

The expression of p53 in AT plays a key role in the development of obesity-related IR (Ahima et al., 2009; Minamino et al., 2009). P53 acts both as a potent senescence inducer and an adipogenesis repressor (Gustafson et al., 2019). Indeed, it needs to be downregulated before APCs can differentiate into insulin-responsive adipocytes (Krstic et al., 2018. Furthermore, the activation of p53 in adipocytes impairs insulin-stimulated glucose transport, enhances lipolysis, and promotes inflammation (Vergoni et al., 2016). *Minamino* et al. elucidated the role of p53 in linking obesity, AT senescence, and metabolic dysfunction (Minamino et al., 2009). Excessive caloric intake induces AT senescence, inflammation, and IR in agouti mice, a widely used model adopted to study nutritionally induced

epigenetic effects on the obesity phenotype (Parrillo et al., 2019). Interestingly, the adipocyte-specific p53 deficiency in the obese agouti mice exposed to a standard chow diet, as well as in obese wild-type mice fed a high-sugar/high fat diet, is sufficient to decrease the expression of senescence and inflammatory markers in AT and to improve insulin sensitivity (Minamino et al., 2009). Therefore, cellular senescence and inflammation, due to high p53 levels in AT, lead to metabolic complications associated with obesity (Tchkonia et al., 2010). There is evidence that similar processes in obese patients are also activated in AT. Obesity is associated to increased AT expression of senescence markers in young/middle-aged subjects, including p53 (Tchkonia et al., 2010; Muñoz-Espín et al., 2014; Gustafson et al., 2019). Additionally, Justice et al. recently provided evidence of the effectiveness of a 5-month resistance training programme with or without CR in lowering these senescence markers in thigh AT in overweight/obese women (Justice et al., 2018). Senescent APCs from SAT of obese individuals show a loss of replicative and differentiation ability (Tchkonia et al., 2010; Muñoz-Espín et al., 2014; Gustafson et al., 2019; Mitterberger et al., 2014; Oñate et al., 2012). Recently, Gustafson et al. provided a mechanistic explanation for the above correlation by showing that increased APC senescence is responsible for impaired SAT adipogenesis in hypertrophic obesity (Gustafson et al., 2019). This study has revealed that senescence markers (i.e., SA-β-gal, p53, and p16) and SASP factors that antagonize differentiation (i.e., PAI-1 and TGFβ-1) are upregulated in SAT biopsies from patients with hypertrophic obesity and T2D and are positively correlated with subcutaneous adipocyte cell size (Gustafson et al., 2019) Interestingly, the impaired adipogenic capacity of APCs isolated from the same specimens of SAT biopsy is linked to the inability to suppress p53 after induction of differentiation (Gustafson et al., 2019)

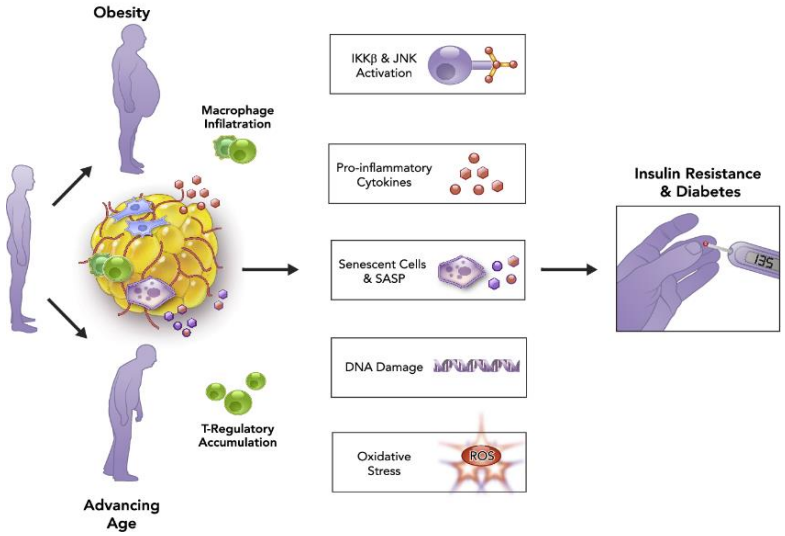

FIGURE 4. Ageing and obesity-related adipose tissue dysfunction: Age and obesity synergistically and independently lead to adipose tissue dysfunction, ultimately resulting in a chronic subclinical pro-inflammatory state, insulin resistance and Type 2 Diabetes. Analysis of processes causing fat tissue dysfunction in obesity could point to mechanisms contributing to metabolic dysfunction with ageing and even the ageing process itself. Stout et al., 2017, Tchkonia et al., 2010.

1.3.2 Type 2 Diabetes

There is a dynamic relationship between T2D and senescence (Palmer et al., 2015; Strycharz et al., 2017; Berná et al., 2014; Hannou et al., 2014; Leslie et al., 2014; Strazhesko et al., 2015; Gardner et al., 2005; Testa et al., 2011). T2D in itself has been proposed to represent a state of accelerated ageing in which senescent cells are part of a pathogenic loop, both as a contributing cause and as a result of the metabolic disturbances observed in the prediabetic and diabetic states (Palmer et al., 2015; Strycharz et al., 2017). Many GWASs also showed that single-nucleotide polymorphisms (SNPs) in genes encoding senescence markers, including p53, p16, and p21, are associated with an increased risk of developing T2D and its complications (Berná et al., 2014; Hannou et al., 2014; Leslie et al., 2014). Notably, SNPs at p53 transcriptional target genes, such as ZMAT3, are also associated with T2D and its related traits (Huynh et al., 2013; Leslie et al., 2014). Focusing on AT, TL shortening is inversely correlated with adipocyte cell size in SAT not only in obese subjects with or without T2D but also in lean diabetic patients, indicating a strong relationship of cellular senescence to the unhealthy metabolic environment related to adipocyte hypertrophy (Monickaraj et al., 2012). This link is also supported by data from adipose-p53-transgenic mice expressing high levels of both p53 and p21 in AT (Minamino et al., 2009). In these mice, the upregulation of these senescence markers is sufcient to induce an infammatory state that drives IR (Minamino et al., 2009). Consistently, individuals with T2D typically display an elevated senescent cell burden in AT, as demonstrated by the high expression levels of SA-

β-gal, p53, p21, and pro-infammatory SASP components (e.g., IL-1α, IL-1β, IL-6, and TNF-α). From a mechanistic perspective, cellular senescence and T2D form a vicious circle where both the obese and the prediabetic microenvironment become permissive for cellular senescence to develop prematurely. Senescence, in turn, exacerbates induction and impairs the clearance of senescent cells, resulting in tissue damage and metabolic derangement (Palmer et al., 2015). p53-mediated premature senescence can result from chronic IGF-1 exposure, the increased levels of which are due to hyper-insulinaemia and the changes in IGF-binding proteins (IGFBPs) (Tran et al., 2014). Among these, IGFBP3 has been recognized among the SASP components responsible for spreading senescence to bystander cells (Elzi et al., 2012). Furthermore, p53 mediates different types of stress responses in which ceramides act as important mediators. High ceramide levels can result in the senescence of adipose, endothelial, and immune cells due to alterations in the metabolism of fatty acids (Trayssac et al., 2018). Altogether these events synergistically promote the accumulation of senescent cells and expression of the related SASP in AT. This event, in turn, drives the local and systemic inflammation and derangement of metabolic homeostasis, contributing to the onset of T2D.

Several studies on human cells from T2D subjects revealed that senescent cells are also spread within aetiological tissues involved in diabetes-related complications (Palmer et al., 2015). In particular, the kidneys of patients with type 2 diabetic nephropathy (DN) exhibit an accelerated senescent phenotype in selected cell populations, particularly tubular cells and podocytes, accounting for DN progression towards renal insufficiency and diabetic kidney disease (DKD) (Verzola et al., 2008). This hypothesis seems also confirmed by the latest interim report from a clinical trial in DKD patients evaluating a combination of senolytic medications, dasatinib plus quercetin (D+Q) (Hickson et al., 2020). Indeed, DKD patients treated with three daily doses of D+Q display a lower senescent cell burden in abdominal SAT (i.e., decreases in SA-β-gal, p21, and p16) and lower plasma levels of the main SASP components (e.g., IL-1α, IL-2, IL-6, and IL-9) within 11 days (Hickson et al., 2020). Since senolytics appear to be more effective in alleviating senescence-associated diabetes complications than the currently available glucose-lowering treatments, the opportunity to introduce these drugs into clinical practice may provide a new way to treat chronic diseases that are still untreatable (Palmer et al., 2019; Hickson et al., 2020; Palmer et al., 2015). Importantly, previous investigations have shown that D+Q exposure eliminated senescent cells from aged mice, mice with IR and other chronic diseases, and AT explants from obese and/or diabetic patients (Hickson et al., 2020; Kim et al., 2019). In additions, preclinical studies in HFD-induced or genetically obese (db/db) mice revealed that D+Q mitigated IR, proteinuria, and dysfunction of the renal podocytes by eliminating senescent cells, primarily senescent APCs, from AT (Palmer et al., 2019).

1.4 Family History of Diabetes: an important risk factor to develop T2D

A family history of T2D, like ageing and obesity, is a key risk factor for the development of T2D (InterAct Consortium et al., 2013; Kirkman et al., 2012). Indeed, FDRs have a risk of developing diabetes up to 10-fold higher than subjects with no familiarity with diabetes (Meigs et al.,2000; Forouhi et al., 2014; InterAct Consortium et al., 2013). FDRs show early signs of molecular and metabolic abnormalities that are linked to an increased T2D risk (Spinelli & Florese., 2022) and reflect hereditary and environmental factors shared by families (Cederberg et al., 2015; Scott et al., 2013). In particular, they feature significantly increased HOMA-IR values, higher fasting plasma insulin and glucose levels and higher glucose levels following 75 g glucose loading. Also, the FDRs have higher triglyceride levels (Arner et al., 2011; Parrillo et al., 2020). Also, even when young and non-obese, FDRs feature anomalies of SAT similar to those observed during ageing. Indeed, they are characterized by inappropriate hypertrophic expansion of adipose cells due to a reduced differentiation capacity of the resident APCs, which drives ectopic fat storage, state of chronic low-grade inflammation, and IR (Parrillo et al., 2020; Arner et al., 2011; Henninger et al., 2014). A recent investigation reported that, in FDRs, the restricted ability of subcutaneous APCs to differentiate in the functional adipocytes is associated with inability to suppress the p53 senescence marker after adipocyte differentiation (Gustafson et al., 2019), suggesting their SAT alterations could reflect the detrimental effects of the accumulation of senescent APCs (Spinelli et al., 2022). Because p53 remains increased also in APCs from individuals with hypertrophic obesity (Gustafson et al., 2019), it is possible that FDRs share the "obese phenotype" characterized by limited ability to recruit and differentiate new adipocytes, inappropriate adipose cell hypertrophy, inflammation, and IR with obese subjects (Arner et al., 2011). The molecular mechanisms responsible for increased T2D susceptibility in FDRs remain unclear (Baig et al., 2020). Despite extensive efforts to identify risk loci for FDR-associated T2D predisposition, no genotype has been identified in the majority of FDRs. However, mounting evidence indicates that epigenetics may contribute to render FDRs more vulnerable to T2D (Parrillo et al., 2020; Ling & Ronn., 2019; Sanabil et al., 2020).

It is well established that epigenetic modifications, including loss of DNA methylation, are key in regulating the senescence phenotype (Atkinson et al., 2007; Cheng et al., 2017). Interestingly, major risk factors for T2D (ageing, obesity, T2D familiarity), which are associated with increased APC senescence, contribute to IR by affecting the AT methylome in non-diabetic subjects (Davegårdh et al., 2018; Parrillo et al., 2019). Furthermore, lifestyle interventions (diet, exercise, weight loss) that prevent T2D development by inducing DNA methylation changes in the AT, further exert their protective effects by preventing APC senescence (Justice et el., 2018; Most et al., 2017). Interestingly, my research

group recently demonstrated that the epigenetic signature of subcutaneous APCs in FDR subjects is characterized by a number of DNA hypomethylation events (Parrillo et al., 2020). Thus, the hypothesis that DNA methylation level determines occurrence of an early senescence phenotype in APCs of FDR individuals and contributes to their predisposition towards T2D, deserves to be investigated.

1.5 Epigenetics

The central dogma of biology describes the flow of genetic information from DNA to RNA to proteins and occurs through two intermediate steps, namely transcription and translation. However, these highly regulated processes can be modified at any point, altering protein expression and thus cellular phenotypes. Epigenetics mechanisms are important modifiers that hinder or promote the intermediate steps of the central dogma (Clark et al., 2020; Barros et al., 2009). Epigenetics consists of heritable modifications that regulate gene expression without altering the DNA sequence as a result of the dynamic and complex interaction between environment and genome. For many years, the heritability of epigenetic information was thought to be limited to mitotic cellular divisions. However, it is now apparent that epigenetic processes are meiotically heritable in organisms (Li et al., 2014). The relative plasticity of epigenetic modifications provides a framework for investigating the relationship between environmental and behavioral influences, human health, and disease development. The identification of epigenetic profiles linked to human chronic diseases has the potential to identify therapeutic targets that can be modulated through epigenetic mechanisms. (Crouch et al., 2022).

Epigenetic modifications changes include DNA methylation, histone posttranslational modifications (PTMs), and noncoding RNAs (ncRNAs) (Fig.5). Although each of these mechanisms is functionally relevant, geroscience research has best characterized the role of DNA methylation dynamics during ageing and their involvement in cellular senescence. The majority of DNA methylation occurs on cytosines that precede a guanine nucleotide (CpG) and acts as an essential transcription regulator. CpG methylation consists in the covalent transfer of a methyl group to the 5-carbon position of a CpG dinucleotide to form 5-methylcytosine (5mC) (More et al., 2013). Although the role of CpG methylation in the regulation of gene expression has been extensively investigated, the exact mechanism by which CpG methylation represses or activates gene expression has not been fully elucidated (Clark et al., 2020). Some experimental evidence indicates that methyl groups in the promoter region may influence protein binding to DNA, promoting modification of chromatin organization. In this way, the ability of transcription factors and other transcriptional machinery to access DNA is negatively modulated, leading to a reduction in gene expression (Clark et al., 2020; Bommarito et al., 2019). Another mechanism by which DNA methylation negatively regulates gene expression is the recruitment of methyl-CpG-binding proteins. The recruitment of methyl-CpG-binding proteins represents a physical

barrier to positive regulators of gene expression (Clark et al., 2020). These “competitor proteins” have been identified in complexes containing histone deacetylases, responsible for histone deacetylation of methylated sites (Boyes and Bird, 1991; Curradi et al., 2002). This phenomenon silences gene expression by creating a closed chromatin. Interestingly, CpG methylation and histone deacetylation in synergies may conspire to silence gene expression state (Boyes and Bird, 1991). PTMs drive the reorganization or remodelling of chromatin structure (Clark et al., 2020). Histone proteins are highly alkaline and positively charged. According to their structure and function, they are classified into five families: histones H1, H2A, H2B, H3 and H4. In the eukaryotic genome, the positively charged histone protein associated with negatively charged DNA forming the nucleosome, which represents a fundamental unit of chromatin. Except for H1, all histones are involved in the nucleosome core's construction. The enzymes carrying histonic modifications are acetyltransferases, deacetylases and methyltransferases, collectively termed histone-modifying proteins (Zhang et al., 2021). Altogether, these modifications allow the remodelling of DNA-histones interactions, which are responsible for chromatin reorganization (Peterson et al., 2004). These events affect the accessibility of nucleosomal DNA to complex transcriptional machinery, thereby influencing gene expression. For example, histone acetylation has been linked to positive transcriptional regulation: adding an acetyl group to positively charged lysine residues on histone tails attenuates histone and DNA interaction. The overall chromatin structure is relaxed, allowing transcriptional factor binding. This event results in increased gene expression. ncRNAs have a role in the post-transcriptional regulation of gene expression (Morceau et al., 2013; Mattick & Makunin., 2007). Regulatory ncRNAs include long ncRNAs (lncRNAs) and small ncRNAs, including the best characterized micro RNAs (miRNA), piwi-interacting RNA (piRNAs) and small interfering RNA (siRNAs) (Nigita et al., 2019; Fiannaca., 2017). The lncRNAs are at least 200 nucleotides long and act through several mechanisms, including transcription degradation, translation interference, and chromatin remodelling (Nigita et al., 2019; Clark et al., 2020). Alternatively, small ncRNAs (21-25 nucleotides) guide the process of mRNA degradation after incorporation into an RNA-induced silencing complex (Yang et al., 2016; Lekka &Hall., 2018).

1.5.1 DNA methylation

DNA methylation is now well recognized as a key epigenetic regulatory mechanism that involves direct chemical modification of DNA and influences gene activity cooperating with other regulators (Jin et al., 2011). DNA methylation is catalyzed by a family of DNA methyltransferases (DNMTs) that transfer a methyl group from S-adenyl methionine to the fifth carbon of a cytosine residue to form 5mC (Clark et al., 2020). The CpG methylation is governed by three critical mechanisms, which include: de novo establishment of methylation patterns (e.g., the establishment of methylation patterns in new cells early

in development), maintenance of methylation patterns, and active removal of methyl groups (demethylation) (Moore et al., 2013). DNMT3A and DNMT3B catalyse *de novo* methylation (Clark et al., 2020). Whether DNMT3A is expressed relatively ubiquitously, DNMT3B is poorly expressed by the majority of differentiated tissues, except for the thyroid, testes, and bone marrow (Moore et al., 2013). The maintenance of methylation patterns is governed by DNMT1. After DNA replication, DNMT1 is responsible for maintaining DNA methylation pattern in the newly replicated DNA strand, in order to maintains the original pattern of DNA methylation in a cell lineage (Long et al., 2017). The active demethylation of CpGs occurs through oxidation of 5mC to 5-hydroxymethylcysteine (5-hmC), both in dividing and non-dividing cells. TET enzyme family regulates this mechanism (Shi et al., 2017). DNMTs expression is greatly reduced after the end of the differentiative process, indicating that the DNA methylation pattern in the postmitotic state is stable. When exposed to environmental stimuli, several cell types, even when differentiated, display changes in DNMT expression (Feng et al., 2005).In the human genome, the total number of CpG is estimated to be around 28 million, and 60-80% of them are generally methylated (Wreczyckaad et al., 2017). Less of 10% of CpG characterizes CG-rich regions, knowns as CpG islands. Most of the gene promoters, about 70%, contain CpG islands. Interestingly CpG islands are mainly unmethylated (Long et al., 2017; Moore et al., 2013; Deaton & Beard., 2011), and they contain fewer nucleosomes than other strands of DNA (Ramirez-Carrozzi et al, 2009; Choi, 2010). This evidence suggests that CpG islands enhance the accessibility of DNA and promote transcription factor binding. Indeed, both hypo-methylated patterns and a reduced number of nucleosomes result in a stable rise in gene expression (Moore et al., 2013). On the other hand, if CpG sites located in promoters or enhancers are hypermethylated, these regions become heterochromatic and are not bound by transcription activators. This leads to transcriptional silencing (Jang et al., 2017; Anastasiadi et al., 2018). DNA methylation works with histone modifications and miRNA to regulate transcription. DNMTs cooperate with histone-modifying enzymes involved in order to induce a repressive and/or enhanced state of gene expression. Moreover, DNA methylation can affect methylation pattern of miRNA CpG islands, modulating miRNA expression (Lujambio et al., 2009).

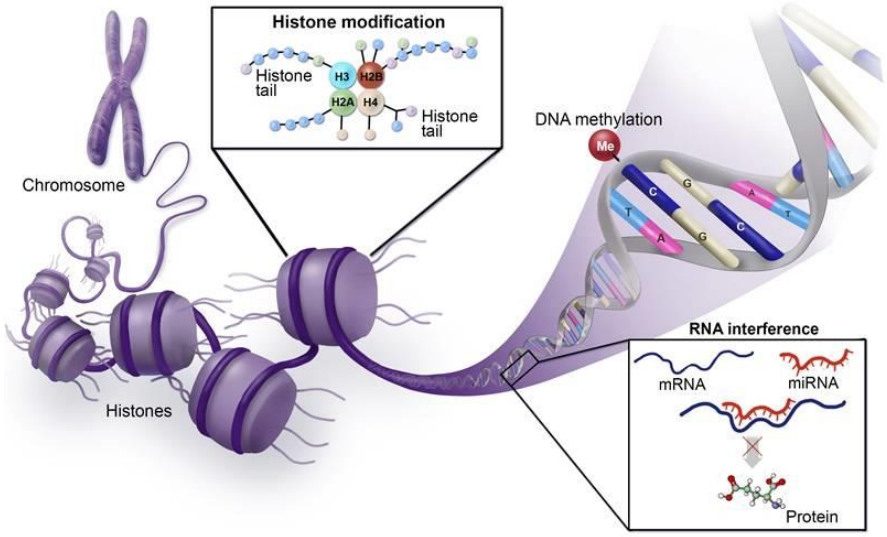

Figure 5. Epigenetic Mechanisms: Epigenetics, which encompasses alterations in gene expression caused by mechanisms other than DNA sequence changes, also plays a significant role in phenotypic diversity and differential sensitivity to environmental stimuli. Chromatin plays a significant role in genome regulation by dictating whether genes are active in a given cell or tissue type and is subject to extensive post-translational modifications that define this activity. As the field of epigenetics has advanced, it has become increasingly clear that epigenetic mechanisms provide a completely new ensemble of therapeutic targets for treating metabolic disorders. American Hematology Society

1.5.2 DNA methylation during ageing and senescence

DNA methylation is a crucial process behind the trajectories of alternative ageing, driving healthy ageing and longevity on one side and unhealthy ageing and chronic metabolic diseases on the other. Indeed, age-related dysregulation of DNA methylation is a common aetiological factor for ARDs ranging from T2D to neurodegenerative diseases (Hadad et al., 2020). Moreover, many effective lifespan-extending interventions act through DNA methylation (Pal et al., 2016). Thus, the opportunity to "reverse" ageing is an intriguing implication of epigenetic ageing regulation (Ghosh et al., 2019). There is a global hypomethylation of CpG over the genome during ageing that is responsible for *i.* loss of heterochromatin and gene de-repression in this region; *ii.* nuclear architecture changes; and, *iii.* increased genomic instability. Interestingly, the hypomethylation-induced loss of silencing at heterochromatic loci appears during ageing in all mammals, and its acceleration and rescue can, respectively, reduce and extend the lifespan (Pal et al., 2016). The age-associated genome-wide pattern in DNA methylation can be due to a progressive reduction in levels of DNMTs and/or their critical substrates [e.g., S-adenosilmetionina (SAM)] (Berná et al., 2014; Strazheskoet al., 2015). Paired methylome and transcriptome analyses in ageing cells and tissues from both mice and humans have

revealed an inverse correlation between gene expression and DNA methylation (Hadad et al., 2019; Rönn et al., 2015). These differences between young and old mammals show that they are in the range of 5-25 % at susceptible genes (Issa., 2014). Notably, these genes are enriched in pathways dysregulated during ageing such as senescence, inflammation, and the insulin-signalling pathway (Hadad et al., 2020). DNA methylation has been recognized as a critical mechanism promoting senescence at the molecular and cellular levels (Sidler et al., 2017; Nacarelli et al., 2016; Cheng et al., 2017; So et al., 2011; Balakrishnan et al., 2018). The DNA methylome of SNCs shows extensive hypomethylation and formation of facultative heterochromatin domains compared to proliferating normal cells. There is extensive evidence of the importance of DNA hypomethylation as a senescence inducer. First, this occurs in pre-senescent cells, but not in immortalized cells where the overall methylation level is relatively stable, indicating that DNA methylation dynamics are related to a limited proliferative lifetime (Nacarelli et al., 2016; Balakrishnan et al., 2018). Thus, DNA hypomethylation may function as a mitotic clock, similar to TL shortening (Issa., 2014). Second, the use of DNMT inhibitors (*e.g.*, 5-azacytidine) or specific small-interfering RNAs to target DNA methylation is sufficient to induce senescence in primary human cells (So et al., 2011). Notably, senescence-related hypomethylation occurs predominantly in genes with reduced expression in proliferating cells but elevated expression in SNCs (Balakrishnan et al., 2018). These include genes that encode p53 targets p21 and p16, as well as the two main SASP pro-inflammatory components IL-6 and IL-8 (Faget et al., 2019; So et al., 2011). Many studies have shown that the pattern of DNA methylation in human tissues can be used as a chronological age estimator, a biomarker for healthy and unhealthy ageing, and a risk factor for ARDs (Field et al., 2018). AT has been extensively studied in this context supporting the notion that age-related changes to the methylome may underlie the AT dysfunction observed in the elderly population (Rönn et al., 2015). In particular, different groups have developed so-called DNA methylation clocks (DNAm-age clocks) based on age-associated DNA methylation changes that are relatively common across individuals and in some cases, across tissues (Horvath et al., 2013; Hannum et al., 2013; Bocklandt et al., 2011; Huang et al., 2015; Zbieć-Piekarska et al., 2015). Each clock utilizes DNA methylation information at specific CpGs (ranging between 3 and 353 CpGs) to calculate the time elapsed after birth (*i.e.*, chronological age). Interestingly, several DNAm-age clocks investigated *in vivo* successfully predict *in vitro* chronological age. Their analysis shows that both systems display global hypomethylation throughout the human lifespan suggesting preservation of an epigenetic ageing signature between human tissues and primary human cells (Sturm et al., 2019). Notably, specific DNAm-age clocks also distinguish senescence from replicative states of cellular lifespan and are sensitive to environmental stimuli (Field et al., 2018; Sturm et al., 2019; Horvath et al., 2014). Accelerated rates of epigenetic ageing, both *in vivo* and *in vitro*, are correlated with metabolic stressors

related to obesity and a shorter lifespan. Insulin, glucose, triglycerides, and total cholesterol serum concentrations are positively correlated with DNAm-age acceleration. Consistently, *ex vivo* experiments have shown that human fibroblasts cultured under chronic hyperglycaemic conditions show an increase in the baseline DNAm-age of approximately three years (Sturm et al., 2019). The effects of environmental stimuli on epigenetic ageing rates offer insight into how and why subjects with the same chronological age can experience dissimilar DNAm-age. The difference between DNAm-age and true chronological age reflects biological age (Δage), which is considered an indicator of human ageing rate and health outcomes (Field et al., 2018; Jones et al., 2015; Gentilini et al., 2013). Individuals can be classified as *i.* biologically old if their DNAm-age is higher than their chronological age; *ii.* biologically young if the reverse is true; or, *iii.* biologically concordant. Several lines of evidence support the notion of an accelerated DNAm-age reflects an advanced biological age. Obesity, BMI, chronic systemic inflammation, T2D, NAFLD and decreased physical fitness accelerate DNAm-age. Instead, interventions that promote longevity, such as CR and rapamycin, decelerate DNAm-age (Field et al., 2018, Horvath et al., 2014; Stevenson et al., 2018; Bacos et al., 2016) (Fig.6). Therefore, understanding DNAm-age molecular biology is essential in deciding how best using DNAm-age as a biomarker in biomedical research and in clinical medicine.

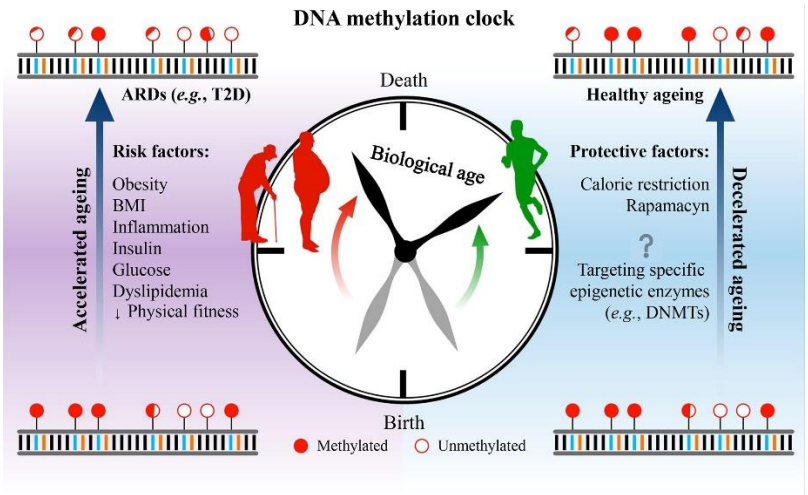

Figure 6. Schematic chart of a DNA methylation clock throughout the human lifetime. The difference between DNA methylation age and chronological age (i.e., the time elapsed since birth) reflects biological age and may be an indicator of ageing rate and health outcomes. ARDs, age-related diseases; T2D, type 2 diabetes. Spinelli et al., 2020

1.6 *ZMAT3* as candidate epi-gene for senescence in APCs

The *Zinc Finger Matrin-Type 3* (*ZMAT3*), also known as *WIG1* or *PAG608*, gene encodes a zinc-finger RNA-binding protein, highly conserved from fish to human, which is involved in post-transcriptional regulation of gene expression by affecting mRNA stability and translation (Hellborg et al., 2001; Bersani et al., 2016). ZMAT3 has been originally identified as a P53 positive regulator that enhances *P53* mRNA levels via a positive feedback loop. ZMAT3 binds to AU-rich locations in the 3'UTR of *P53* mRNA and protects it from deadenylation, resulting in *P53* mRNA stabilization and increased P53 protein expression, as well as an expanded P53 network. P53, on the other hand, acts as a transcriptional activator of ZMAT3 (Bersani et al., 2014; Vilborg et al., 2009). A recent study also uncovered a novel function for ZMAT3 in RNA homeostasis by modulating alternative splicing, resulting in multifaceted effects on several cellular processes. ZMAT3 regulates hundreds of transcripts through alternative splicing, including the transcripts encoding the P53 negative regulators MDM2 and MDM4 (Bieging-Rolett et al., 2021). The ZMAT3 positive feedback to P53 may account for some ZMAT3 tumor suppressor activity. Indeed, ZMAT3 belongs to the p53-dependent growth-inhibiting and tumor suppressor pathways (Hellborg et al., 2001; Janic et al., 2018). Accordingly, ZMAT3 has been identified as a tumour suppressor in lung and liver cancers, as well as human carcinomas (Bieging-Rolett et al., 2020).

In humans, ZMAT3 is expressed in all tissues, with the highest expression in brain, smooth muscle, cardiac myocytes, and adipocytes (Vilborg et al., 2011). *ZMAT3* upregulation has been reported in both human SNC and aged tissues (Chaturvedi et al., 2015; Lee et al., 2014; Marthandan et al., 2016; Yang et al., 2016). In a recent analysis of 17,382 whole transcriptome profiles in 54 tissue types from 979 human donors aged 20 to 79 and included in the GTEx database (V.8), *ZMAT3* emerged as one of the top ten age-related and differentially expressed genes. According to this data, *ZMAT3* mRNA levels are positively correlated with age in several human tissues (*e.g.*, artery, heart, nerve, liver, thyroid, lung), including the SAT (Chaturvedi et al., 2015; Marthandan et al., 2016; Yang et al., 2016; Avelar et al., 2020; Dong et al., 2021). Furthermore, ZMAT3 hypomethylation has been found in the cerebellum of subjects with Down Syndrome, which has been described as a human condition of accelerated ageing (Gensous et al., 2019; Mendioroz et al., 2016). ZMAT3 was found to be increased in human fibroblasts, during both stress-induced premature senescence and replicative senescence (Lee et al., 2014). *ZMAT3* gene was also upregulated in human blood cells following exposure to ionizing radiation (Lacombe et al., 2018), as well as and in endothelial cells after nickel irradiation (Beck et al., 2014). Both these environmental stressors are responsible for p53-dependent induction of senescence in human cells (Wang et al., 2016; Luczak et al., 2017). Altogether these findings suggest that ZMAT3 upregulation

is linked to cellular senescence. Other pathways, such as oxidative stress response, inflammation mediated by chemokines and cytokines, Insulin/IGF-protein kinase B, support the involvement of ZMAT3 in the P53 network for regulating cell growth and senescence (Vilborg et al., 2011). However, whether and how ZMAT3 induces senescence deserves to be investigated.

2. EXPERIMENTAL PROCEDURES

2.1 Study participants

Twenty-four individuals were selected from the EUGENE2 consortium (Laakso et al., 2008). These subjects were healthy and non-obese with (*n*=12; FDRs) or without (*n*=12; CTRLs) one first-degree relative with T2D. Male/female in the study group was 1; mean age was 40.6 years (SEM:1.6 years); mean BMI was 24.9 Kg/m^2 (SEM:0.4 Kg/m^2). Detailed clinical characteristics of these individuals have been previously reported in (Laakso et al., 2008) and are synoptically presented in Tab.1. Subjects who were FDRs exhibited a significantly reduced insulin sensitivity and larger subcutaneous adipocytes when compared to CTRL subjects. No significant differences were shown between two groups regarding age, sex, BMI, and body fat percent. All of the enrolled subjects signed their informed consent and were subjected to abdominal subcutaneous adipose tissue (SAT) sampling from the paraumbilical region. The study protocol was approved by the Ethical Committee of the University of Gothenburg (ethical approval numbers S655-03 and T492-17) according to the Declaration of Helsinki.

2.2 Isolation and culture of APCs

After harvesting, adipose precursor cells (APCs) were isolated from SAT specimens as previously reported in (Gustafson et al., 2019). Minced adipose tissue was aseptically processed by incubation with collagenase (Roche Diagnostics) at 37 ºC for 45 min. The digest was filtered through nylon mesh with a pore size of 250 μm and collected in enzyme quenching media. The layer with floating adipocytes was removed and used for adipocyte size measurement as described in (Arner et al., 2011). The remaining media containing the APC fraction was centrifuged for 15 min at 1500 g at 20 ºC. The isolated APCs were washed twice, and the erythrocytes were lysed with 155 mmol/l NH_4Cl for 5 min before seeding APCs. After 3 days, the inflammatory cells ($CD14^+/CD45^+$) and endothelial cells ($CD31^+$) were removed from the APC fraction by immune magnetic separation (Miltenyi) as described in (Arner et al., 2011). The APCs were then cultured with DMEM/F-12 medium (ThermoFisher Scientific) supplemented with 10% fetal bovine serum (FBS, ThermoFisher Scientific), 2 mmol/l

glutamine, 100 U/ml penicillin and 100 μg/ml streptomycin (ThermoFisher Scientific). APCs were finally expanded in culture for three passages to prepare for experimentations.

2.3 Adipogenic differentiation of APCs

APCs were grown and allowed to differentiate into mature adipocytes as described in (Gustafson et al., 2019). APCs were induced to differentiate after 3 days of confluence (differentiation day 0) with a cocktail consisting of 850 nmol/l insulin, 10 μmol/l dexamethasone (Sigma-Aldrich), 0.5 mmol/l isobutylmethylxanthine (MP Biomedicals), 10 μmol/l rosiglitazone (Cayman Chemical) in DMEM/F12 supplemented with 3 % FBS, 2 mmol/l glutamine, and antibiotics. After 3 days, the medium was replaced to adipocyte medium consisting of 850 nmol/l insulin, 1 μmol/l dexamethasone, 1 μmol/l rosiglitazone in DMEM/F12 supplemented with 10 % FBS, 2 mmol/l glutamine, and antibiotics. The adipocyte medium was changed every 3 days throughout the differentiation period until day 15 (differentiation day 15). To examine lipid accumulation, differentiated APCs were fixed with 4 % formaldehyde for 5 min at room temperature and stained with Oil Red O (Sigma-Aldrich) as previously reported in (Mirra et al., 2021).

2.4 Flow cytometry analysis

Flow cytometry was performed with a BD LSRFortessa Flow Cytometer (BD). For each experiment, 10,000 cells per APC sample were counted. Flow cytometric forward scatter (FSC-A) and side scatter (SSC-A) density plots were applied to analyze APC size and structure, respectively, as described (Ratushnyy et al., 2020). Senescence-associated beta-galactosidase (SA-β-gal) activity was assessed as indicated in (Debacq-Chainiaux et al., 2009). APCs (3×10^4 cells) were seeded in a 6-well plate. Cells at 70–80% confluence were treated with bafilomycin A1 (Sigma-Aldrich) for 1 hour to induce lysosomal alkalynization. This step was followed by 2 hours incubation with 5-dodecanoylaminofluorescein di-β-D-galactopyranoside (C_{12}FDG, ThermoFisher Scientific). Once inside the cells, the C_{12}FDG substrate is cleaved by SA-β-gal producing a green fluorescent product. SA-β-gal positive APCs were quantified by flow cytometry. Cell cycle analysis was performed as reported in (Raciti et al., 2018). APCs (3×10^4 cells) were seeded in a 6-well plate and left until they had reached 70–80% confluency. Then, the cells were harvested, fixed in cold ethanol 70%, washed twice with cold PBS, and incubated in PBS containing 20 μg/mL PI and 1 mg/mL RNase A for 30 min at room temperature in the dark. DNA content of the PI-stained APCs were analyzed by flow cytometry. The histogram of cell cycle distribution was generated from 10,000 events per APC sample.

2.5 Primer sequences

Sequences of all the used primers are shown in Tab.2

2.6 Bisulphite sequencing

Bisulphite treatment of genomic DNA (gDNA) extracted from APCs by the AllPrep DNA/RNA Mini Kit (Qiagen) was carried out using the EZ DNA Methylation Kit (Zymo Research). Converted gDNA was amplified by PCR using specific primers for the *ZMAT3* DMR (*hg38_dna range=chr3:179032279-179033001*). Bisulphite sequencing was performed as previously reported in (Desiderio et al., 2019; Raciti et al., 2017). PCR products were cloned into the pGEM T-Easy vector (Promega) and 10 clones for sample were sequenced with an AB 3500 genetic analyzer (ThermoFisher Scientific). We first calculated the percentage of DNA methylation levels at all the 42 CpGs within the *ZMAT3* DMR in each clone and then averaged the DNA methylation level for 10 clones of the same sample. DNA methylation % = [methylated CpGs/ (methylated CpGs + unmethylated CpGs)] *100. Bioinformatics analysis was carried out using EMBOSS CpGplot (available from www.ebi.ac.uk/Tools/seqstats/emboss_ cpgplot/; accessed November 2015).

2.7 RNA isolation and qPCR

Total RNA was extracted from APCs using the AllPrep DNA/RNA Mini Kit (Qiagen). Reverse transcription of 1 μg of total RNA was performed using SuperScript III (ThermoFisher Scientific), following the manufacturer's instructions. qPCR reactions were run with SYBR Green PCR Master Mix (Bio-Rad) as previously described in (Longo et al., 2016; Nigro et al., 2019). Human *RPL13A* or *28S* were used as reference genes as mentioned in the corresponding figure legend. qPCR conditions were as follows: 95 °C for 30 s, 40 × (95 °C for 5 s and 60 °C for 30 s). All reactions were run in triplicate on a QuantStudio 7 Flex Real-Time PCR System (ThermoFisher Scientific).

2.8 Western Blot

Protein extracts were prepared in ice-cold RIPA buffer as previously described in (Pirone et al., 2019). Protein concentration was assessed using the protein assay based on Bradford's method (Bio-Rad). Total cell extracts in equal amounts were separated by SDS-PAGE and blotted on nitrocellulose membrane (Millipore) as reported in (Ungaro et al., 2012). Upon incubation with primary antibodies against ZMAT3 (ab191536, Abcam), P53 (sc-126, Santa Cruz), or Vinculin (sc-73614, Santa Cruz), and secondary antibodies (Bio-Rad), immunoreactive bands were detected by an enhanced

chemiluminescence kit (Bio-Rad) and quantified by the ImageJ software. Protein abundance was calculated after Vinculin normalization.

2.9 Construction and functional analysis of luciferase reporter vectors

The intronic *ZMAT3* DMR (*hg38_dna range=chr3:179032279-179033001*) was amplified by PCR and cloned into the CpG-free promoter firefly luciferase reporter vector (InvivoGen) in both forward and reverse orientations (Bakshi et al., 2018). Luciferase assay was performed as described in (Desiderio et al., 2019). Constructs were amplified in E. coli GT115 cells (InvivoGen). *In vitro* methylation was carried out using the M.SssI CpG methyltransferase (New England Biolabs) and S-adenosylmethionine (SAM; New England Biolabs), following manufacturer's instructions. Un-methylated constructs were treated as the methylated construct, including application of SAM, but in the absence of *M.SssI* (mock-treated). *In vitro* methylation was confirmed by resistance to *HhaI* or *HpaII* (New England Biolabs) digestion. Transfection with an equimolar amount of the mock-treated empty vector was used to control for background firefly luciferase activity. Firefly luciferase activity of each transfection was normalized against renilla luciferase activity (Promega).

The wild-type *CDKN1A* promoter region (*hg38_dna range=chr6: 36676412-36676502*) containing the P53 response element (RE) from -2281 to -2261 bp upstream the TSS (el-Deiry et al., 1993; Laptenko et al., 2011) was amplified by PCR and cloned into the CpG-free promoter firefly luciferase reporter vector (InvivoGen). Complementary oligonucleotides corresponding the above-mentioned *CDKN1A* promoter region were synthesised by Sigma-Aldrich to incorporate the desired point mutations of the invariant G/C basepairs within the P53 RE to prevent P53 from binding to this nucleotide sequence (Kaeser & Iggo, 2004). These oligonucleotides were annealed *in vitro* and then cloned into the CpG-free promoter firefly luciferase reporter vector (InvivoGen). The wild-type or mutagenized *CDKN1A* reporter construct was transfected in APCs from CTRL subjects in the presence of the pCMV6-*ZMAT3* or pCMV6-*TP53* expression vector, or an equimolar amount of the pCMV6 empty vector. Co-transfection of the wild-type *CDKN1A* reporter construct with the pCMV6 empty vector was used to control for the basal *CDKN1A* promoter activity. Firefly luciferase activity of each transfection was normalized against renilla luciferase activity (Promega).

All final constructs were validated by sequencing. Transfections were carried out by Lipofectamine 3000 reagent (ThermoFisher Scientific) in serum-free Opti-MEM media (ThermoFisher Scientific), following manufacturer's instructions. Luciferase activities were measured by a dual-luciferase reporter system and a GloMax Luminometer (Promega). All luciferase assays were performed at least three times.

2.10 Construction and transfection of *ZMAT3* expression vector

The *ZMAT3* expression vector was engineered using the pCMV6-Entry mammalian expression plasmid (Origene). The complete ORF of *ZMAT3* (RefSeq NM_022470.4) was amplified from full-length cDNA by PCR. The *ZMAT3* ORF was cloned into the pCMV6 plasmid digested with NheI and XhoI (New England BioLabs) to generate the recombinant vector pCMV6-*ZMAT3*. The final construct was verified by sequencing. APCs from CTRL donors were transfected with the pCMV6-*ZMAT3* expression vector or an equimolar amount of the pCMV6 empty vector using Lipofectamine 3000 reagent (ThermoFisher Scientific) in serum-free Opti-MEM media (ThermoFisher Scientific), following manufacturer's instructions. Senescence markers were evaluated 3 days after transfection.

2.10.1 Construction and transfection of *TP53* expression vector

The *TP53* expression vector was engineered using the pCMV6-Entry mammalian expression plasmid (Origene). The complete ORF of *TP53* (RefSeq NM_000546) was amplified from full-length cDNA by PCR. The *TP3* ORF was cloned into the pCMV6 plasmid digested with NheI and XhoI (New England BioLabs) to generate the recombinant vector pCMV6-*TP53*. The final construct was verified by sequencing. APCs from CTRL donors were transfected with the pCMV6-*TP53* expression vector or an equimolar amount of the pCMV6 empty vector using Lipofectamine 3000 reagent in serum-free Opti-MEM media and following manufacturer's instructions.

2.11 Multiplex SASP protein analysis

Conditioned media (CM) were prepared by pre-washing APC cultures with PBS, then exposing them to serum-free DMEM/F-12 medium (ThermoFisher Scientific) for 24 hours. CM were centrifuged at 14,000 g to remove debris and stored at -80 °C for subsequent analysis. Bioplex Multiplex human cytokine and chemokine assays (Bio-Rad) were used to quantify SASP factors in CM as specified by the supplier.

2.12 Chromatin immunoprecipitation (ChIP)

ChIP experiments were performed by True MicroChIP kit (Diagenode), following manufacturer's instructions. APCs from CTRL donors transfected with the pCMV6-*ZMAT3* expression vector or an equimolar amount of the pCMV6 empty vector, as well as APCs from FDR and CTRL subjects, were cross-linked with 1 % formaldehyde for 10 min at room temperature and then quenched with 125 mmol/l glycine for 5 min. The samples were sonicated for chromatin shearing using a Bioruptor (Diagenode). After centrifugation, the supernatants were diluted according to the manufacturer’s instructions. The samples of sheared chromatin were divided into Input, P53-IP, and IgG control

aliquots. At the latter two aliquots were added 2 µg of anti-P53 monoclonal antibody (sc-126, Santa Cruz) or mouse IgG (sc-2025, Santa Cruz) as a negative control (IgG control), respectively, and incubated for 16 hours at 4 °C with rotation. Protein G-coated magnetic beads (ThermoFisher Scientific) were added to each sample, which was then incubated for 2 hours at 4 °C. The immunoprecipitated DNA was eluted from coated magnetic beads and subsequently purified with QIAquick PCR Purification Kit (Qiagen). The DNA samples (Input, P53-IP, and IgG control) were subjected to qPCR amplification using primers flanking the region of interest within the *CDKN1A* promoter.

2.13 Senescence induction

To induce senescence, APCs obtained from CTRL donors were exposed to hydrogen peroxide (H_2O_2; Sigma-Aldrich) or 5-azacytidine (5-AZA; Sigma-Aldrich). H_2O_2 was dissolved in culture medium at a concentration of 200 µM and APCs were treated as described in (Wang et al., 2013) 5-AZA was dissolved in culture medium at a concentration of 10 µM and APCs were treated for 72 hours.

2.14 RNA interfering

siRNA targeting *ZMAT3* ($siRNA^{ZMAT3}$) and scrambled siRNA as negative control ($siRNA^{C}$) were purchased from ThermoFisher Scientific. APCs from CTRL donors were transfected with 25 pmol of $siRNA^{ZMAT3}$ or $siRNA^{C}$ using Lipofectamine 3000 reagent (ThermoFisher Scientific) in serum-free Opti-MEM media (ThermoFisher Scientific), following manufacturer's instructions. After 24 hours from the transfection, the cells were treated for 72 hours with or without 10 µM 5-AZA in the absence or presence of either $siRNA^{ZMAT3}$ or $siRNA^{C}$.

2.15 PFTα treatment

PFTα was purchased from Santa Cruz (sc-45050). PFTα was dissolved in DMSO to generate stock solution (50 mM). Then, it was diluted in DMEM/F12 medium to a final concentration of 50 nM. APCs from CTRL donors were transfected with the pCMV6-*ZMAT3* vector in the presence or absence of 50 nM PFTα for 72 hours.

2.16 Senolytic treatment

Dasatinib (D) and Quercetin (Q) were purchased from Sigma-Aldrich. D and Q were dissolved in DMSO to generate stock solutions (100 mM and 10 mM, respectively). Then, D plus Q was diluted in DMEM/F12 medium to get the indicated final concentration. APCs from FDR donors were exposed to 0.5 μM D plus 20 μM Q or vehicle only (DMSO) for 3 days as reported in (Zhu et al., 2015).

2.17 SAT bioptical samples

Discovery cohort - Human abdominal SAT samples were obtained in the fasting state by needle biopsy from *n*=29 subjects aged 26 to 67. This group included both T2D individuals (*n*=10) and subjects who featured normal glucose tolerance (*n*=19). Their clinical characteristics have been previously reported (Gustafson et al., 2019). Prior to sample collection, all subjects provided informed consent in full compliance with and strict adherence to the guidelines approved by the Ethical Committee of the University of Gothenburg in agreement with the Declaration of Helsinki. Whole tissue was used for adipose cell isolation (Gustafson et al., 2019). The isolated adipose cells were directly processed for RNA extraction. Gene expression was analysed with the Quant Studio6 sequence detection system (ThermoFisher Scientific). mRNA results were first normalized to *28S* and then normalized to expression levels in one individual (=1). Values are presented as relative expression units (REU).

Replication cohort - Human SAT samples were obtained from women (*n*=20; age 18–61 years; BMI 22.0–43.3) undergoing surgical mammary reduction. Sample size was calculated by using the G*Power 3.1.9.2 software (Heinrich-Heine-Universität Düsseldorf, Germany). A sample size of 20 participants, *n*=10 for group, achieved 95% power to detect a difference of 0.3692 between the null hypothesis that both group means are equal to 0.2299 and the alternative hypothesis that the mean of group 2 is different and equal to 0.5491, considering a two-sample t test (two tails), a significance level (α) of 0.01, an estimated group standard deviations of 0.0908 and 0.1843, and an allocation ratio N2/N1 = 1. For calculations, values of the *ZMAT3* mRNA (mean ± SD) in high- and low-expressor subjects from our discovery cohort were applied. All of the women were otherwise healthy, with no metabolic or endocrine diseases. Their characteristics have been previously described (D'Esposito et al., 2012). Before the surgical procedure, each study participant provided informed consent. This procedure was approved by the ethical committee of the University of Naples. The mammary adipose tissue specimens were directly processed for RNA extraction and gene expression analysis. Among them, twelve samples were available for protein extraction and expression analysis.

2.18 Statistical analysis

Data are presented according to proposed guidelines for basic science data visualization (Weissgerber et al., 2017). Biological replicates were collected from different samples, each isolated from different human specimens. The number of independent biological replicates (*n*) used in each experiment was indicated in the figure. Statistical analysis was performed with GraphPad Prism 6.0 software (GraphPad Software Inc) and R statistical platform. Normal distribution of continuous variables was tested using the Shapiro-Wilk test. Normally distributed data were compared between groups by unpaired Student's *t*-test (two-tailed). Within-group comparisons between matched samples were performed using paired two-tailed Student *t*-test or one-way repeated measures ANOVA followed by Tukey's multi-comparison test, as appropriate. Not normally distributed data were compared between groups by Mann Whitney test (two-tailed). The correlation between quantitative variables was tested using Spearman's rank correlation test. The association between age or *TP53* mRNA levels and *ZMAT3* expression in both subcutaneous adipose cells and SAT was tested by multiple regression analysis adjusting for BMI. BMI was fixed as covariate to account for the potential confounding effect of the association between this variable and cellular senescence and mRNA expression in human SAT. *p*-value ≤ 0.05 was considered statistically significant

Table 1. Clinical characteristics of FDR and CTRL subjects

Phenotypes	*FDR subjects*	*CTRL subjects*	*p value*
N (female/male)	12 (6/6)	12 (6/6)	>0.9999
Age, years	45.0 [35.0; 49.7]	38.0 [35.0; 46.0]	0.1386
BMI, Kg/m^2	25.0 [23.9; 26.6]	24.9 [22.8; 26.7]	0.5800
Fat percent, %	27.7 [19.8; 31.4]	23.2 [20.1; 31.2]	0.5516
Waist to Hip Ratio (WHR)	0.92 [0.87; 0.96]	0.82 [0.74; 0.86]	*0.0021*
Subcutaneous adipocyte size, µm	101.0 [99.6; 104.6]	90.4 [87.0; 92.0]	*<0.0001*
f-insulin, pmol/L	53.4 [49.3; 66.2]	31.9 [23.6; 44.4]	*0.0091*
fb-glucose, mmol/L	4.7 [4.5; 5.2]	4.3 [4.1; 4.6]	*0.0070*
OGTT p-glucose 2 h, mmol/L	6.5 [3.4; 8.1]	4.6 [4.0; 6.1]	*0.0346*

Gender (female/male) is expressed as number. Other data are shown as median [first quartile-Q1; third quartile-Q3]. Statistical differences between the two groups were tested using Mann Whitney test (continuous variables) or Fisher's exact test (categorical variable). *p* value *vs* CTRLs.

FDRs, first-degree relatives of T2D subjects; CTRLs, subjects with no diabetes familiarity; BMI, body mass index; f-insulin, fasting insulin; fb-glucose, fasting blood glucose; OGTT, oral glucose tolerance test; p-glucose, plasma glucose.

Table 2. List of primers used in this study

Technique	Gene/Region	Oligonucleotide sequences (5' ® 3')
qPCR	*RPL13A*	F: CTTTCCGCTCGGCTGTTTTC R: GCCTTACGTCTGCGGATCTT
	CDKN1A	F: GCAGACCAGCATGACAGATTTC R: ATGTAGAGCGGGCCTTTGAG
	LMNB1	F: GCCCAGATCAAGCTTCGAGA R: GCTTCCAACTGGGCAATCTG
	ZMAT3	F: TATCGAAGGGAGGGGAGCAA R: TTAAAGGAGCCCATCTGCGG
	TP53	F: CGCTTCGAGATGTTCCGAGA R: CTTCAGGTGGCTGGAGTGAG
	28S	F: CCCAGTGCTCTGAATGTCAA R: AGTGGGAATCTCGTTCATCC
	IL6	F: CAATGAGGAGACTTGCCTGGT R: AGCTGCGCAGAATGAGATGA
	MCP1	F: CCCAAAGAAGCTGTGATCTTCA R: TCTGGGGAAAGCTAGGGGAA
	PPARG2	F: TCAGTGAATTACAGCAAACCC R: AGTGTATCAGTGAAGGAATCGCT
Bisulfite sequencing	*ZMAT3* DMR	F: GGATTGTAGATAGAGTTT R: TATTAAATACACCTCCCAAATA
Cloning	*ZMAT3* DMR forward	F: CGCCCTAGGCAGACAGAGTCTCGCTCACT R: CGCGGATCCATGAGCTGTTGGGTACACCT
	ZMAT3 DMR reverse	F: CGCGGATCCCAGACAGAGTCTCGCTCACT R: CGCCCTAGGATGAGCTGTTGGGTACACCT
	wild-type *CDKN1A* promoter	F: CGCCCTAGGAGCAGGCTGTGGCTCTGATT R: CGCGGATCCCAAAATAGCCACCAGCCTCTTCT
	mutated *CDKN1A* promoter	F: CGCCCTAGGAGCAGGCTGTGGCTCTGATTGGC TTTCTGGCCGTCAGGAA**G**AT**C**TCCCAA**G**AT**T**TTGAGCTC TGGCATAGAAGAGGCTGGTGGCTATTTTGGGATCCCGC R:GCGGGATCCCAAAATAGCCACCAGCCTCTTCTATG CCAGAGCTCAAAATCTTGGGAGATCTTCCTGACGGCC AGAAAGCCAATCAGAGCCACAGCCTGCTCCTAGGGCG
	ZMAT3 ORF	F: CTAGCTAGCATGATCCTCTTGCAACACGCCG R:CCGCTCGAGTACATATCCCAGATTCTCCATCTC
	TP53 ORF	F: CTAGCTAGCATGGAGGAGCCGCAGTC R: CCGCTCGAGTCAGTCTGAGTCAGGCCCTT
ChIP	*CDKN1A* promoter	F: AGCAGGCTGTGGCTCTGATT R: CAAAATAGCCACCAGCCTCTTCT

3. RESULTS

3.1 Senescence phenotyping in APCs from FDRs of T2D subjects

To test the hypothesis that the early senescence of APCs occurs in individuals at high risk for developing T2D, we have first compared senescence markers in APCs from FDRs of T2D patients and subjects with no familiarity for diabetes (CTRLs). We examined a panel of senescence markers in these cells because none of them has absolute specificity (Wiley et al., 2017). A threefold increase in the percentage of senescence-associated beta-galactosidase (SA-β-gal)-positive APCs was observed in the FDRs compared to the CTRLs (Fig.7a). Based on flow cytometric forward scatter and side scatter evaluation, this difference was accompanied, respectively, by enlarged size and increased cytoplasmic granularity in the FDR APCs (Fig.8), along with upregulation of the p21-encoding *CDKN1A* gene (Fig.7b) and a consistent increase in the percentage of cells arrested in the G1 phase of cell cycle (Fig.9a). Accordingly, FDR APCs showed a significant slower growth rate compared to controls (Fig.9b) The *Lamin B1* (*LMNB1*) mRNA levels were also reduced in the FDR APCs (Fig.7c). Subsequently, to see if APCs from FDR subjects released SASP factors, we compared conditioned media (CM) obtained from FDR and CTRL cells cultured for 24 hours. As shown in Tab.3, several key SASP factors were present at higher levels in the media conditioned by FDR compared to CTRL APCs. These include interleukin 6 (IL6), monocyte chemotactic protein 1 (MCP1), regulated on activation normal T-cell- expressed and T-cell- secreted (RANTES), interleukin 8 (IL8), and macrophage inflammatory protein 1 beta (MIP1b). Thus, APCs from subjects who are FDRs exhibit increased signs of senescence when compared to individuals with no familiarity for diabetes. Because these cells develop a distinct SASP, their presence is likely to have an effect on the surrounding AT.

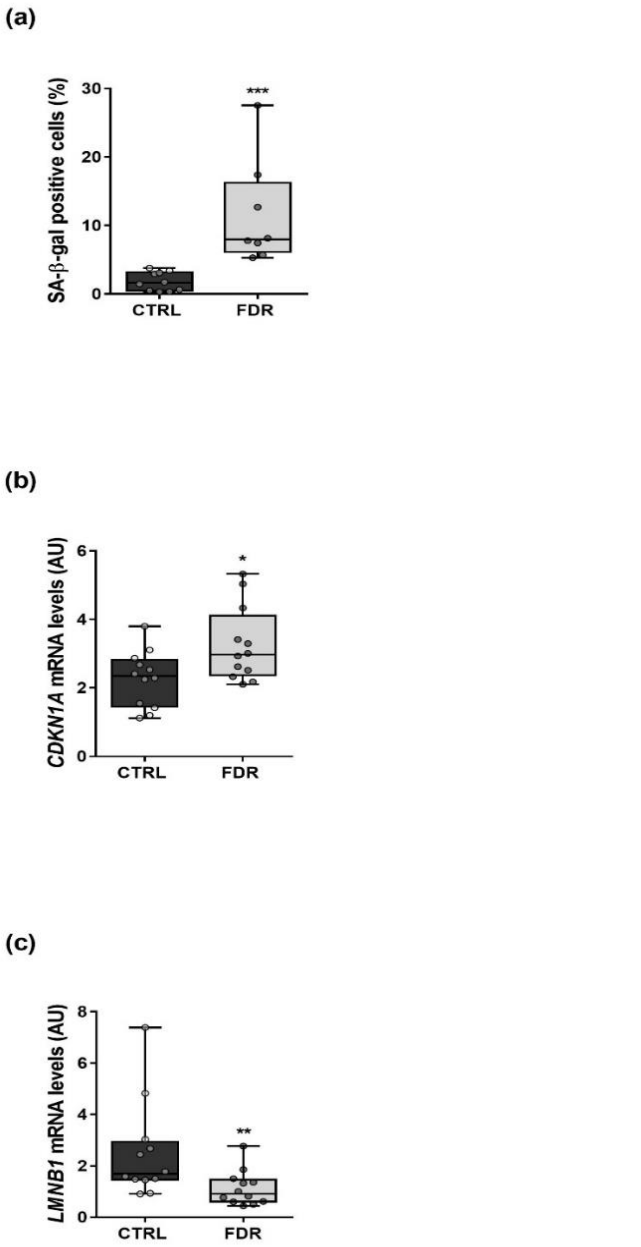

FIGURE 7. Senescence markers in APCs from FDRs and CTRLs. (**a**) Flow cytometric detection of the SA-β-gal-positive cells in APCs from FDR (n = 8) and CTRL (n = 10) subjects available from our study cohort. Values are presented as percentage (%). The mRNA levels of CDKN1A (**b**) and LMNB1 (**c**) were measured by qPCR and normalized to RPL13A expression in APCs from FDR (n = 12) and CTRL (n = 12) subjects. Values are presented as absolute units (AU). (**a-c**) Data are shown as boxplots (min-max) with all individual values. Significance was determined by Mann–Whitney test (**a, c**) or unpaired Student's *t*-test (b). **p* < 0.05, ***p* < 0.01, ****p* < 0.001 *vs* CTRLs

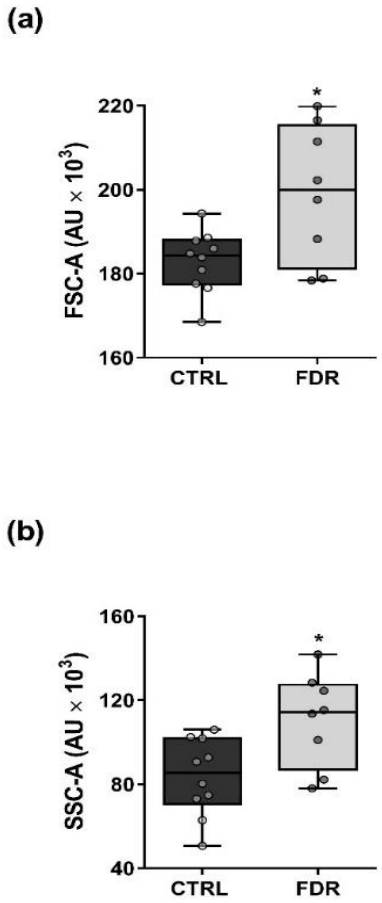

FIGURE 8. Flow cytometry analysis of forward scattering (FSC-A) and side scattering (SSC-A) in APCs from FDR and CTRL subjects. Flow Cytometric detection of FSC-A (**a**) and SSC-A (**b**) to illustrate size and cytoplasm vacuolization, respectively, of APCs from FDR (n=8) and control (CTRL; n=10) subjects available from our study cohort. (**a, b**). All values are expressed as arbitrary units (AU x 10^3). Data are shown as boxplots (mini-max) with all individual values. Significance was determined by unpaired Student's *t*-test. $^*p<0.05$ *vs* CTRLs

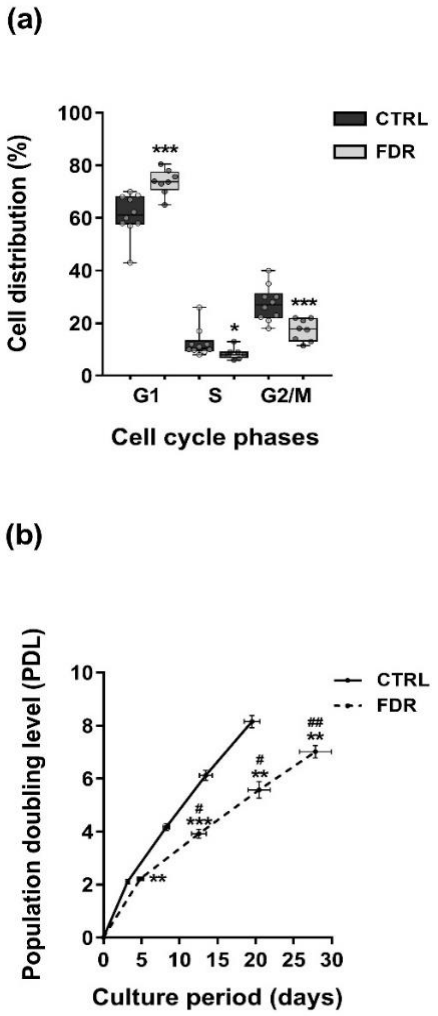

FIGURE 9. Cell Cycle and population doubling rate analyses in APCs from FDR and CTRL subjects. (a) Flow Cytometric detection of cell cycle distribution of APCs from FDR (n=8) and control (CTRL=10) subjects available from our study cohort. 1 x 10^4 cells were quantified per each sample. Data are shown as boxplots (mini-max) with all individual values and represent the percentage of APCs in G1, S, and G2/M phases. Significance was determined by Mann Whitney test. $^{*}p<0.05$, $^{***}p<0.001$ *vs* CTRLs. (**b**). The indicated cells were plated at an initial density of 3x 10^4 and allowed to grow to 70%-80% confluence for the time indicated before counting. Cells were replated at the same density at each point on the curve. Each culture was maintained for 4 passages. Population doubling level (PDL) and doubling times were calculated at the end of each passage. PDL= (logN -log N0)] + X, where N represents the cell yield at the point, N0 represents the cell number used as inoculum to begin that subculture, and X=the doubling level of the inoculum used to initiate the subculture being quantitated. Data shown are the mean ± SEM of biologically independent APC samples from FDR (n=8) and CTRL (N=10) subjects available from our study cohort. Significance was determined by Mann Whitney test. $p<0.01$, $^{***}p<0.001$ *vs* culture period in CTRLs; $^{\#}p<0.05$, $^{\#\#}p<0.01$ *vs* PDL in CTRLs.

Table 3. SASP factor protein levels in the media conditioned by FDR and CTRL APCs.

Variables	*FDR APCs*	*CTRL APCs*	*p value*
IL6 (pg/ml/10^5 cells)	**1099.0 [809.1; 1171.0]**	**193.0 [60.2; 633.0]**	***0.0021***
MCP1 (pg/ml/10^5 cells)	**118.0 [82.2; 245.0]**	**42.0 [12.4; 117.1]**	***0.0430***
RANTES (pg/ml/10^5 cells)	**6.4 [2.6; 7.7]**	**1.6 [0.3; 3.0]**	***0.0165***
IL8 (pg/ml/10^5 cells)	**112.0 [49.3; 340.6]**	**30.0 [15.7; 60.7]**	***0.0260***
MIP1b (pg/ml/10^5 cells)	**1.0 [1.8;3.8]**	**0.9 [0.3; 1.9]**	***0.0322***
EOTAXIN (pg/ml/10^5 cells)	**0.5 [0.3; 2.3]**	**0.4 [0.1; 1.0]**	**0.2735**
FGF (pg/ml/10^5 cells)	**5.9 [4.6; 7.3]**	**3.9 [1.8; 6.2]**	**0.1522**
G-CSF (pg/ml/10^5 cells)	**24.5 [15.8; 36.1]**	**7.4 [4.3; 90.5]**	**0.3042**
IFNɣ (pg/ml/10^5 cells)	**5.7 [3.4; 6.1]**	**3.9 [0.9; 7.7]**	**0.2370**
VEGF (pg/ml/10^5 cells)	**80.3 [29.5; 135.3]**	**55.4 [30.7; 140.9]**	**0.6170**
TNFα (pg/ml/10^5 cells)	**1.7 [0.7; 2.7]**	**0.7 [0.1; 2.6]**	**0.2646**
IL15 (pg/ml/10^5 cells)	**68.5 [43.7; 94.7]**	**37.0 [23.5; 72.1]**	**0.1220**

SASP factor protein levels in the media conditioned by FDR (*n*=8) and CTRL (*n*=10) APCs were measured by multiplex assay and normalized by cell number. Detectable APC-released SASP factors are reported. Results are shown as median [first quartile-Q1; third quartile-Q3] and compared between groups using Mann Whitney test. *p* value *vs* CTRL APCs. FDRs, first-degree relatives of T2D subjects; CTRLs, subjects with no diabetes familiarity; APCs, adipose precursor cells; IL, interleukin; MCP1, monocyte chemotactic protein 1; RANTES, regulated on activation normal T-cell-expressed and -secreted; MIP1b, macrophage inflammatory protein 1 beta; FGF, fibroblast growth factor; G-CSF, granulocyte-colony stimulating factor; IFNɣ, interferon gamma; VEGF, vascular endothelial cell growth factor; TNFα, tumour necrosis factor alpha.

3.2 The role of *ZMAT3* in premature senescence of FDR APCs

We focused on the RNA-binding protein ZMAT3 to gain new insight into the potential mechanisms responsible for the senescence phenotype displayed by APCs from FDR subjects because its role in senescence, ageing, and age-related diseases is well-established (Dong et al., 2018; Kim et al., 2017). In addition, our previous MeDIP-Seq study in APCs from these same FDR subjects (Parrillo et al., 2020) have identified a CpG island in the intronic *chr3:179032279-179033001* region at the *ZMAT3* gene showing significant hypomethylation compared to CTRL individuals, providing a potential basis for altered *ZMAT3* gene transcription in FDRs. To address this issue, bisulphite sequencing was used to confirm that the DNA methylation level at this *ZMAT3* region is significantly lower in FDR compared to CTRL APCs (Fig.10a). Consistently, as shown in Fig.10b,c, FDR subjects had increased ZMAT3 expression at both the mRNA and protein levels. The SA-β-gal senescence marker strongly correlated with *ZMAT3* DNA methylation, mRNA and protein levels in both FDR and CTRL subjects (Fig.10d-f). Overall, these findings raised the possibility that epigenetic dysregulation of *ZMAT3* is involved in the early APC senescence observed in subjects who are FDRs of T2D patients.

3.3 Functional analysis of the *ZMAT3* intronic region

To confirm the regulatory role of CpG island in the intronic *chr3:179032279-179033001 ZMAT3* region, we have cloned the region in both the forward and reverse orientations in a luciferase reporter vector. The constructs were either methylated in vitro or mock-treated (un-methylated) before being transfected into HEK-293 cells. Subsequent analysis revealed that the un-methylated construct containing the *ZMAT3* intronic differentially methylated region (DMR) had higher luciferase activity in both forward and reverse orientations compared to the mock-treated empty vector (Fig.10g,h). Importantly, when *in vitro* methylated, both of these constructs showed reduced transcriptional activity (Fig.10g,h), indicating that the intronic DMR functions as a DNA methylation-sensitive region regulating *ZMAT3* transcription. To further test if, in the APCs, methylation-induced changes in *ZMAT3* transcription associate with premature senescence in APCs, we have exposed the cells from CTRL subjects to 5-azacytidine (5-AZA). This hypomethylating agent has been previously shown to induce senescence in both human primary cells and cancer cell lines (So et al., 2011). After treatment with 10 μM 5-AZA for 72 hours, more than 10% of APCs became positive for SA-β-gal (Fig.11a). 5-AZA had a similar effect on these cells as the senescence inducer hydrogen peroxide, which was used as a positive control for stress-induced premature senescence (Chen et al., 2007). Interestingly, the appearance of senescence in 5-AZA-treated APCs was accompanied by decreased DNA methylation at the *ZMAT3* intronic DMR (Fig.11b) and upregulation of *ZMAT3* expression

(Fig.11c,d), implying a causal link between epigenetic dysregulation of *ZMAT3* and early APC senescence. To demonstrate that 5-AZA-induced senescence is caused, at least in part, by upregulation of *ZMAT3*, we knocked down its expression in CTRL APCs, followed by 5-AZA treatment. As shown in Fig.12, following 5-AZA exposure, a higher percentage of senescent cells was detected. This effect was significantly reduced by siRNA-mediated *ZMAT3* knockdown, supporting the hypothesis that decreased *ZMAT3* methylation increases its expression and causes premature senescence in APCs.

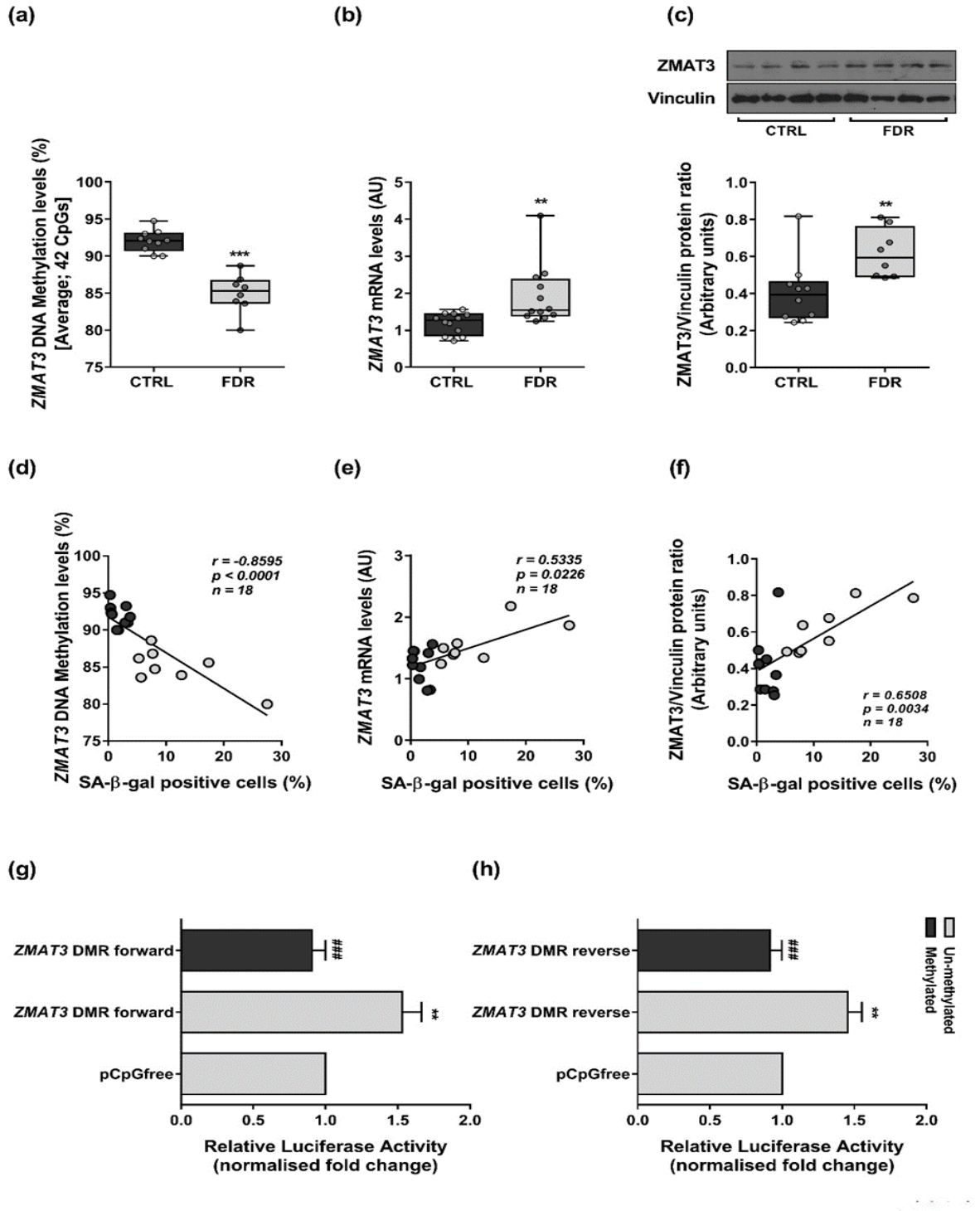

FIGURE 10. DNA methylation and expression of *ZMAT3* in APCs from FDRs and CTRLs. (**a**) Changes in average DNA methylation levels at 42 CpGs within the *ZMAT3* DMR were detected by bisulfite sequencing (BS) in APCs from FDR (*n*=8) and CTRL (*n*=10) subjects available from our study cohort. (**b**) The *ZMAT3* mRNA levels were measured by qPCR and normalized to *RPL13A* expression in APCs from FDR (*n*=12) and CTRL (*n*=12) subjects. Data are presented as absolute units (AU). (**c**) The ZMAT3 protein levels were assessed by Western blot in APCs from FDR (*n*=8) and CTRL (*n*=10) subjects available from our study cohort. Vinculin served as a loading control. The upper figure shows representative blots; the lower figure shows result quantitation. (**a**-**c**) Data are shown as boxplots (min-max) with all

individual values. Significance was determined by unpaired Student's *t*-test (**a**) or Mann Whitney test (**b,c**). ***p*<0.01, ****p*<0.001 *vs* CTRLs. (**d-f**) Correlation between the percentage of SA-β-gal-positive cells and *ZMAT3* DNA methylation or mRNA or protein levels in the same APC samples from FDRs and CTRLs. Spearman's correlation coefficient *r*, *p*-value and number of samples (*n*) are indicated in the graph. Dark gray circles represent CTRLs, light gray circles represent FDRs. (**g**,**h**) The *ZMAT3* DMR was cloned into a luciferase reporter vector devoid of CpGs in both forward (*ZMAT3* DMR forward) and reverse (*ZMAT3* DMR reverse) orientations. These constructs were either methylated or mock-treated (un-methylated). The results were normalized using a co-transfected renilla luciferase control vector and are presented as fold change relative to the mock-treated empty vector (pCpGfree). Data are shown as mean ± SEM of three independent experiments. Significance was determined by one-way repeated measures ANOVA followed by Tukey's multi-comparison test. ***p*<0.01 *vs* pCpGfree; $^{\#\#\#}p$<0.001 *vs* un-methylated *ZMAT3* DMR forward (**g**) or un-methylated *ZMAT3* DMR reverse (**h**)

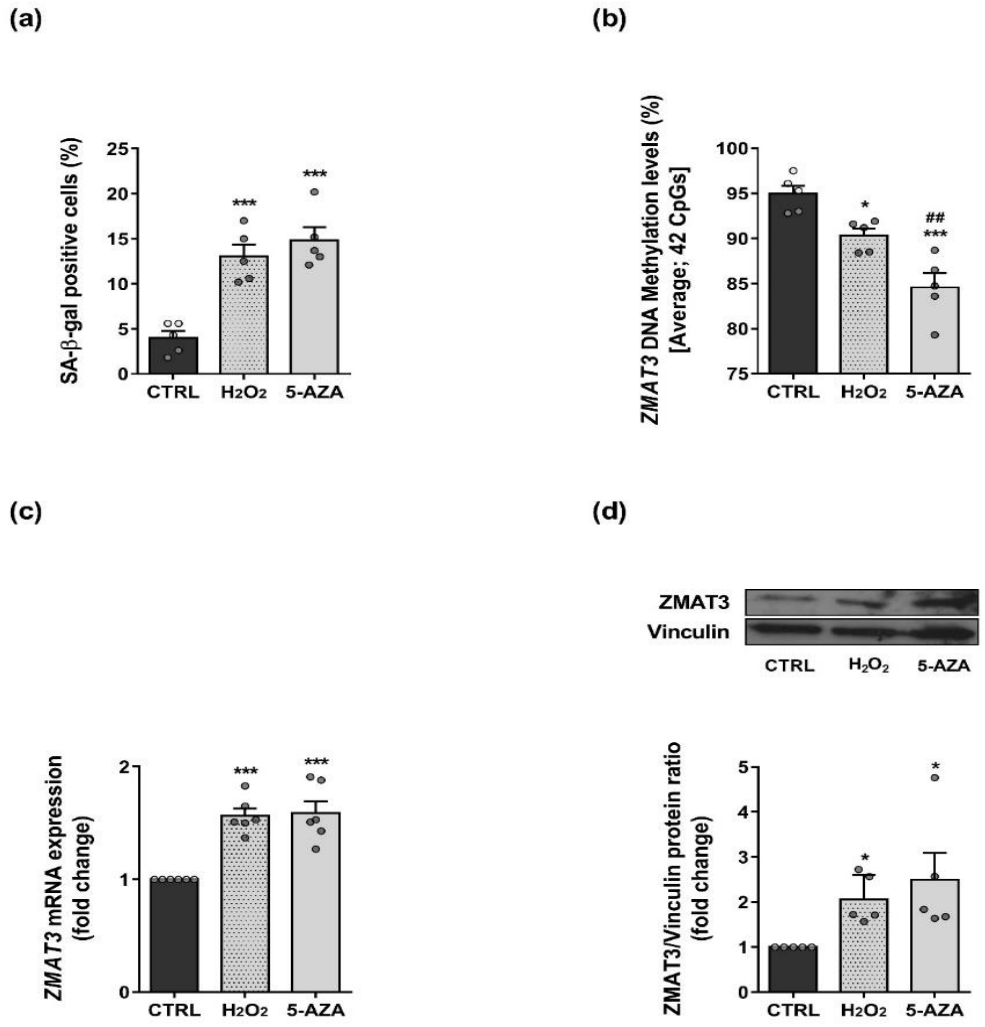

FIGURE 11. Effect of 5-AZA on both senescence induction and *ZMAT3* epigenetic regulation in CTRLs APCs. APCs from CTRL subjects (n=5) were treated with or without 10 µM 5-AZA for 72 h. Treatment with 200 µM hydrogen peroxide (H_2O_2) was used as positive control for stress-induced premature senescence. (**a**) Flow cytometric detection of the SA-β-gal-positive cells in APCs treated with or without 5-AZA or H_2O_2. Values are presented as percentage (%). (**b**) Changes in average DNA methylation levels at 42 CpGs within the *ZMAT3* DMR were detected by BS in APCs treated with 5-AZA or H_2O_2 compared to un-treated APCs (CTRLs). (**c**) The fold change of mRNA expression of *ZMAT3* was measured by qPCR. Expression was normalized first to *RPL13A* and the to expression in un-treated APCs (CTRLs). (**d**) The fold change of protein expression of ZMAT3 was assessed by Western Blot in APCs treated with 5-AZA or H_2O_2 compared to un-treated APCs (CTRLs). Vinculin served as a loading control. The upper figure shows representative blots; the lower figure presents result quantitation. (**a-d**) Data are shown as mean ± SEM of five biologically independent APC samples randomly selected in the CTRL group. Data represent individual level data. Significance was determined by one-way repeated measures ANOVA followed by Tukey's multi-comparison test. *p<0.05, ***p<0.001 vs un-treated APCs (CTRLs); $^{\#\#}p$<0.01 vs H_2O_2-treated APCs.

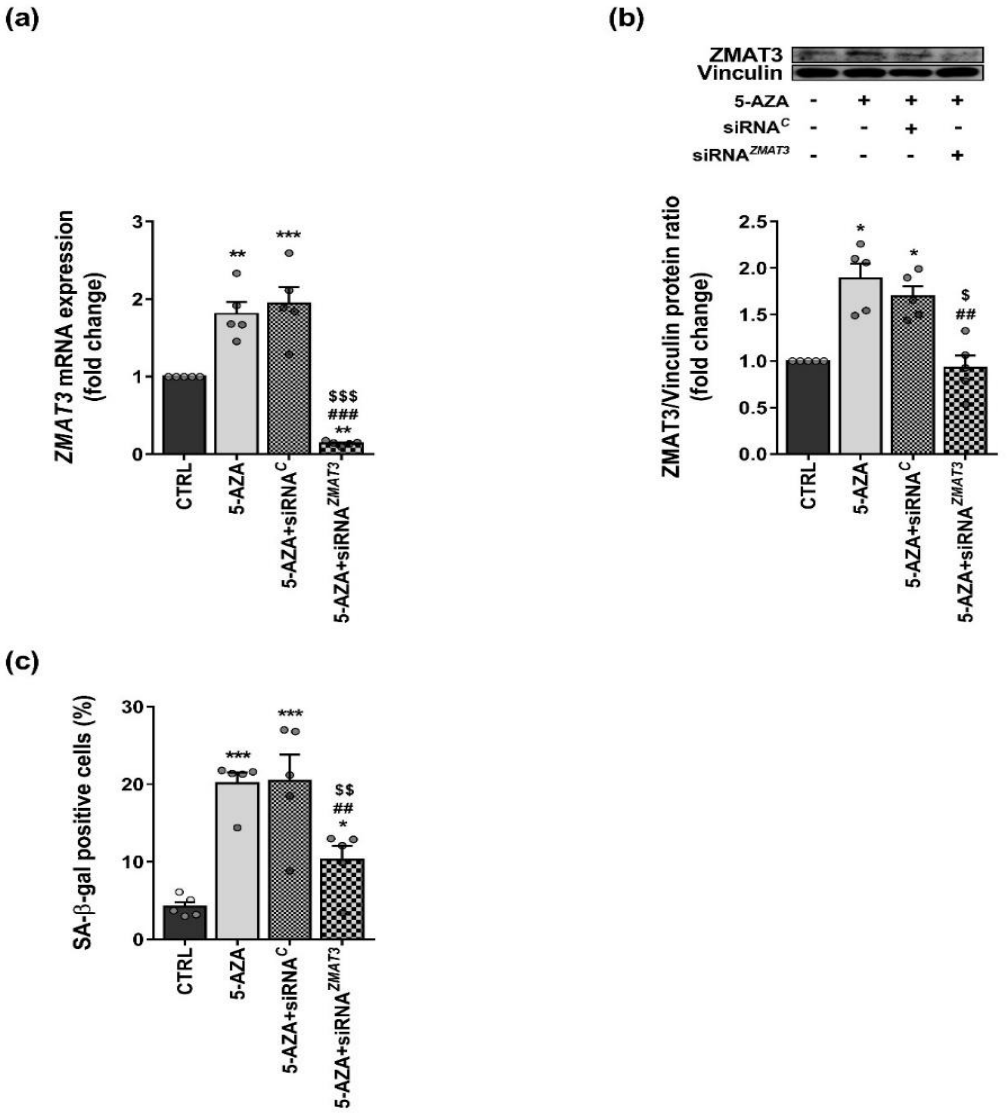

FIGURE 12. Effect of siRNA-mediated silencing of *ZMAT3* on 5-AZA induced senescence in CTRL APCs. APCs from CTRL subjects (n=5) were treated for 72h with or without 10μM 5-AZA in the absence or in presence of 25 pmol of siRNA targeting ZMAT3 (siRNA ^{ZMAT3}) or scrambled siRNA (siRNA^{C}). (**a**) The fold change of mRNA expression of *ZMAT3* was measured by Qpcr. Expression was normalized first to *RPL13A* and the to expression in un-treated APCs (CTRLs). (**b**) The fold change of protein expression of *ZMAT3* was assessed by Western Blot in APCs treated with 5-AZA compared to un-treated APCs (CTRLs). Vinculin served as a loading control. The upper figure shows representative blot; the lower figure presents result quantitation. (**c**) Flow cytometric detection of SA-β-gal-positive cells. Values are presented as percentage (%). (**a-c**) Data are shown as mean ± SEM of five biologically independent APC samples randomly selected in the CTRL group. Dots represent individual level data. Significance was determined by one-way repeated measures ANOVA followed by Tukey's multi-comparison test. $^{*}p<0.05$, $^{**}p<0.01$, $^{***}p<0.001$ vs un-treated APCs (CTRLs); $^{\#\#}p<0.01$, $^{\#\#\#}p<0.001$ vs 5-AZA-treated APCs; $^{\$}P<0.05$, $^{\$\$}p<0.01$, $^{\$\$\$}p<0.001$ vs 5-AZA+siRNA ^{C}-treated APCs.

3.4 Senescence induction by *ZMAT3* overexpression in human APCs

To directly demonstrate whether *ZMAT3* enhanced expression causes senescence in human preadipocytes, we transfected the pCMV6-*ZMAT3* construct in APCs from donors with no diabetes familiarity. This procedure resulted in a 2-fold increase in ZMAT3 protein levels after 72 hours (Fig.13a). This increase was comparable to that seen in APCs from FDR subjects and was large enough to cause cell senescence, as evidenced by a threefold increase in the percentage of SA-β-gal positive APCs (Fig.13b). In cells transfected with the pCMV6-*ZMAT3* construct, mRNA levels of *CDKN1A* were consistently increased while those of *LMNB1* were significantly reduced (Fig.13c). The levels of the major SASP components IL6 (mRNA and protein), MCP1 (mRNA and protein), and MIP1b (protein) were also significantly enhanced in these cells (Tab.4; Fig.14), identifying a SASP pattern in *ZMAT3* overexpressing APCs similar to that observed in APCs from FDR subjects.

Next, we wanted to figure out how *ZMAT3* causes senescence in APCs. ZMAT3 has been shown to inhibit *TP53* mRNA deadenylation, resulting in *TP53* mRNA stabilization and, as a result, increased P53 protein expression (Vilborg et al., 2009). Interestingly, 5-AZA-induced ZMAT3 upregulation was accompanied by an increase in P53 expression, which was reversed by siRNA-mediated *ZMAT3* silencing (Fig.15). Furthermore, overexpression of *ZMAT3* in APCs from CTRL donors increased P53 mRNA and protein levels (Fig.13a,c), supporting the hypothesis that ZMAT3 mediated APC senescence via P53. Interestingly, a significant upregulation of P53 was detected also in FDR APCs compared to CTRL APCs (Fig.13d; Fig.16). The protein levels of ZMAT3 significantly correlated with the P53 mRNA and protein levels in the same APC samples from FDR and CTRL subjects (Fig.17a,b), supporting upregulation of P53 by ZMAT3 also in FDR individuals. The evidence that the mRNA levels of the p21-encoding *CDKN1A* gene, a pro-senescence mediator of p53, increased in both *ZMAT3* overexpressing APCs and FDR APCs, led us to investigate the possibility that *ZMAT3* acts through the p53/p21 pathway. To explore this further hypothesis, we examined whether upregulation of ZMAT3 causes activation of a validated P53 response element (RE) in the upstream regulatory region of the *CDKN1A* promoter (el-Deiry et al., 1993; Laptenko et al., 2011). To this end, we cloned the *CDKN1A* promoter region (-2297 to -2207 bp upstream the TSS) containing the P53 RE (-2281 to -2261 bp upstream the TSS) in a reporter gene plasmid to perform luciferase assays. Furthermore, the *CDKN1A* reporter construct was mutagenized at the invariant G/C basepairs within the P53 RE, to prevent P53 from binding to this nucleotide sequence (Fig.18a). The wild-type or mutagenized *CDKN1A* reporter construct was transfected in APCs from CTRL donors, and promoter activity was assessed in the absence or presence of the pCMV6-*TP53* expression vector (Fig.18b). P53 overexpression significantly increased the luciferase activity of the wild-type *CDKN1A* reporter

construct but did not affect that of the mutagenized *CDKN1A* reporter construct (Fig.18c), confirming that P53-dependent transactivation of the *CDKN1A* promoter was effectively prevented by point mutations in the P53 RE. Subsequently, the wild-type or the mutated *CDKN1A* reporter construct was co-transfected in CTRL APCs with the pCMV6-*ZMAT3* expression vector. P53 upregulation following *ZMAT3* overexpression (Fig.12d) resulted in increased luciferase activity of the wild-type *CDKN1A* reporter construct, while this effect was completely lost when the P53 RE in the *CDKN1A* reporter construct was mutagenized (Fig.18e), indicating that *ZMAT3* promotes the transcriptional activation of *CDKN1A* by P53. To strengthen this finding, we analysed the P53 occupancy at the same *CDKN1A* promoter region in *ZMAT3* overexpressing APCs. Chromatin immunoprecipitation (ChIP) experiments revealed that *ZMAT3* overexpression increased the binding of P53 at the *CDKN1A* promoter (Fig.13e), confirming that ZMAT3 regulates *p21* expression at the transcriptional level by increasing the capability of P53 to bind its RE within the *CDKN1A* promoter. Consistently, we also found a 2-fold increase in P53 abundance at the *CDKN1A* promoter in the FDR compared to the CTRL APCs (Fig.13f). Interestingly, the P53 binding at the *CDKN1A* promoter positively correlated with the *CDKN1A* mRNA levels in the same APC samples from FDR and CTRL subjects (Fig.19), supporting that transcription of *CDKN1A* in FDR APCs was enhanced by P53. To verify that activation of the p53/p21 pathway is necessary for the induction of senescence by ZMAT3, we blocked the transcriptional activity of P53 using the specific inhibitor pifithrin alpha (PFTα) (Sohn et al., 2009). To this end, we transfected the pCMV6-*ZMAT3* construct in APCs from subjects with no diabetes familiarity in the presence or the absence of 50 nM PFTα. As shown in Fig.20, the levels of *CDKN1A* mRNA and the percentage of SA-β-gal positive cells were significantly lower in the presence of PFTα, indicating that the p53/p21 pathway plays a major role in the *ZMAT3*-induced senescence in APCs. Overall, these results indicated that *ZMAT3* causes APC senescence through the p53/p21 pathway.

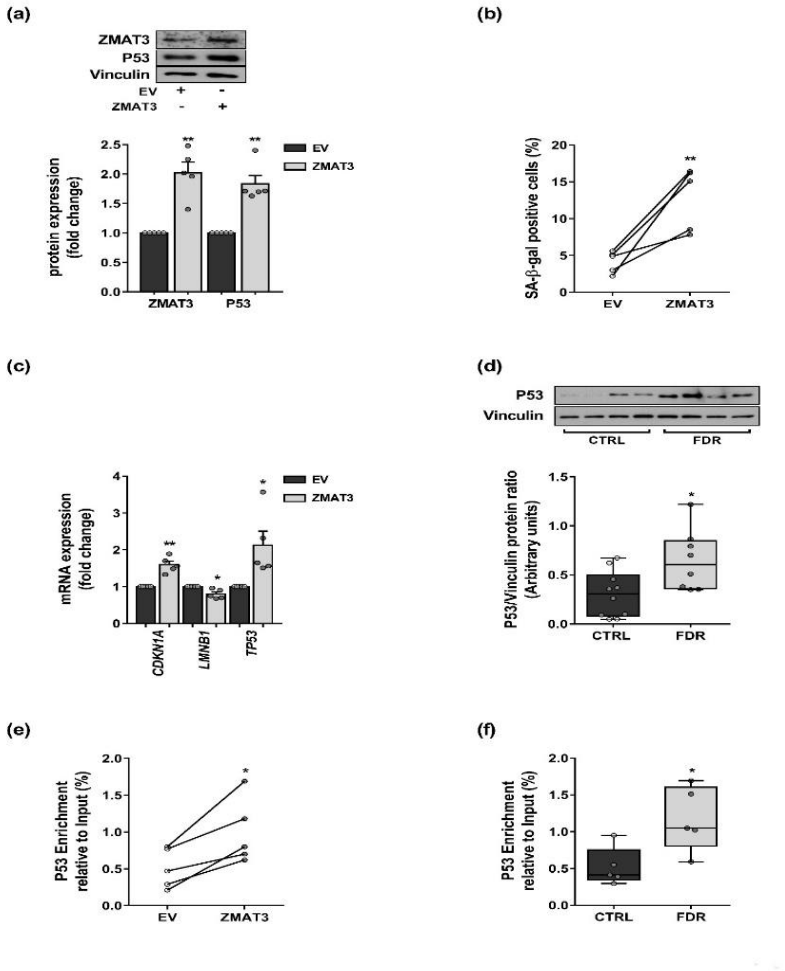

Figure 13. Mechanism of senescence in *ZMAT3* overexpressing APCs. (**a**-**c**,**e**) Five biologically independent APC samples randomly selected in the CTRL group were transfected with the pCMV6-*ZMAT3* expression vector (ZMAT3) or the empty vector (EV). (**a**) The fold change of ZMAT3 and P53 proteins was assessed by Western blot in ZMAT3- *vs* EV-transfected APCs. Vinculin served as a loading control. The upper figure shows representative blots; the lower figure shows result quantitation. (**b**) Flow cytometric detection of the SA-β-gal-positive cells in ZMAT3- or EV-transfected APCs. Values are presented as percentage (%). (**c**) mRNA levels of *CDKN1A*, *LMNB1* and *TP53* were measured by qPCR and are presented as fold change in figure. mRNA expression was normalized first to *28S* and then to expression in EV-transfected APCs. (**d**) The P53 protein levels were assessed by Western blot in APCs from FDR (n=8) and CTRL (n=10) subjects available from our study cohort. Vinculin served as a loading control. The upper figure shows representative blots; the lower figure shows result quantitation. (**e,f**) ChIP analysis for P53 binding at the *CDKN1A* promoter region containing the validated P53 RE in ZMAT3- or EV-transfected APCs and APCs from FDR (n=5) and CTRL (n=5) subjects randomly selected in each study group. Results are expressed as per cent enrichment relative to input DNA. (**a**,**c**) Data are shown as mean ± SEM. Dots represent individual level data. (**b**,**e**) Data are shown as scatterplot with lines joining paired points. (**a**-**c**,**e**) Significance was determined by paired Student's *t*-test. *p<0.05, **p<0.01 *vs* EV. (**d**,**f**) Data are shown as boxplots (min-max) with all individual values. Significance was determined by unpaired Student's *t*-test. *p<0.05 *vs* CTRLs

Table 4. SASP factor levels in the media conditioned by *ZMAT3* overexpressing APCs

Variables	*ZMAT3*	*EV*
IL6 (pg/ml/10^5 cells)	*1509.0 ± 476.1**	*150.2 ± 147.9*
MCP1 (pg/ml/10^5 cells)	*186.6 ± 47.0**	*82.9 ± 31.8*
RANTES (pg/ml/10^5 cells)	*441.6 ± 170.5*	*124.1 ± 42.8*
IL8 (pg/ml/10^5 cells)	*1452.0 ± 646.3*	*80.5 ± 33.6*
MIP1b (pg/ml/10^5 cells)	*12.1 ± 2.3**	*4.2 ± 1.4*

SASP factor protein levels in the media conditioned by APCs from CTRL donors (*n*=5) transfected with the pCMV6-*ZMAT3* expression vector (ZMAT3) or an equimolar amount of thepCMV6 empty vector (EV) were measured by a custom multiplex assay and normalized by cellnumber. All data shown are the mean ± SEM of five biologically independent APC samples randomly selected in the CTRL group. Significance was determined by paired Student's *t*-test. **p*<0.05 *vs* EV. IL, interleukin; MCP1, monocyte chemotactic protein 1; RANTES, regulated on activation normal T-cell-expressed and -secreted; MIP1b, macrophage inflammatory protein 1 beta

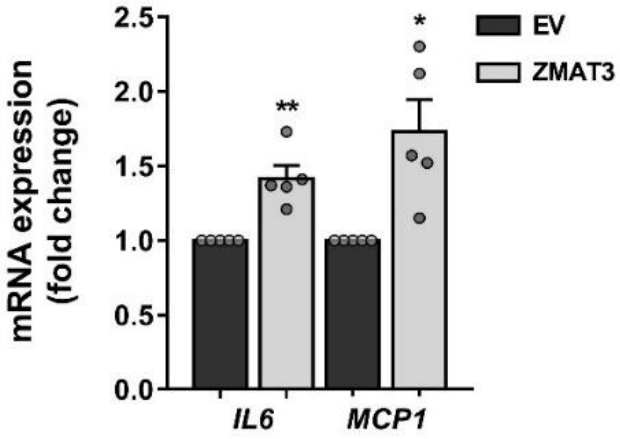

Figure 14. mRNA expression of SASP components in *ZMAT3* overexpressing APCs. APCs from CTRL donors (*n*=5) were transfected with the pCMV6-*ZMAT3* expression vector (ZMAT3) or the pCMV6 empty vector (EV). After 72 hours, APCs were analyzed for expression of SASP factors. mRNA levels of *IL6* and *MCP1* were measured by qPCR and presented as fold change in figure. mRNA expression was normalized first to *28S* and then to expression in EV-transfected APCs. Data are shown as mean ± SEM of five biologically independent APC samples randomly selected in the CTRL group. Dots represent individual level data. Significance was determined by paired Student's t-test. *p<0.05, **p<0.01 vs EV

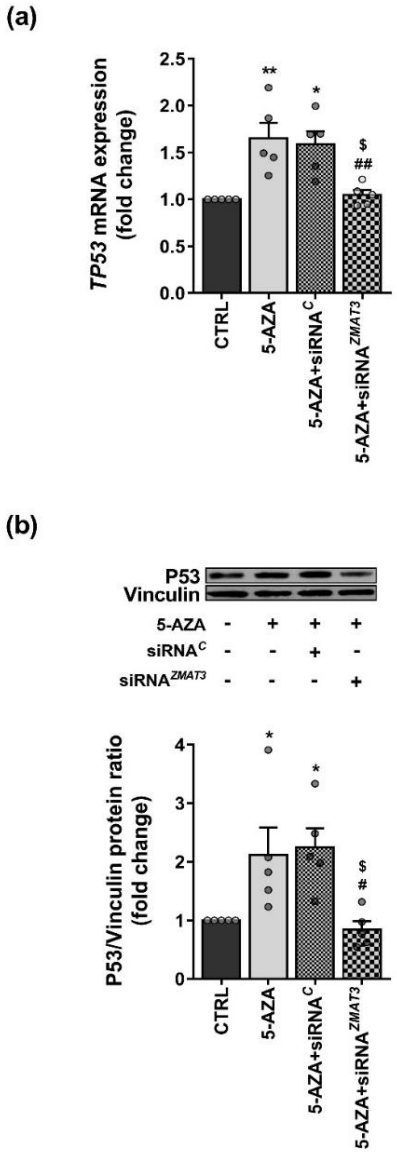

Figure 15. Effect of siRNA-mediated silencing of *ZMAT3* on 5-AZA induced upregulation of the *TP53* gene in CTRL APCs. APCs from CTRL donors (n=5) were treated for 72 hours with or without 10 µM 5-AZA in the absence or in presence of 25 pmol of siRNA targeting *ZMAT3* (siRNA ^{ZMAT3}) or scrambled siRNA (siRNA ^{C}). (**a**) The fold change of mRNA expression of *TP53* was measured by qPCR. Expression was normalized first to *RPL13A* and the to expression in un-treated APCs (CTRLs). (**b**) The fold change of protein expression of P53 was assessed by Western Blot in APCs treated with 5-AZA compared to un-treated APCs (CTRLs). Vinculin served as a loading control. The upper figure shows representative blot; the lower figure presents result quantitation. (**a,b**) Data are shown as mean ± SEM of five biologically independent APC samples randomly selected in the CTRL group. Dots represent individual level data. Significance was determined by one-way repeated measures ANOVA followed by Tukey's multi-comparison test. $^{*}p<0.05$, $^{**}p<0.01$ vs un-treated APCs (CTRLs); $^{\#}p<0.05$, $^{\#\#}p<0.01$ *vs* 5-AZA-treated APCs; $^{\$}P<0.05$ *vs* 5-AZA+ siRNA ^{C}- treated APCs

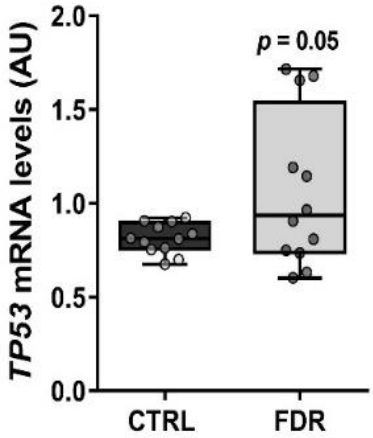

Figure 16. mRNA expression of *TP53* gene in APCs from FDR and CTRL subjects. The *TP53* mRNA levels were measured by qPCR and normalized to *RPL13* expression in APCs from FDR (*n*=12) and CTRL (*n*=12) subjects. Values are shown as absolute units (AU). Data are shown as boxplots (min-max) with all individual values. Significance was determined by unpaired Student's t-test. P-value *vs* CTRLs

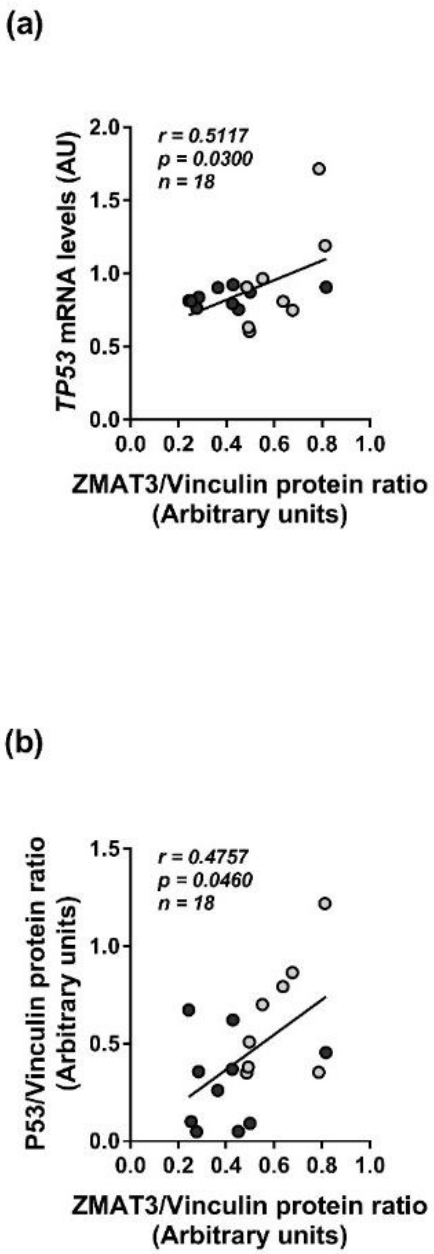

Figure 17. Correlation analyses in APCs from FDR and CTRL subjects. Correlation between the ZMAT3 protein levels and *TP53* mRNA levels (**a**) or P53 protein levels (**b**) in the same APC samples from FDR (*n*=8) and CTRL (*n*=10) subjects. (**a,b**) Spearman's correlation coefficient *r*, *p*-value and number of samples (*n*) are indicated in the graph. Dark gray circles represent CTRLs while light gray circles represent FDRs

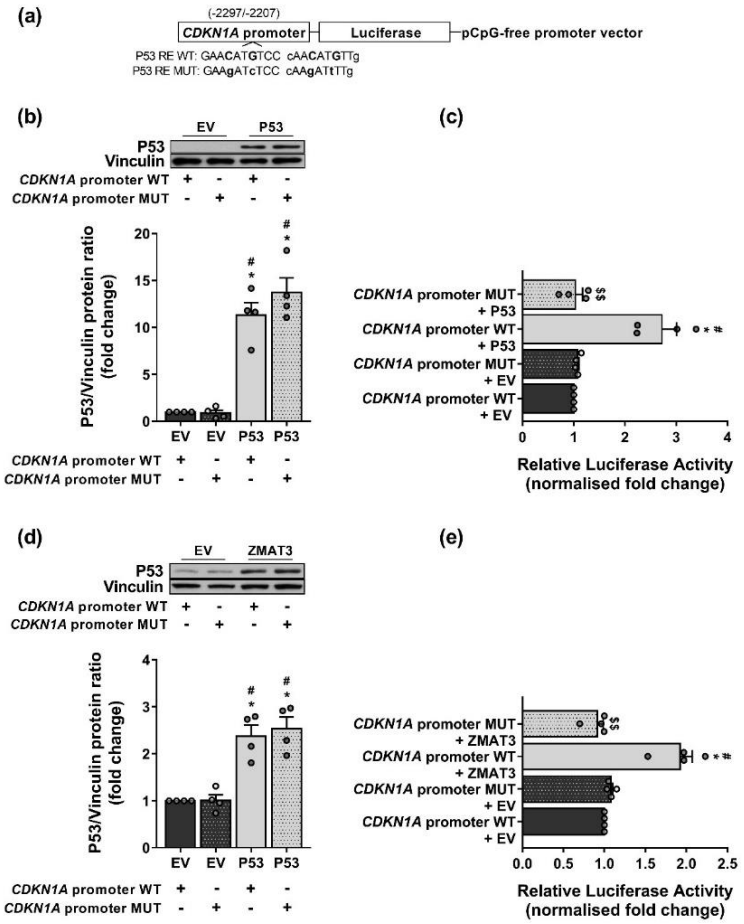

Figure 18. ZMAT3 induces P53-mediated transactivation of the *CDKN1A* promoter. (a) Schematic diagram showing the structure of *CDKN1A* reporter construct. The *CDKN1A* promoter region (from -2297 to -2207 bp upstream the TSS) containing a validated P53 response element (RE) was cloned into luciferase reporter vector (pGpG-free promoter vector). Residues matching the P53 response RE are in capital, with the invariant C/G basepairs in bold. Residues mutagenized to abolish P53 binding to its RE are in lowercase bold. (**b-e)** The wild-type *CDKN1A* promoter (*CDKN1A* promoter wild-type) or its mutant (*CDKN1A* promoter MUT) construct was co-transfected with the pCMV6 empty vector (EV) in APCs from CTRL donors (*n*=4). (**b** and **d**) The expression of P53 was measured by Western Blot. P53 protein fold changes were assessed in comparison with APCs co-transfected with the cdkn1a promoter WT and EV. Vinculin served as a loading control. The upper figures show representative blots; the lower figure presents result quantitation. (**c** and **e**) Luciferase activity of CDKN1A promoter (WT or MUT) was measured and normalized using a co-transfected renilla Luciferase control vector. Results are presented as fold change relative to APCs co-transfected with the *CDKN1A* promoter WT and EV. (**b-e**) Data are show as mean ± SEM of four biologically independent APC samples randomly selected in the CTRL group. Dots represent individual level data. Significance was determined by one-way repeated measures ANOVA followed by Tukey's multi-comparison test. $^{*}p<0.05$ vs CDKN1A promoter WT + EV; $^{\#}p<0.05$ vs *CDKN1A* promoter MUT+ EV; $^{\$\$}p<0.01$ vs CDKN1A promoter WT+ZMAT3

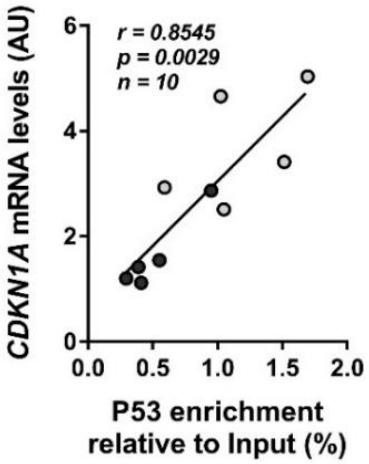

Figure 19. Correlation analyses in APCs from FDR and CTRL subjects. Correlation between the occupancy of P53 at the *CDKN1A* promoter and *CDKN1A* mRNA levels in the same APC samples from FDR (*n*=5) and CTRL (*n*=5) subjects. Spearman's correlation *r*, *p*-value and number of samples (*n*) are indicated in the graph. Dark grey circles represent CTRLs while light gray circles represent FDR.

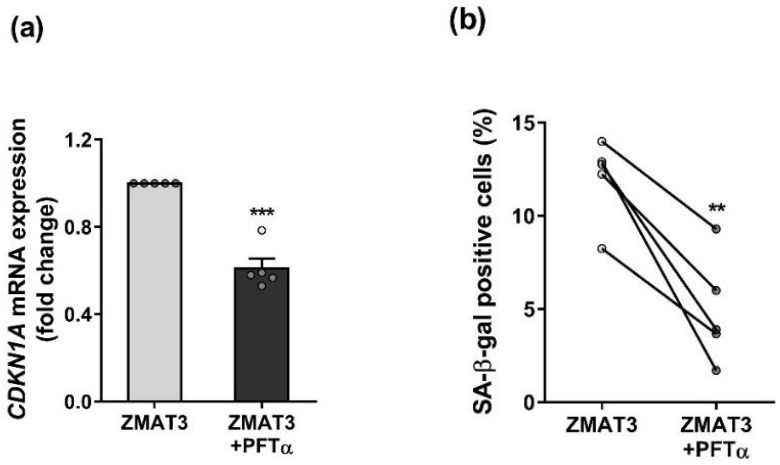

Figure 20. Effect of pifithrin alpha (PTFα) a specific inhibitor of P53, on the ZMAT3-induced APC senescence. Five biologically independent APC samples randomly selected in the CTRL group were transfected with pCMV6-ZMT3 expression vector (ZMAT3) in the presence or absence of 50 nM PTFα for 72h. (**a**) The fold change of the CDKN1A mRNA was measured by qPCR. mRNA expression was normalized first to 28S and then to expression in APCs transfected with ZMAT3 alone. (**b**) Flow Cytometric detection of the SA-β-gal-positive cells in APCs transfected with ZMAT3 alone or ZMAT3 plus PTFα. Values are presented as percentage (%). (**a**) Data are shown as scatterplot with lines joining paired points. (**b**) Data are shown as mean ± SEM. Dots represent individual level data. (**a,b**) Significance was determined by paired Student's *t*-test. $^{**}p<0.01$, $^{***}p<0.001$ *vs* APCs transfected with ZMAT3 alone.

3.5 Adipocyte differentiation of *ZMAT3* overexpressing APCs

Increased APC senescence contributes to the reduced subcutaneous adipogenesis observed in hypertrophic obesity (Gustafson et al., 2019). Non-obese FDR individuals also feature SAT hypertrophy due to impaired differentiation of resident APCs (Arner et al., 2011). Thus, we examined the relationship between APC senescence and adipocyte hypertrophy - as an *in vivo* marker of adipogenic impairment (Henninger et al., 2014) - in the FDR and CTRL subjects of our study cohort. Interestingly, we found that increased percentage of SA-β-gal positive APCs showed a strongly positive correlation with increased subcutaneous adipocyte size (Fig.21), indicating that senescence may be involved in the inability of APCs to undergo differentiation in the FDR subjects as well. Based on this finding, we investigated whether the *ZMAT3*-induced senescence impairs adipogenesis in APCs. Thus, *ZMAT3* overexpressing APCs were subjected to adipogenic differentiation. As shown in Fig.22a,b, after differentiation, these cells accumulated significantly less lipids than EV-transfected APCs, demonstrating that the overexpression of *ZMAT3* in APCs causes senescence and is accompanied by inhibition of adipogenesis. We also examined the ZMAT3 expression in both FDR and CTRL APCs in relation to the ability of these progenitor cells to differentiate. As presented in Fig.22c,d the ZMAT3 protein was increased in poorly differentiated FDR APCs while remaining unchanged in normally differentiated CTRL APCs. Thus, the expression of ZMAT3 needs to be tightly controlled in APCs to preserve their ability to undergo normal adipocyte differentiation. Together, these findings imply that increased ZMAT3 expression in APCs contributes to reduced subcutaneous adipogenesis in FDR subjects by a senescence-dependent mechanism.

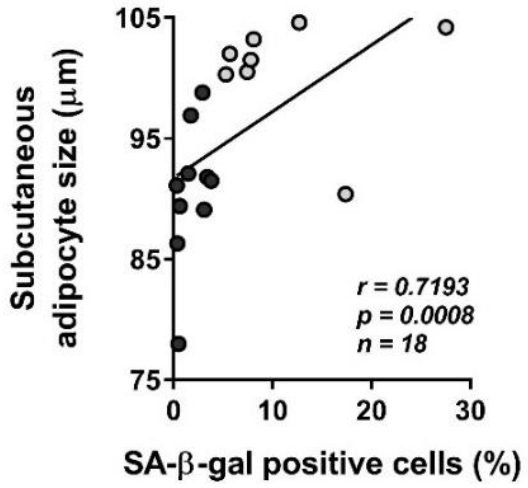

Figure 21. Correlation between the percentage of SA-β-gal positive APCs and subcutaneous adipocyte size in the same FDR (*n*=8) and CTRL (*n*=10) subjects. Spearman's correlation coefficient *r*, *p*-values and number of samples (*n*) are indicated in graph. Dark gray circles represent CTRLs while light gray circles represent FDRs

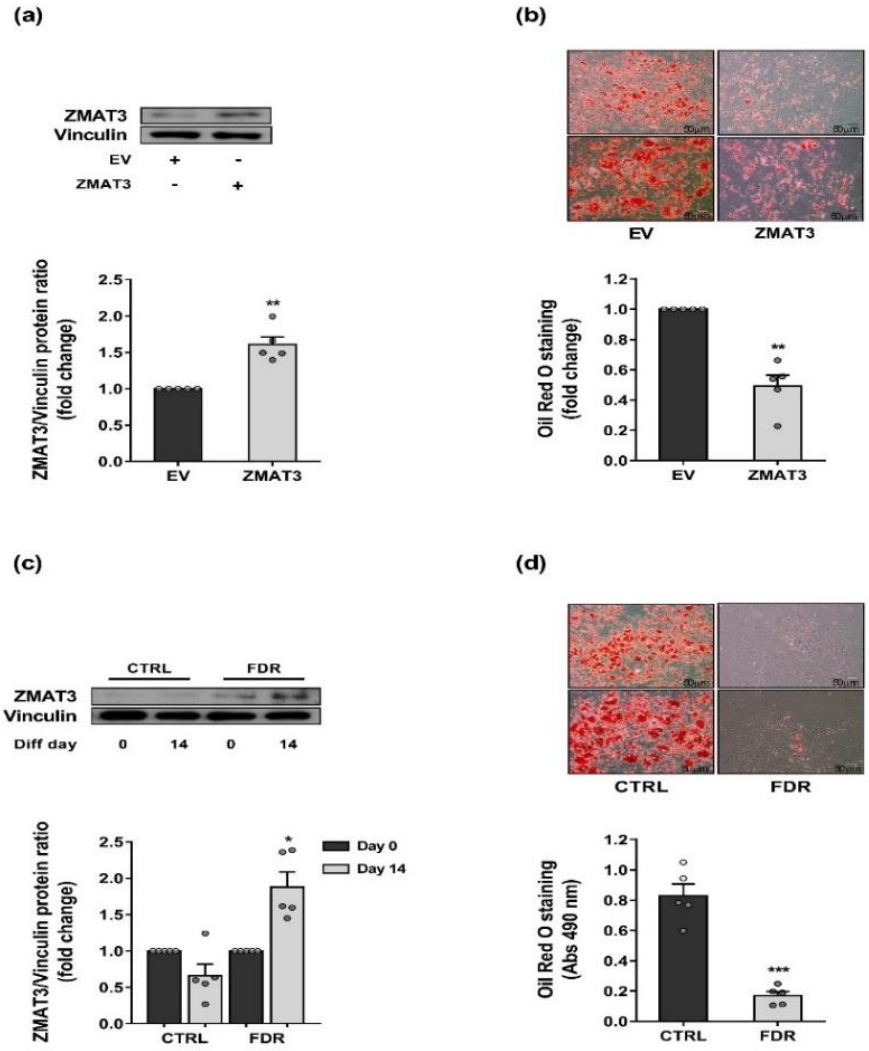

Figure 22. *ZMAT3* upregulation in s is linked to impaired adipogenesis. (**a**,**b**) APCs from CTRL donors (*n*=5) were transfected with the pCMV6-*ZMAT3* expression vector (ZMAT3) or the empty vector (EV) and differentiated for 15 days. (**a**) *ZMAT3* overexpression was confirmed by Western blot in ZMAT3- *vs* EV-transfected APCs at differentiation day 15. The upper figure shows representative blots; the lower figure shows result quantitation. (**b**) Oil Red O staining was used to assess the degree of differentiation. Representative microphotographs showing lipid accumulation of *ZMAT3*- (right) and EV-transfected (left) APCs at differentiation day 15. Upper panel at 10x magnification; bottom panel at 20x magnification. Scale bar 50 μm. Bar graph shows photometric quantification of Oil Red O staining measured at 490 nm. Results are normalized to the absorbance in EV-transfected APCs. (**a**,**b**) Data are shown as mean ± SEM of five biologically independent APC samples randomly selected in the CTRL group. Significance was determined by paired Student's *t*-test. ***p*<0.01 *vs* EV. (**c**,**d**) APCs from FDR (*n*=5) and CTRL (*n*=5) subjects randomly selected in each study group were differentiated for 15 days. (**c**) The fold change of ZMAT3 protein was measured by Western blot in differentiated APCs (diff. day 15) *vs* APCs before adipogenic induction (diff. day 0) in each group. The upper figure shows representative blots; the lower figure shows result quantitation. Data are shown as mean ± SEM. Significance was determined by paired Student's *t*-test. **p*<0.05 *vs* APCs at diff. day 0. (**d**) Oil Red O staining of differentiated APCs from. Representative microphotographs showing lipid accumulation of APCs from FDRs (right) and CTRLs (left) at diff. day 15. Upper panel at 10x magnification; bottom panel at 20x magnification. Scale bar 50 μm. Bar graph shows photometric

quantification of Oil red O staining measured at 490 nm. Data are shown as mean ± SEM. Significance was determined by unpaired Student's *t*-test. ***$p<0.001$ *vs* CTRLs

3.6 Effects of senolytics treatment on *ZMAT3* DNA methylation profile and adipocyte differentiation in FDR APCs

To support the involvement of *ZMAT3* epigenetic dysregulation in senescence induction and the consequent adipogenic impairment in APCs of FDR subjects, we assessed the effects of senolytic combination Dasatinib plus Quercetin (D+Q) on these progenitor cells. D+Q treatment was adopted as this combination has been previously reported to be effective in clearing senescent APCs from mouse and human cell cultures, from old as well as insulin-resistant mice, AT from obese diabetics and individuals with diabetic kidney disease nevertheless preserving viability of cycling-competent cells (Kirkland & Tchkonia, 2020; Zhu et al., 2015). As shown in Fig. 24a, treatment of APCs from FDR subjects with D+Q for 3 days reduced the percentage SA-β-gal positive cells by 60%. This reduction was paralleled by downregulation of both the P53 senescence marker and its target *CDKN1A* gene (Fig.23a,b). We further observed that the SASP factors IL6, MCP1, RANTES, IL8 and MIP1b were lower in the media conditioned by FDR APCs treated with D+Q as compared to the media conditioned by vehicle-treated FDR APCs (Tab.5). Importantly, the removal of senescent cells after D+Q treatment restored higher DNA methylation levels at the *ZMAT3* intronic DMR in FDR APCs (Fig. 24b), while *ZMAT3* expression declined both at mRNA and protein levels in FDR APCs upon D+Q treatment (Fig.24c,d). Thus, in these subjects, hypomethylation of the *ZMAT3* intronic DMR seemed to represent an epigenetic signature of senescent APCs, and senolytic removal of the senescent APCs abrogated this aberrant signature. Finally, we evaluated whether FDR individuals benefit from senotherapy. To this end, we evaluated the ability of FDR APCs to undergo adipocyte differentiation after D+Q treatment. Gene expression of the key adipogenic factor *peroxisome proliferator-activated receptor gamma 2* (*$PPARG_2$*) was increased in the D+Q-treated FDR APCs *versus* vehicle-treated FDR APCs (Fig.23c). Since *$PPARG_2$* is necessary for adipogenesis (Rosen et al., 2000), these data indicated that senolytics improve adipogenic potential of FDRs APCs. To corroborate this evidence, D+Q- and vehicle-treated FDR APCs were then subjected to adipocyte differentiation. As shown in Fig.24e,f, D+Q treatment was capable to improve adipocyte differentiation of FDR APCs. Overall, these data confirmed the direct contribution of senescent APCs to restricted adipogenesis in FDRs and proved that functional impairment of FDR APCs can be reverted by senolytics.

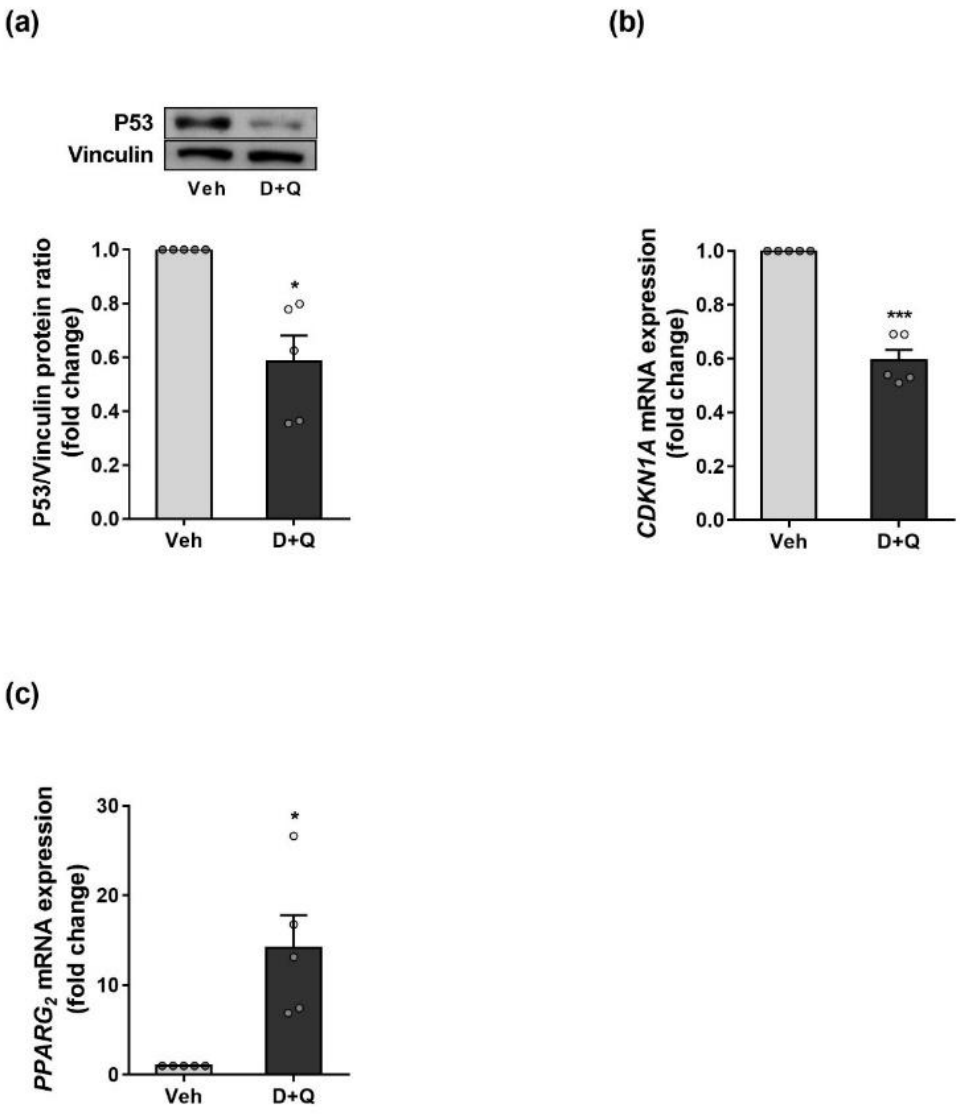

Figure 23. Effects of senolytic combination D+Q on senescence markers and adipogenic potential of FDR APCs. APCs from FDR subjects (*n*=5) were treated with the combination of 0.5 µM Dasatinib and 20 µM Quercitin (D+Q) or vehicle only (Veh)for 72h (**a**) The fold change of protein expression of P53 was assessed by Western Blot in FDR APCs treated with D+Q compared to vehicle-treated FDR APCs. Vinculin served as a loading control. The upper figure shows representative blots which are constructed from the same gel shown in 18**d**; the lower figure is the quantitation of results. The fold change of mRNA expression of *CDKN1A* (**b**) and *PPARG2* (**c**) was measured by qPCR. Expression was normalized first to *RPL13* and the to expression in vehicle-treated FDR APCs. (**a-c**) Data shown are the mean ± SEM of five biologically independent APC samples randomly selected in the FDR group. Dots represent individual level data. Significance was determined by paired Student's *t*-test. $^{*}p<0.05$, $^{***}p<0.001$ vs Veh

Table 5. SASP factor protein levels in the media conditioned by FDR APCs treated with Dasatinib plus Quercetin or vehicle only.

Variables	*D+Q*	*Veh*
IL6 (pg/ml/10^5 cells)	*93.6 ±20.6* **	*1383.0 ± 215.0*
MCP1 (pg/ml/10^5 cells)	*12.2 ± 4.1***	*190.1 ± 28.3*
RANTES (pg/ml/10^5 cells)	*2.9 ± 0.3***	*6.9 ± 1.4*
IL8 (pg/ml/10^5 cells)	*53.1 ± 14.0***	*179.7 ± 20.3*
MIP1b (pg/ml/10^5 cells)	*0.4 ± 0.2*$^{p=0.06}$	*2.4 ± 0.3*

SASP factor protein levels in the media conditioned by FDR APCs (n=5) treated with the combination of 0.5 μM Dasatinib and 20 μM Quercetin (D+Q) or vehicle only (Veh) for 72 h were measured by a custom multiplex assay and normalized by cell number. All data shown are the mean ± SEM of five biologically independent APC samples randomly selected in the FDR group. Significance was determined by paired Student's *t*-test. **p<0.01 *vs* Veh. IL, interleukin; MCP1, monocyte chemotactic protein 1; RANTES, regulated on activation normal T-cell expressed and -secreted; MIP1b, macrophage inflammatory protein 1 beta.

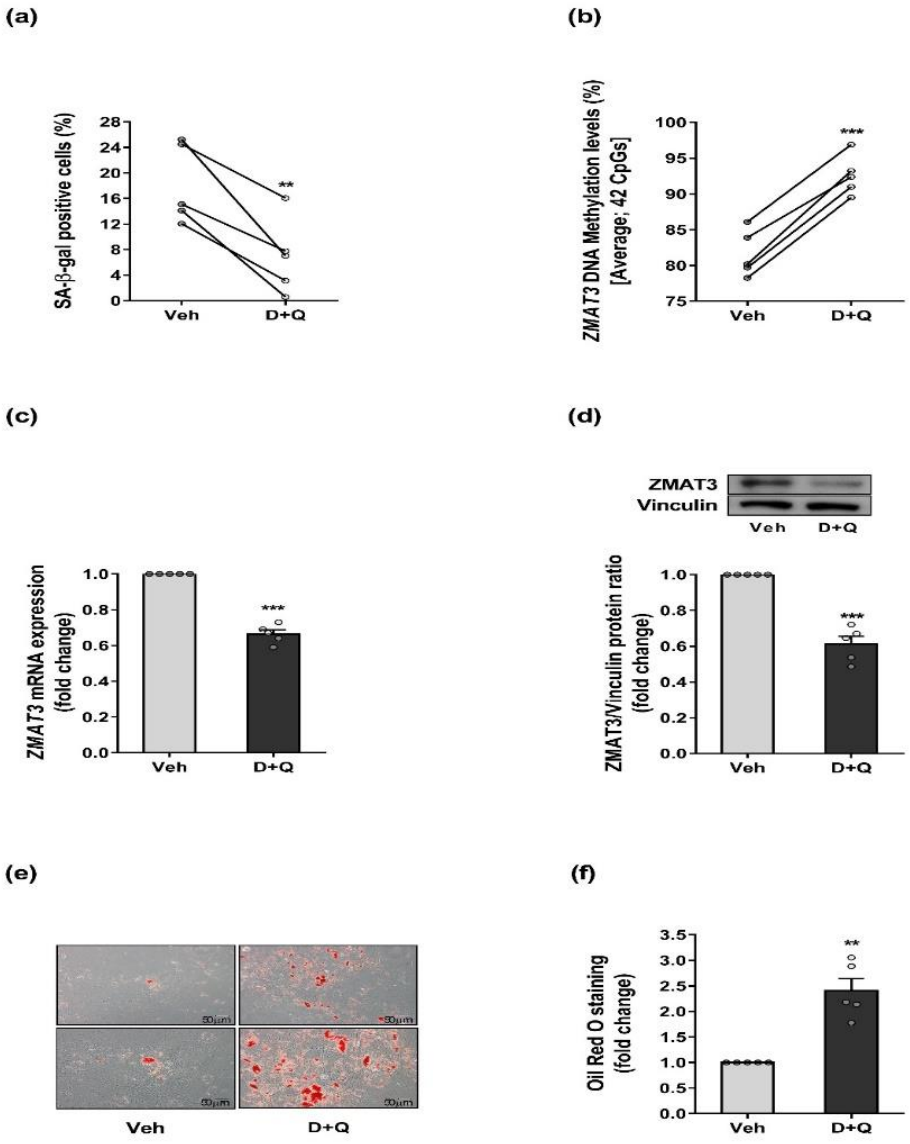

Figure 24. Effects of senolytics on *ZMAT3* DNA methylation and adipocyte differentiation in FDRs APCs. Five biologically independent APC samples randomly selected in the FDRs group were treated with D+Q or vehicle (Veh) for 72 h. (**a**) Flow cytometric detection of the SA-β-gal-positive cells in FDR APCs treated with D+Q or Veh. Values are presented as percentage (%). (**b**) Changes in average DNA methylation levels at 42 CpGs within the *ZMAT3* DMR were detected by BS in D+Q-treated FDR APCs compared to Veh-treated FDR APCs. (**c**) The fold change of the *ZMAT3* mRNA was assessed by qPCR. Expression was normalized first to *RPL13A* and then to expression in Veh-treated FDR APCs. (**d**) The fold change of the ZMAT3 protein was measured by Western blot in D+Q- *vs* Veh-treated FDR APCs. Vinculin served as a loading control. The upper figure shows representative blots; the lower figure shows result quantitation. (**e**,**f**) After either D+Q or Veh treatment, the FDR APCs were differentiated for 15 days. Oil Red O staining was used to assess the degree of differentiation. (**e**) Representative microphotographs showing lipid accumulation of FDR APCs treated with D+Q (right) or Veh (left) at diff. day 15. Upper panel at 10x magnification; bottom panel at 20x magnification. Scale bar 50 μm. (**f**) Bar graph shows photometric quantification of Oil Red O staining measured at 490 nm. Results are normalized to the absorbance in Veh-treated FDR APCs. (**a**,**b**). Data are shown as scatterplot with lines

joining paired points. (**c**,**d**,**f**) Data are shown as mean ± SEM. Dots represent individual level data. (**a**-**d**,**f**) Significance was determined by paired Student's *t*-test. ***p*<0.01, ****p*<0.001 *vs* Veh

3.7 Age-, senescence- and T2D-associated *ZMAT3* expression in SAT

Increased senescent cell burden in SAT contributes to the development of T2D in elderly (Spinelli at al., 2020). Thus, we have investigated whether, *in vivo*, the upregulation of *ZMAT3* transcription, previously identified as a major age-related gene in most tissues including SAT (Dong et al., 2021), associates with human ageing and T2D. To this end, we measured mRNA levels of *ZMAT3* in subcutaneous adipose cells from individuals aged 26 to 67. The clinical characteristics of these subjects have been previously reported (Gustafson et al., 2019). The subjects were then stratified according to *ZMAT3* expression levels and two subgroups expressing *ZMAT3* levels above (*n*=14) or below (*n*=15) *ZMAT3* median values were identified. As shown in Tab.6, the higher *ZMAT3* expressors also featured higher *TP53* mRNA levels, were significantly older, had significantly greater T2D prevalence and showed higher BMI. Importantly, multiple regression analysis further revealed that age was significantly associated with *ZMAT3* gene expression in this group, similar to *TP53* expression (Fig.25a,b). To validate the association between *ZMAT3* expression and age, we sought to replicate the age-related upregulation of *ZMAT3* in the SAT from an independent cohort of healthy women with similar age range as those in the previously analysed cohort (D'Esposito et al., 2012). Accordingly, these subjects were divided, based on *ZMAT3* mRNA levels, in two groups, low (*n*=10) and high (*n*=10) expressors, defined, respectively, by expression levels below or above the median value. As previously shown, the higher *ZMAT3* expressors were significantly older and had higher *TP53* mRNA levels (Table 7). Nevertheless, age was positively associated with *ZMAT3* mRNA in this group, as was *TP53* expression (Fig.25c,d). In addition, we examined the ZMAT3 protein in all of the available SAT samples in the replication cohort and compared the high versus low *ZMAT3* expressors. Once again, this comparison revealed that protein analysis of ZMAT3 largely reproduced the transcriptional data (Fig.26a). Furthermore, a positive correlation between *ZMAT3* mRNA and protein measurements across the same SAT samples was observed (Fig.26b). Overall, these findings indicate that, in human SAT, an increase in *ZMAT3* transcription is a feature of the elderly and T2D subjects. Thus, the age-related *ZMAT3* upregulation may have functional consequences in SAT through senescence induction, thereby impacting T2D risk.

Table 6. Characteristics of subjects in the discovery cohort stratified according to *ZMAT3* mRNA expression in subcutaneous adipose cells.

Phenotypes	***High ZMAT3 mRNA expression***	***Low ZMAT3 mRNA expression***	***p value***
N	14	15	
***ZMAT3* mRNA levels (REU)**	0.52 [0.39; 0.64]	0.21 [0.18; 0.31]	*<0.0001*
***TP53* mRNA levels (REU)**	0.53 [0.38; 0.91]	0.26 [0.19; 0.35]	*<0.0001*
Age, years	59.0 [32.8; 62.5]	45.0 [32.0; 47.0]	*0.0150*
T2D: N (%)	10 (71%)	0 (0%)	*<0.0001*
BMI, Kg/m^2	33.2 [30.5;35.0]	26.6 [23.1; 29.2]	*<0.0001*

Clinical study participants were stratified according to *ZMAT3* mRNA expression in subcutaneous adipose cells into two categories, low (Lexp) and high (Hexp) expression, definedby values below or above the median, respectively. Study participants are expressed as number (N). Data are shown as median [first quartile-Q1; third quartile-Q3]. Statistical differences between the two groups were tested using Mann Whitney test (continuous variables) or Fisher's exact test (categorical variable). *p* value *vs* Lexp participants. REU, relative expression units; BMI, body mass index; T2D, Type 2 Diabetes

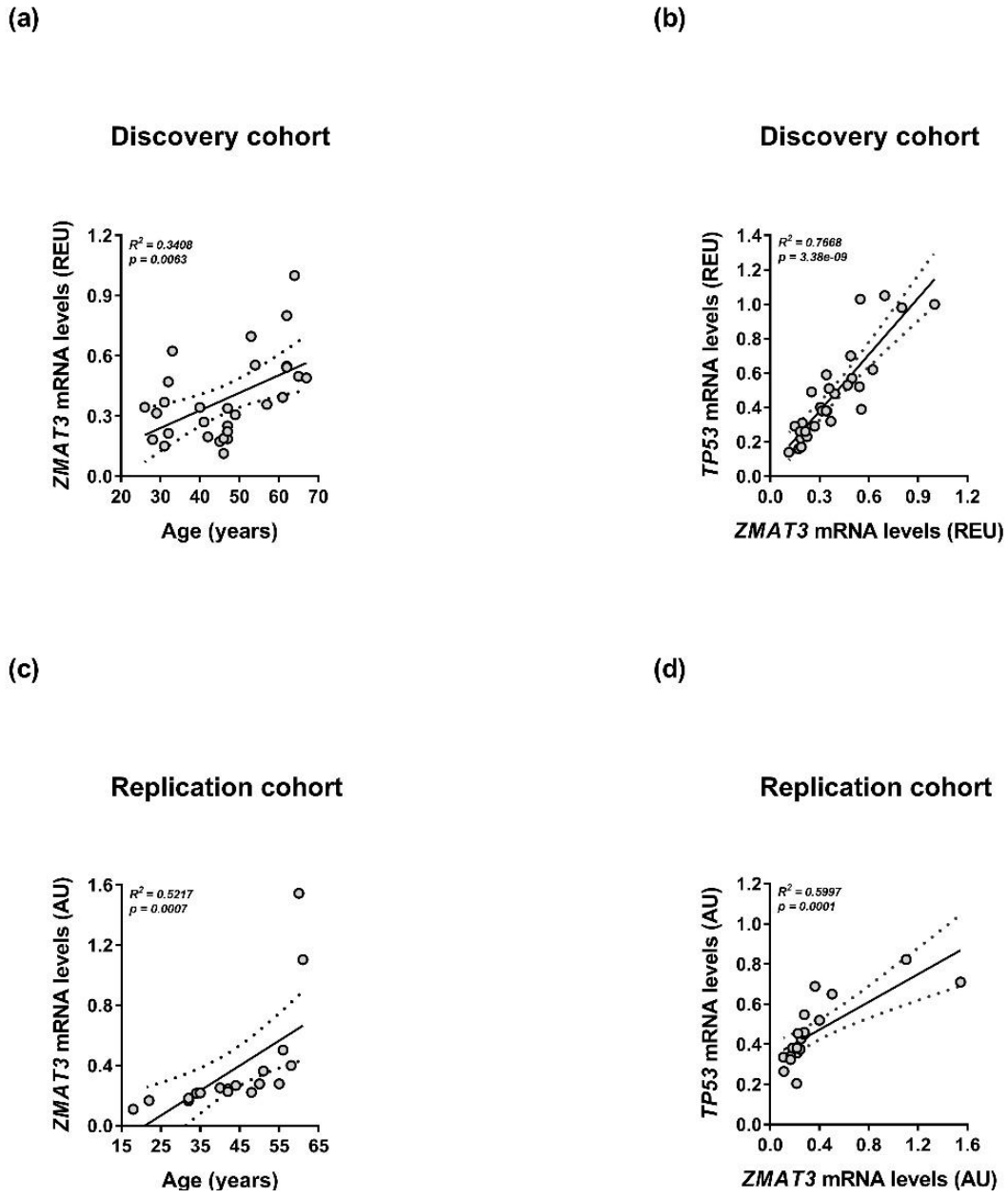

Figure 25. Age and senescence association with *ZMAT3* expression in SAT. (**a**,**b**) *ZMAT3* and *TP53* mRNA levels were measured by qPCR in subcutaneous adipose cells from 29 individuals aged 26 to 67. Values are presented as relative expression units (REU). (**a**) Scatter plot shows the association between the age of study participants and *ZMAT3* mRNA levels (*regression coefficient*=0.0080, adjusted for BMI). (**b**) Scatter plot depicts the association between *ZMAT3* and *TP53* mRNA levels in subcutaneous adipose cells (*regression coefficient*=1.1004, adjusted for BMI). (**c**,**d**) *ZMAT3* and *TP53* mRNA levels were measured by qPCR in SAT from 20 women aged 18 to 61. Values are presented as absolute units (AU). (**c**) Scatter plot shows the association between the age of study participants and *ZMAT3* mRNA levels (*regression coefficient*=0.0186, adjusted for BMI). (**d**) Scatter plot depicts the association between *ZMAT3* and *TP53* mRNA levels in SAT (*regression coefficient*=0.3558, adjusted for BMI). (**a-d**) The association analyses were adjusted for BMI by using multiple linear regression models. R^2 and *p* values for the whole models are shown in the graphs. Dashed lines indicate the 95% confidence intervals for the regression line

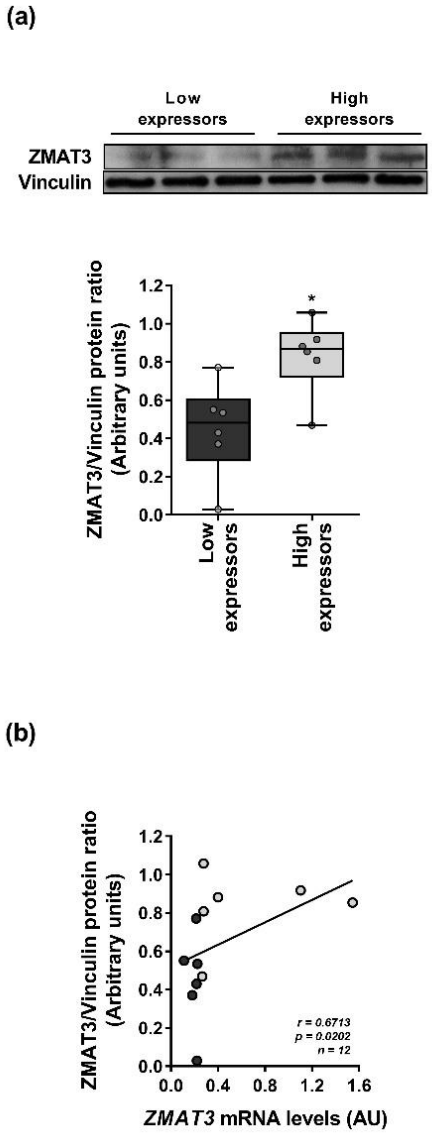

Figure 26. Protein analysis of ZMAT3 in the SAT samples from the replication cohort. (a) The ZMAT3 protein levels were assessed by Western Blot in the SAT from High (*n*=6) and Low (*n*=6) ZMAT3 mRNA expressors available from our study cohort. Vinculin served as a loading control. The upper figure shows representative blots; the lower figure shows result quantitation. Data are shown as boxplots (min-max) with all individual values. Significance was determined by unpaired Student's t-test. * $p<0.05$ *vs* Low expressors. (**b**) Correlation between the ZMAT3 mRNA and protein levels in the same SAT samples from High (*n*=6) and Low *(n*=6) expressors. Spearman's correlation coefficient *r*, *p* -value and number of samples (*n*) are indicated in the graph. Dark gray circles represent Low expressors, light gray circles represent High expressors

Table 7. Characteristics of subjects in the replication cohort stratified according to *ZMAT3* mRNA expression in subcutaneous adipose tissue.

Phenotypes	***High ZMAT3 mRNA expression***	***Low ZMAT3 mRNA expression***	***p value***
N	10	10	
***ZMAT3* mRNA levels (AU)**	0.32 [0.27; 0.65]	0.20 [0.15; 0.22]	*<0.0001*
***TP53* mRNA levels (AU)**	0.53 [0.45; 0.69]	0.35 [0.31; 0.38]	*<0.0001*
Age, years	53.0 [48.5; 58.5]	33.0 [21.0; 42.0]	*<0.0001*
BMI, Kg/m^2	29.6 [25.0;33.7]	27.6 [24.6; 30.8]	0.4030

Clinical study participants were stratified according to *ZMAT3* mRNA expression in subcutaneous adipose tissue into two categories, low (Lexp) and high (Hexp) expression, defined by values below or above the median, respectively. Study participants are expressed as number (N). Data are shown as median [first quartile-Q1; third quartile-Q3]. Statistical differences between the two groups were tested using Mann Whitney test. *p* value *vs* Lexp participants. AU, absolute units; BMI, body mass index

4. DISCUSSION

The ability to activate SAT hyperplasia mechanisms in response to obesity and ageing is critical for metabolic health because the development of T2D in obesity and/or the elderly can be prevented in part if SAT expansion is driven by recruitment of new adipocytes rather than hypertrophy of pre-existing cells (Gao et al., 2020; Smith & Kahn, 2016). As a result, it has been proposed that APC senescence contributes to the increased risk of T2D in both elderly and obese subjects by impairing de novo adipogenesis (Wissler et al., 2020). Despite this evidence, the molecular mechanisms underlying APC senescence and their implications for T2D risk are unknown. The FDR individuals investigated in this study showed both decreased adipogenesis and adipocyte hypertrophy in SAT (Smith & Kahn, 2016). Even though these subjects were young and non-obese, we hypothesized that their SAT abnormalities were caused by APC senescence. Furthermore, we have recently shown that the methylome of SAT-derived APCs from these same FDRs is characterized by extensive hypomethylation (Parrillo et al., 2020), as has been shown in other SNC (Cruickshanks et al., 2013). Thus, we investigated whether the DNA hypomethylation associated with T2D familiarity causes early senescence in the APCs of FDR subjects, contributing to their high risk of developing T2D.

SNCs are characterized by irreversible growth arrest and undergo structural and molecular changes. Indeed, they appear larger than normal cells, have more granules in their cytoplasm, and appear to have vanishing cell borders under light microscopy. Their lysosomal compartment is typically expanded, indicating increased activity of lysosomal β-galactosidase (senescence-associated β-galactosidase [SA-β-gal]), and nuclear integrity is compromised due to the downregulation of the *Lamin B1* (*LMNB1*) gene (Spinelli et al., 2020; Song et al., 2020; Hernandez-Segura et al., 2017; Wiley et al., 2017). All of these changes are accompanied by the activation of the tumor suppressor protein 53 (p53), which increases the expression of the CDK inhibitors p21 and p16 (Rufini et al., 2013). Although SNCs can no longer divide or proliferate, they can still produce and secrete a variety of factors that collectively define the state known as SASP. These secreted molecules include cytokines, chemokines, growth factors, matrix remodelling factors, non-coding RNA, exosomes, and other mediators linked to chronic inflammation and tissue damage (Spinelli et al., 2020). We show that the burden of SNCs, as measured by analyzing all of these marks, is significantly higher in APCs from FDR subjects. These cells have increased cytoplasmic granularity and enlarged size, as well as upregulation of the p21-encoding *CDKN1A* gene, a consistent increase in the percentage of cells arrested in the G1 phase of the cell cycle, and decreased mRNA levels of *LMNB1*. Furthermore, FDR APCs have increased secretion of the proinflammatory SASP factors IL6, MCP1, RANTES, IL8, and MIP1b, which are characteristic of senescence-associated low-grade inflammation (Freund et al.,

2010, Gourgulis et al., 2019; Khosla et al., 2020). Following senolytic clearance of SNCs, secretion of these molecules in the conditioned media of FDR APCs was significantly reduced, demonstrating that these senescent APCs have acquired a proinflammatory SASP. Importantly, the above mentioned SASP factors have been shown to cause defective adipogenesis, inflammation, aberrant adipocytokine production and IR in both elderly and obese individuals (Liu et al., 2020; Tchkonia et al., 2020). Thus, senescent APCs may represent a source of multiple factors that contribute to SAT dysfunction and metabolic abnormalities associated with T2D familiarity in FDR subjects.

Linkage analysis, candidate gene approaches, genome-wide association studies, and sequencing have all identified common, low-frequency, and rare T2D variants. However, the common variants discovered explain only a small portion of T2D inheritability, introducing the concept of "missing heritability," which can be gene-environment interactions and epigenetics (Alì., 2013; Stancàkovà & Laasko, 2016). Based on this evidence, we hypothesized that the SAT anomalies associated with FDRs are due to environmental factors that are widely shared within family groups and are epigenetically regulated. Epigenetic modifications, and in particular the loss of DNA methylation, play an important role in regulating the senescence phenotype (Atkinson et al., 2007; Cheng et al., 2017). Interestingly, the major risk factors for T2D (ageing, obesity, T2D familiarity), which are associated with increased APC senescence, contribute to IR in non-diabetic subjects by affecting the DNA methylation profile of AT (Davegårdh et al., 2018; Parrillo et al., 2019). Additionally, lifestyle modifications (diet, exercise, and weight loss) that prevent the onset of T2D by inducing DNA methylation changes in the AT also exert their protective effects by reducing APC senescence (Justice et al., 2018; Most et al., 2017). Therefore, in this work, it has been of interest to establish how DNA methylation contributes to T2D risk by promoting premature senescence in APCs. Our previous methylome analysis of the APCs from FDR subjects revealed that the majority of genomic regions differentially methylated in these individuals were less methylated and many overlapped with ageing- and senescence-related genes (Parrillo et al., 2020; Gorgoulis et al., 2019). These genes include *ZMAT3*, which belongs to the p53-dependent growth-inhibiting and tumor suppressor pathways (Hellborg et al., 2001; Janic et al., 2018). The *ZMAT3* gene encodes a zinc-finger RNA-binding protein, highly conserved from fish to human, which is involved in post-transcriptional regulation of gene expression by affecting mRNA stability and translation (Hellborg et al., 2001). A recent study also revealed an intriguing role for ZMAT3 in modulating alternative splicing, which has multiple effects on various cellular processes (Bieging-Rolett et al., 2020). ZMAT3 expression has been found to be higher in both human SNCs and aged tissues (Chaturvedi et al., 2015; Lee et al., 2014; Marthandan et al., 2016; Yang et al., 2016, Avelar et al., 2020). In particular, *ZMAT3* was

identified as one of the top ten age-related and differentially expressed genes in a recent analysis of 17,382 whole transcriptome profiles in 54 tissue types from 979 human donors aged 20 to 79 and included in the Genotype-Tissue Expression (GTEx) database (V.8). Importantly, *ZMAT3* showed a significant positive association with age in multiple tissues, including SAT (Dong et al., 2021). In addition, *ZMAT3* hypomethylation has been found in the cerebellum of subjects with Down Syndrome, which has been described as a human condition of accelerated ageing (Gensous et al., 2019;Mendioroz et al., 2016). However, our study is the first to investigate whether and how changes in the DNA methylation profile of *ZMAT3* cause premature senescence in APCs of FDR individuals.

In this study, we found that decreased methylation at the ZMAT3 DMR is associated with increased ZMAT3 expression in APCs from FDRs. In addition, we demonstrated that hypomethylation at this gene region directly increased ZMAT3 transcriptional activity *in vitro*, which may also occur *in vivo*. Indeed, the ZMAT3 DMR overlaps with the intronic chr3:179032651-179039599 region of the ZMAT3 gene annotated as regulatory feature based on the Ensembl regulatory build (Zerbinio et al., 2015). Although there is a significant difference in *ZMAT3* DNA methylation between FDR and CTRL subjects, the percentage changes are small, with only an 8% difference in mean DNA methylation between groups. This result, however, is consistent with previous findings that environmental factors linked to metabolic diseases such as T2D alter DNA methylation at specific genes in a subtle manner (Kirchner et al., 2016). We found that DNA methylation levels at the ZMAT3 DMR were negatively correlated with the appearance of the senescence phenotype in the APCs, whereas ZMAT3 mRNA and protein levels were positively correlated, supporting the hypothesis that methylation changes causing ZMAT3 upregulation contribute to the premature APC senescence seen in FDRs. In addition to this, we provided evidence that premature senescence caused by APC exposure to the demethylating agent 5-AZA was accompanied by decreased DNA methylation at the *ZMAT3* DMR and increased expression of the gene. Importantly, the pro-senescence effect of 5-AZA treatment was prevented by ZMAT3 silencing, confirming that hypomethylation-induced senescence is, at least in part, mediated by ZMAT3 upregulation. Consistently, senolytic removal of senescent cells in the FDR APCs resulted in a significant reestablishment of higher DNA methylation levels at the FDR-associated DMR of the ZMAT3 gene same intronic region, accompanied by a decrease in ZMAT3 expression. Collectively, these findings indicate that *ZMAT3* epigenetic dysregulation could be a reliable marker of senescent APCs. This conclusion is further strengthened by the evidence that *ZMAT3*-overexpressing APCs mimic the senescence phenotype observed in FDR APCs based upon SA-β-gal

expression, *CDKN1A* upregulation, loss of *LMNB1,* and SASP acquisition. The SASP profile acquired by the *ZMAT3* overexpressing APCs does not fully replicate that seen in FDR APCs. Nonetheless, increased RANTES and IL8 secretion was detected in media conditioned by APCs where senescence was induced by *ZMAT3* overexpression, indicating that other factors, in addition to ZMAT3, likely contribute to determining inflammatory SASP in FDR APCs.

After confirming the efficacy of *ZMAT3* overexpression and analyzing its effects on the acquisition of the senescence phenotype, we looked into the molecular mechanism by which ZMAT3 could cause senescence in APCs. ZMAT3 is an ARE-binding protein regulating a wide range of transcripts which are implicated in several biological processes, including cell cycle, immune system function and metabolic responses (Bersani et al., 2014, 2016; Vilborg et al., 2011). In particular, it is also a positive regulator of p53, which is critical for senescence induction. Indeed, ZMAT3 maintains high levels of P53 by blocking deadenylation of its mRNA (Vilborg et al., 2009). In addition, Bieging-Rolett et al. have recently demonstrated that ZMAT3 promotes full P53 activity by triggering mRNA decay of its MDM4 and MDM2 inhibitors (Bieging-Rolett et al., 2020). These reports have highlighted the growth-suppressive role of ZMAT3 in human cells, particularly when P53 function is intact, suggesting that ZMAT3 is most active when its signalling occurs through the P53-dependent pathways (Bieging-Rolett et al., 2020). In line with this evidence, we found that FDR APCs and ZMAT3 overexpressing APCs had significant P53 upregulation at both the mRNA and protein levels. Furthermore, we discovered that 5-AZA-induced ZMAT3 upregulation was associated with an increase in P53 expression and could be reversed by siRNA-mediated silencing of *ZMAT3*. Based on this evidence, we propose that hypomethylation-dependent ZMAT3 upregulation promotes APC senescence by increasing P53 activity. A positive correlation between ZMAT3 and P53 expression levels in FDR APCs supports this.

The *CDKN1A* gene is a well-known transcriptional target of P53. This gene encodes for the P21 protein, which acts as primary mediator of cell cycle arrest in by binding to and inhibiting the kinase activity of the cyclin-dependent kinases Cdk2 and Cdk1 (Meng et al., 2002). We demonstrated that *CDKN1A* gene expression was increased in both FDR APCs and ZMAT3 overexpressing APCs, confirming the pro-senescence role of ZMAT3 by increasing P53 activity. This evidence is further supported by data demonstrating that *ZMAT3* directly regulates *P21* expression at the transcriptional level by enhancing the ability of P53 to bind the *CDKN1A* promoter *in vitro*, which may also occur *in vivo*. Accordingly, we found a reduced *CDKN1A* expression in *ZMAT3* overexpressing APCs after treatment with PFT-α, a small molecule that has been widely used as a specific inhibitor of P53 transcription activity (Zhu et al., 2020), confirming that ZMAT3 promotes *CDKN1A* expression in a

P53-dependent manner. Overall, the findings indicate that *ZMAT3* induces premature senescence in APCs of FDRs by activating the p53/p21 pathway. Our findings are consistent with the study by Minamino et al., which demonstrated the critical role of the p53/p21 pathway in the induction of premature senescence in the AT in both obese and insulin-resistant mice, as well as T2D patients. These researchers demonstrated that adipocyte-specific p53 ablation reduced AT senescence and inflammation while improving IR in diabetic mice. In contrast, p53 overexpression resulted in AT senescence and inflammation that reduced insulin sensitivity (Minamino et al., 2009). Thus, the activation of the p53/p21 pathway by ZMAT3 links premature APC senescence to the accelerated development of IR in FDR subjects. These findings prompted us to investigate whether *ZMAT3* upregulation occurs *in vivo* and whether it is associated with chronological ageing and T2D. As a result, we investigated *ZMAT3* expression in SAT from elderly and T2D individuals. Interestingly, we discovered that *ZMAT3* mRNA levels increase with age and that this upregulation is strongly associated with increased expression of the *P53* senescence marker in these subjects.

Inappropriate expansion of adipose cell in the SAT due to impaired adipogenesis of APCs is a feature of non-obese FDR individuals (Gustafson et al., 2019). APC senescence is a major negative regulator of adipogenesis (Spinelli et al., 2020). Thus, we investigated the role of *ZMAT3* also in this process and discovered that ZMAT3 overexpression in APCs causes senescence as well as impaired adipogenesis. As previously demonstrated for its target P53, we also observed an increase in ZMAT3 expression in poorly differentiated APCs of FDR subjects, which may contribute to the establishment of this phenotype. Indeed, it is well established that P53 is a negative regulator of the adipogenic process, and its expression must be suppressed before APCs can differentiate into insulin-responsive adipocytes (Lee et al., 2020; Krstic et al., 2018). Thus, in FDR APCs, hypomethylation-induced upregulation of *ZMAT3* may keep P53 upregulated, induce senescence, and increase T2D risk by restraining adipogenesis.

In light of this evidence, APC senescence represent a promising target for alleviating the SAT dysfunction and metabolic abnormalities observed in FDR subjects. In support to this, we have provided the first evidence that FDRs might benefit from senolytic therapy. The combination of D+Q has recently emerged as an attractive therapeutic strategy by allowing selective clearance of senescent APCs both *in vitro* and *in vivo* (Robbins et al., 2020). Indeed, intermittent oral administration of D+Q improves insulin sensitivity in obese mice by restoring the ability of APCs to differentiate into insulin-responsive adipocytes and by reducing AT hypertrophy and inflammation (Palmer et al., 2019). Furthermore, in patients with T2D complicated by renal dysfunction a 3-day oral administration of D+Q is effective in reducing SNC burden and macrophage infiltration in abdominal SAT and in

reducing plasma levels of the main SASP mediators (Hickson et al., 2020). In this study, we found that after three days of D+Q treatment, the expression of senescence markers and SASP factors decreased in FDR APCs. We also discovered that after D+Q treatment, cultured APCs from FDRs have improved adipogenic capacity. Based on the evidence that the positive effect of D+Q on adipogenesis persisted after these agents were removed from the culture medium, we can conclude that senescent APCs are directly involved in the adipogenic impairment observed in FDRs.

Finally, our findings identify premature APC senescence as a key player in the SAT dysfunction occurring in healthy individuals who are FDRs of T2D patients and reveal a previously unknown role of ZMAT3 hypomethylation in determining these events. Furthermore, we show that senolytic-induced clearance of SNC improves adipogenesis of APCs and might contribute to decreasing diabetes risk in these FDRs (Fig.27).

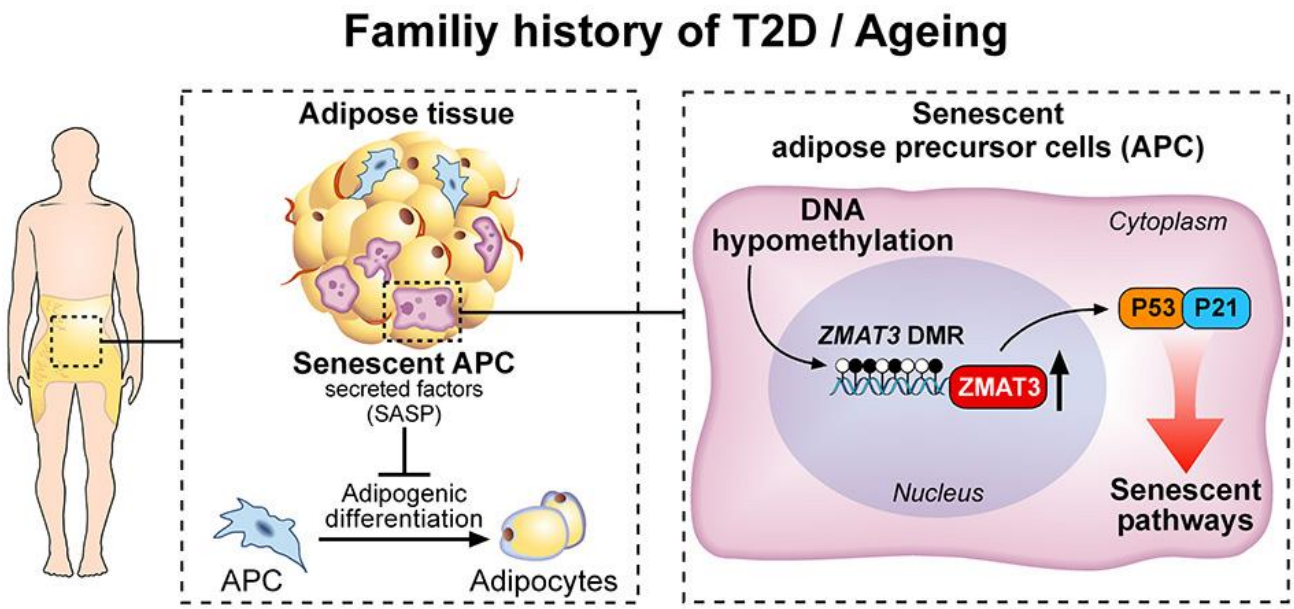

Figure 27. Schematic representation of the increased risk of type 2 diabetes in FDR subjects: DNA hypomethylation-induced ZMAT3 overexpression in FDR APCs caused premature senescence and impaired adipogenesis by activating p53/p21 pathway, resulting in higher FDRs predisposition for T2D

5. REFERENCES

Ahima RS. Connecting obesity, aging and diabetes. Nat Med. 2009 Sep;15(9):996-7. doi: 10.1038/nm0909-996.

Ahmed SAH, Ansari SA, Mensah-Brown EPK, Emerald BS. The role of DNA methylation in the pathogenesis of type 2 diabetes mellitus. Clin Epigenetics. 2020 Jul 11;12(1):104. doi: 10.1186/s13148-020-00896-4.

Ali O. Genetics of type 2 diabetes. World J Diabetes. 2013 Aug 15;4(4):114-23. doi: 10.4239/wjd.v4.i4.114.

Alt EU, Senst C, Murthy SN, Slakey DP, Dupin CL, Chaffin AE, Kadowitz PJ, Izadpanah R. Aging alters tissue resident mesenchymal stem cell properties. Stem Cell Res. 2012 Mar;8(2):215-25. doi: 10.1016/j.scr.2011.11.002.

Anastasiadi D, Esteve-Codina A, Piferrer F. Consistent inverse correlation between DNA methylation of the first intron and gene expression across tissues and species. Epigenetics Chromatin. 2018 Jun 29;11(1):37. doi: 10.1186/s13072-018-0205-1.

Argmann C, Dobrin R, Heikkinen S, Auburtin A, Pouilly L, Cock TA, Koutnikova H, Zhu J, Schadt EE, Auwerx J. Ppargamma2 is a key driver of longevity in the mouse. PLoS Genet. 2009 Dec;5(12):e1000752. doi: 10.1371/journal.pgen.1000752.

Arner P, Arner E, Hammarstedt A, Smith U. Genetic predisposition for Type 2 diabetes, but not for overweight/obesity, is associated with a restricted adipogenesis. PLoS One. 2011 Apr 12;6(4): e18284. doi: 10.1371/journal.pone.0018284.

Atkinson SP, Keith WN. Epigenetic control of cellular senescence in disease: opportunities for therapeutic intervention. Expert Rev Mol Med. 2007 Mar 13;9(7):1-26. doi: 10.1017/S1462399407000269.

Atzmon G, Yang XM, Muzumdar R, Ma XH, Gabriely I, Barzilai N. Differential gene expression between visceral and subcutaneous fat depots. Horm Metab Res. 2002 Nov-Dec;34(11-12):622-8. doi: 10.1055/s-2002-38250.

Avelar RA, Ortega JG, Tacutu R, Tyler EJ, Bennett D, Binetti P, Budovsky A, Chatsirisupachai K, Johnson E, Murray A, Shields S, Tejada-Martinez D, Thornton D, Fraifeld VE, Bishop CL, de Magalhães JP. A multidimensional systems biology analysis of cellular senescence in aging and disease. Genome Biol. 2020 Apr 7;21(1):91. doi: 10.1186/s13059-020-01990-9.

Bacos K, Gillberg L, Volkov P, Olsson AH, Hansen T, Pedersen O, Gjesing AP, Eiberg H, Tuomi T, Almgren P, Groop L, Eliasson L, Vaag A, Dayeh T, Ling C. Blood-based biomarkers of age-associated epigenetic changes in human islets associate with insulin secretion and diabetes. Nat Commun. 2016 Mar 31;7: 11089. doi: 10.1038/ncomms11089.

Baig S, Shabeer M, Parvaresh Rizi E, Agarwal M, Lee MH, Ooi DSQ, Chia C, Aung N, Ng G, Teo Y, Chhay V, Magkos F, Vidal-Puig A, Seet RCS, Toh SA. Heredity of type 2 diabetes confers increased susceptibility to oxidative stress and inflammation. BMJ Open Diabetes Res Care. 2020 Jan;8(1):e000945. doi: 10.1136/bmjdrc-2019-000945.

Bakshi A, Bretz CL, Cain TL, Kim J. Intergenic and intronic DNA hypomethylated regions as putative regulators of imprinted domains. Epigenomics. 2018 Apr 1;10(4):445-461. doi: 10.2217/epi-2017-0125.

Balakrishnan A, Guruprasad KP, Satyamoorthy K, Joshi MB. Interleukin-6 determines protein stabilization of DNA methyltransferases and alters DNA promoter methylation of genes associated with insulin signaling and angiogenesis. Lab Invest. 2018 Sep;98(9):1143-1158. doi: 10.1038/s41374-018-0079-7.

Barros SP, Offenbacher S. Epigenetics: connecting environment and genotype to phenotype and disease. J Dent Res. 2009 May;88(5):400-8. doi: 10.1177/0022034509335868.

Beck M, Rombouts C, Moreels M, Aerts A, Quintens R, Tabury K, Michaux A, Janssen A, Neefs M, Ernst E, Dieriks B, Lee R, De Vos WH, Lambert C, Van Oostveldt P, Baatout S. Modulation of gene expression in endothelial cells in response to high LET nickel ion irradiation. Int J Mol Med. 2014 Oct;34(4):1124-32. doi: 10.3892/ijmm.2014.1893.

Berná G, Oliveras-López MJ, Jurado-Ruíz E, Tejedo J, Bedoya F, Soria B, Martín F. Nutrigenetics and nutrigenomics insights into diabetes etiopathogenesis. Nutrients. 2014 Nov 21;6(11):5338-69. doi: 10.3390/nu6115338.

Bersani C, Huss M, Giacomello S, Xu LD, Bianchi J, Eriksson S, Jerhammar F, Alexeyenko A, Vilborg A, Lundeberg J, Lui WO, Wiman KG. Genome-wide identification of Wig-1 mRNA targets by RIP-Seq analysis. Oncotarget. 2016 Jan 12;7(2):1895-911. doi: 10.18632/oncotarget.6557.

Bersani C, Xu LD, Vilborg A, Lui WO, Wiman KG. Wig-1 regulates cell cycle arrest and cell death through the p53 targets FAS and 14-3-3σ. Oncogene. 2014 Aug 28;33(35):4407-17. doi: 10.1038/onc.2013.594.

Bieging-Rolett KT, Kaiser AM, Morgens DW, Boutelle AM, Seoane JA, Van Nostrand EL, Zhu C, Houlihan SL, Mello SS, Yee BA, McClendon J, Pierce SE, Winters IP, Wang M, Connolly AJ, Lowe SW, Curtis C, Yeo GW, Winslow MM, Bassik MC, Attardi LD. Zmat3 Is a Key Splicing Regulator in the p53 Tumor Suppression Program. Mol Cell. 2020 Nov 5;80(3):452-469.e9. doi: 10.1016/j.molcel.2020.10.022.

Bocklandt S, Lin W, Sehl ME, Sánchez FJ, Sinsheimer JS, Horvath S, Vilain E. Epigenetic predictor of age. PLoS One. 2011;6(6):e14821. doi: 10.1371/journal.pone.0014821.

Bommarito PA, Fry RC (2019) Chapter 2–1: The role of DNA methylation in gene regulation. In: McCullough SD, Dolinoy DC (eds) Toxicoepigenetics. Academic Press, pp 127–151. doi: 10.1016/B978-0-12-812433-8.00005-8

Boyes J, Bird A. DNA methylation inhibits transcription indirectly via a methyl-CpG binding protein. Cell. 1991 Mar;64(6):1123-34. doi: 10.1016/0092-8674(91)90267-3.

Burton DGA, Faragher RGA. Obesity and type-2 diabetes as inducers of premature cellular senescence and ageing. Biogerontology. 2018 Dec;19(6):447-459. doi: 10.1007/s10522-018-9763-7.

Bussè C, Barnini T, Zucca M, Rainero I, Mozzetta S, Zangrossi A, Cagnin A. Depression, anxiety and sleep alterations in caregivers of persons with dementia after 1-year of COVID-19 pandemic. Front Psychiatry. 2022 Feb 10;13:826371. doi: 10.3389/fpsyt.2022.826371.

Carninci P, Sandelin A, Lenhard B, Katayama S, Shimokawa K, Ponjavic J, Semple CA, Taylor MS, Engström PG, Frith MC, Forrest AR, Alkema WB, Tan SL, Plessy C, Kodzius R, Ravasi T, Kasukawa T, Fukuda S, Kanamori-Katayama M, Kitazume Y, Kawaji H, Kai C, Nakamura M, Konno H, Nakano K, Mottagui-Tabar S, Arner P, Chesi A, Gustincich S, Persichetti F, Suzuki H, Grimmond SM, Wells CA, Orlando V, Wahlestedt C, Liu ET, Harbers M, Kawai J, Bajic VB, Hume DA, Hayashizaki Y. Genome-wide analysis of mammalian promoter architecture and evolution. Nat Genet. 2006 Jun;38(6):626-35. doi: 10.1038/ng1789. Strategies for analyzing bisulfite sequencing data. Katarzyna Wreczyckaad1 Alexander Gosdschana1 Dilmurat Yusufa Björn Grüningb Yassen Assenov cAltuna Akali.

Cartwright MJ, Tchkonia T, Kirkland JL. Aging in adipocytes: potential impact of inherent, depot-specific mechanisms. Exp Gerontol. 2007 Jun;42(6):463-71. doi: 10.1016/j.exger.2007.03.003.

Caso G, McNurlan MA, Mileva I, Zemlyak A, Mynarcik DC, Gelato MC. Peripheral fat loss and decline in adipogenesis in older humans. Metabolism. 2013 Mar;62(3):337-40. doi: 10.1016/j.metabol.2012.08.007.

Cederberg H, Stančáková A, Kuusisto J, Laakso M, Smith U. Family history of type 2 diabetes increases the risk of both obesity and its complications: is type 2 diabetes a disease of inappropriate lipid storage? J Intern Med. 2015 May;277(5):540-51. doi: 10.1111/joim.12289.

Charrière G, Cousin B, Arnaud E, André M, Bacou F, Penicaud L, Casteilla L. Preadipocyte conversion to macrophage. Evidence of plasticity. J Biol Chem. 2003 Mar 14;278(11):9850-5. doi: 10.1074/jbc.M210811200.

Chatterjee S, Khunti K, Davies MJ. Type 2 diabetes. Lancet. 2017 Jun 3;389(10085):2239-2251. doi: 10.1016/S0140-6736(17)30058-2.

Chaturvedi P, Neelamraju Y, Arif W, Kalsotra A, Janga SC. Uncovering RNA binding proteins associated with age and gender during liver maturation. Sci Rep. 2015 Mar 31;5:9512. doi: 10.1038/srep09512.

Chawla A, Nguyen KD, Goh YP. Macrophage-mediated inflammation in metabolic disease. Nat Rev Immunol. 2011 Oct 10;11(11):738-49. doi: 10.1038/nri3071.

Chen JH, Ozanne SE, Hales CN. Methods of cellular senescence induction using oxidative stress. Methods Mol Biol. 2007;371:179-89. doi: 10.1007/978-1-59745-361-5_14.

Cheng LQ, Zhang ZQ, Chen HZ, Liu DP. Epigenetic regulation in cell senescence. J Mol Med (Berl). 2017 Dec;95(12):1257-1268. doi: 10.1007/s00109-017-1581-x.

Childs BG, Durik M, Baker DJ, van Deursen JM. Cellular senescence in aging and age-related disease: from mechanisms to therapy. Nat Med. 2015 Dec;21(12):1424-35. doi: 10.1038/nm.4000.

Cho NH, Shaw JE, Karuranga S, Huang Y, da Rocha Fernandes JD, Ohlrogge AW, Malanda B. IDF Diabetes Atlas: Global estimates of diabetes prevalence for 2017 and projections for 2045. Diabetes Res Clin Pract. 2018 Apr;138:271-281. doi: 10.1016/j.diabres.2018.02.023

Choe SS, Huh JY, Hwang IJ, Kim JI, Kim JB. Adipose Tissue Remodeling: Its Role in Energy Metabolism and Metabolic Disorders. Front Endocrinol (Lausanne). 2016 Apr 13; 7:30. doi: 10.3389/fendo.2016.00030.

Chronic disease management in ageing populations. Lancet. 2012 May 19;379(9829):1851. doi: 10.1016/S0140-6736(12)60790-9.

Chung S, Lapoint K, Martinez K, Kennedy A, Boysen Sandberg M, McIntosh MK. Preadipocytes mediate lipopolysaccharide-induced inflammation and insulin resistance in primary cultures of newly differentiated human adipocytes. Endocrinology. 2006 Nov;147(11):5340-51. doi: 10.1210/en.2006-0536.

Clark J., Rager J. E. Epigenetics: An overview of CpG methylation, chromatin remodeling, and regulatory/non-coding RNAs. In Environmental Epigenetics in Toxicology and Public Health (Fry R. C., Ed.), pp. 3–32. Elsevier. 2020. doi:10.1016/b978-0-12-819968-8.00001-9.

Clarke SL, Robinson CE, Gimble JM. CAAT/enhancer binding proteins directly modulate transcription from the peroxisome proliferator-activated receptor gamma 2 promoter. Biochem Biophys Res Commun. 1997 Nov 7;240(1):99-103. doi: 10.1006/bbrc.1997.7627.

Cousin B, Munoz O, Andre M, Fontanilles AM, Dani C, Cousin JL, Laharrague P, Casteilla L, Pénicaud L. A role for preadipocytes as macrophage-like cells. FASEB J. 1999 Feb;13(2):305-12. doi: 10.1096/fasebj.13.2.305.

Crossno JT Jr, Majka SM, Grazia T, Gill RG, Klemm DJ. Rosiglitazone promotes development of a novel adipocyte population from bone marrow-derived circulating progenitor cells. J Clin Invest. 2006 Dec;116(12):3220-8. doi: 10.1172/JCI28510.

Crouch J, Shvedova M, Thanapaul RJRS, Botchkarev V, Roh D. Epigenetic Regulation of Cellular Senescence. Cells. 2022 Feb 15;11(4):672. doi: 10.3390/cells11040672. PMID: 35203320; PMCID: PMC8870565.

Cruickshanks HA, McBryan T, Nelson DM, Vanderkraats ND, Shah PP, van Tuyn J, Singh Rai T, Brock C, Donahue G, Dunican DS, Drotar ME, Meehan RR, Edwards JR, Berger SL, Adams PD. Senescent cells harbour features of the cancer epigenome. Nat Cell Biol. 2013 Dec;15(12):1495-506. doi: 10.1038/ncb2879.

Curradi M, Izzo A, Badaracco G, Landsberger N. Molecular mechanisms of gene silencing mediated by DNA methylation. Mol Cell Biol. 2002 May;22(9):3157-73. doi: 10.1128/MCB.22.9.3157-3173.2002.

da Silva PFL, Ogrodnik M, Kucheryavenko O, Glibert J, Miwa S, Cameron K, Ishaq A, Saretzki G, Nagaraja-Grellscheid S, Nelson G, von Zglinicki T. The bystander effect contributes to the

accumulation of senescent cells in vivo. Aging Cell. 2019 Feb;18(1):e12848. doi: 10.1111/acel.12848.

Davegårdh C, García-Calzón S, Bacos K, Ling C. DNA methylation in the pathogenesis of type 2 diabetes in humans. Mol Metab. 2018 Aug;14:12-25. doi: 10.1016/j.molmet.2018.01.022.

Delmonico MJ, Harris TB, Visser M, Park SW, Conroy MB, Velasquez-Mieyer P, Boudreau R, Manini TM, Nevitt M, Newman AB, Goodpaster BH; Health, Aging, and Body. Longitudinal study of muscle strength, quality, and adipose tissue infiltration. Am J Clin Nutr. 2009 Dec;90(6):1579-85. doi: 10.3945/ajcn.2009.28047

Desiderio A, Longo M, Parrillo L, Campitelli M, Cacace G, de Simone S, Spinelli R, Zatterale F, Cabaro S, Dolce P, Formisano P, Milone M, Miele C, Beguinot F, Raciti GA. Epigenetic silencing of the ANKRD26 gene correlates to the pro-inflammatory profile and increased cardio-metabolic risk factors in human obesity. Clin Epigenetics. 2019 Dec 4;11(1):181. doi: 10.1186/s13148-019-0768-0.

Desiderio A, Longo M, Parrillo L, Campitelli M, Cacace G, de Simone S, Spinelli R, Zatterale F, Cabaro S, Dolce P, Formisano P, Milone M, Miele C, Beguinot F, Raciti GA. Epigenetic silencing of the ANKRD26 gene correlates to the pro-inflammatory profile and increased cardio-metabolic risk factors in human obesity. Clin Epigenetics. 2019 Dec 4;11(1):181. doi: 10.1186/s13148-019-0768-0.

D'Esposito V, Passaretti F, Hammarstedt A, Liguoro D, Terracciano D, Molea G, Canta L, Miele C, Smith U, Beguinot F, Formisano P. Adipocyte-released insulin-like growth factor-1 is regulated by glucose and fatty acids and controls breast cancer cell growth in vitro. Diabetologia. 2012 Oct;55(10):2811-2822. doi: 10.1007/s00125-012-2629-7

Dong Q, Wei L, Zhang MQ, Wang X. Regulatory RNA binding proteins contribute to the transcriptome-wide splicing alterations in human cellular senescence. Aging (Albany NY). 2018 Jun 24;10(6):1489-1505. doi: 10.18632/aging.101485.

Dong X, Sun S, Zhang L, Kim S, Tu Z, Montagna C, Maslov AY, Suh Y, Wang T, Campisi J, Vijg J. Age-related telomere attrition causes aberrant gene expression in sub-telomeric regions. Aging Cell. 2021 Jun;20(6):e13357. doi: 10.1111/acel.13357.

Drong AW, Lindgren CM, McCarthy MI. The genetic and epigenetic basis of type 2 diabetes and obesity. Clin Pharmacol Ther. 2012 Dec; 92(6):707-15. doi: 10.1038/clpt.2012.149.1,2,3.

el-Deiry WS, Tokino T, Velculescu VE, Levy DB, Parsons R, Trent JM, Lin D, Mercer WE, Kinzler KW, Vogelstein B. WAF1, a potential mediator of p53 tumor suppression. Cell. 1993 Nov 19;75(4):817-25. doi: 10.1016/0092-8674(93)90500-p.

Elzi DJ, Lai Y, Song M, Hakala K, Weintraub ST, Shiio Y. Plasminogen activator inhibitor 1--insulin-like growth factor binding protein 3 cascade regulates stress-induced senescence. Proc Natl Acad Sci U S A. 2012 Jul 24;109(30):12052-7. doi: 10.1073/pnas.1120437109.

Epigenetics & Cellular Senescence Group, Blizard Institute, Barts and the London School of Medicine and Dentistry, Queen Mary University of London, London, United Kingdom

Faget DV, Ren Q, Stewart SA. Unmasking senescence: context-dependent effects of SASP in cancer. Nat Rev Cancer. 2019 Aug;19(8):439-453. doi: 10.1038/s41568-019-0156-2.

Fajas L, Schoonjans K, Gelman L, Kim JB, Najib J, Martin G, Fruchart JC, Briggs M, Spiegelman BM, Auwerx J. Regulation of peroxisome proliferator-activated receptor gamma expression by adipocyte differentiation and determination factor 1/sterol regulatory element binding protein 1: implications for adipocyte differentiation and metabolism. Mol Cell Biol. 1999 Aug;19(8):5495-503. doi: 10.1128/MCB.19.8.5495.

Fajas L. Adipogenesis: a cross-talk between cell proliferation and cell differentiation. Ann Med. 2003;35(2):79-85. doi: 10.1080/07853890310009999.

Farr JN, Xu M, Weivoda MM, Monroe DG, Fraser DG, Onken JL, Negley BA, Sfeir JG, Ogrodnik MB, Hachfeld CM, LeBrasseur NK, Drake MT, Pignolo RJ, Pirtskhalava T, Tchkonia T, Oursler MJ,

Feng J, Chang H, Li E, Fan G. Dynamic expression of de novo DNA methyltransferases Dnmt3a and Dnmt3b in the central nervous system. J Neurosci Res. 2005 Mar 15;79(6):734-46. doi: 10.1002/jnr.20404.

Ferrucci L, Fabbri E. Inflammageing: chronic inflammation in ageing, cardiovascular disease, and frailty. Nat Rev Cardiol. 2018 Sep;15(9):505-522. doi: 10.1038/s41569-018-0064-2.

Fiannaca A, La Rosa M, La Paglia L, Rizzo R, Urso A. nRC: non-coding RNA Classifier based on structural features. BioData Min. 2017 Aug 1;10:27. doi: 10.1186/s13040-017-0148-2.

Field AE, Robertson NA, Wang T, Havas A, Ideker T, Adams PD. DNA Methylation Clocks in Aging: Categories, Causes, and Consequences. Mol Cell. 2018 Sep 20;71(6):882-895. doi: 10.1016/j.molcel.2018.08.008.

Florath I, Butterbach K, Müller H, Bewerunge-Hudler M, Brenner H. Cross-sectional and longitudinal changes in DNA methylation with age: an epigenome-wide analysis revealing over 60 novel age-associated CpG sites. Hum Mol Genet. 2014 Mar 1;23(5):1186-201. doi: 10.1093/hmg/ddt531.

Fontana L, Klein S. Aging, adiposity, and calorie restriction. JAMA. 2007 Mar 7;297(9):986-94. doi: 10.1001/jama.297.9.986.

Forouhi NG, Wareham NJ. The EPIC-InterAct Study: A Study of the Interplay between Genetic and Lifestyle Behavioral Factors on the Risk of Type 2 Diabetes in European Populations. Curr Nutr Rep. 2014;3(4):355-363. doi: 10.1007/s13668-014-0098-y.

Franceschi C, Garagnani P, Morsiani C et al (2018) The continuum of aging and age-related diseases: common mechanismsbut different rates. Front Med (Lausanne) 5:61.

Freund A, Orjalo AV, Desprez PY, Campisi J. Inflammatory networks during cellular senescence: causes and consequences. Trends Mol Med. 2010 May;16(5):238-46. doi: 10.1016/j.molmed.2010.03.003.

Fuhrmann-Stroissnigg H, Ling YY, Zhao J, McGowan SJ, Zhu Y, Brooks RW, Grassi D, Gregg SQ, Stripay JL, Dorronsoro A, Corbo L, Tang P, Bukata C, Ring N, Giacca M, Li X, Tchkonia T, Kirkland JL, Niedernhofer LJ, Robbins PD. Identification of HSP90 inhibitors as a novel class of senolytics. Nat Commun. 2017 Sep 4;8(1):422. doi: 10.1038/s41467-017-00314-z.

Fujisaka S, Usui I, Nawaz A, Takikawa A, Kado T, Igarashi Y, Tobe K. M2 macrophages in metabolism. Diabetol Int. 2016 Nov 1;7(4):342-351. doi: 10.1007/s13340-016-0290-y.

Galicia-Garcia U, Benito-Vicente A, Jebari S, Larrea-Sebal A, Siddiqi H, Uribe KB, Ostolaza H, Martín C. Pathophysiology of Type 2 Diabetes Mellitus. Int J Mol Sci. 2020 Aug 30;21(17):6275. doi: 10.3390/ijms21176275.

Gao Z, Daquinag AC, Fussell C, Zhao Z, Dai Y, Rivera A, Snyder BE, Eckel-Mahan KL, Kolonin MG. Age-associated telomere attrition in adipocyte progenitors predisposes to metabolic disease. Nat Metab. 2020 Dec;2(12):1482-1497. doi: 10.1038/s42255-020-00320-4

Gardner JP, Li S, Srinivasan SR, Chen W, Kimura M, Lu X, Berenson GS, Aviv A. Rise in insulin resistance is associated with escalated telomere attrition. Circulation. 2005 May 3;111(17):2171-7. doi: 10.1161/01.CIR.0000163550.70487.0B.

Gastaldelli A, Gaggini M, De Fronzo RA. Role of Adipose Tissue Insulin Resistance in the Natural History of Type 2 Diabetes: Results From the San Antonio Metabolism Study. Diabetes. 2017 Apr; 66(4):815-822. doi: 10.2337/db16-1167.

Gensous N, Franceschi C, Salvioli S, Garagnani P, Bacalini MG. Down Syndrome, Ageing and Epigenetics. Subcell Biochem. 2019;91:161-193. doi: 10.1007/978-981-13-3681-2_7. PMID: 30888653.

Gensous N, Franceschi C, Salvioli S, Garagnani P, Bacalini MG. Down Syndrome, Ageing and Epigenetics. Subcell Biochem. 2019;91:161-193. doi: 10.1007/978-981-13-3681-2_7.

Gentilini D, Mari D, Castaldi D, Remondini D, Ogliari G, Ostan R, Bucci L, Sirchia SM, Tabano S, Cavagnini F, Monti D, Franceschi C, Di Blasio AM, Vitale G. Role of epigenetics in human aging and longevity: genome-wide DNA methylation profile in centenarians and centenarians' offspring. Age (Dordr). 2013 Oct;35(5):1961-73. doi: 10.1007/s11357-012-9463-1.

Ghosh AK, O'Brien M, Mau T, Qi N, Yung R. Adipose Tissue Senescence and Inflammation in Aging is Reversed by the Young Milieu. J Gerontol A Biol Sci Med Sci. 2019 Oct 4;74(11):1709-1715. doi: 10.1093/gerona/gly290.

Gillett M, Royle P, Snaith A, et al. Non-Pharmacological Interventions to Reduce the Risk of Diabetes in People with Impaired Glucose Regulation: A Systematic Review and Economic Evaluation. Southampton (UK): NIHR Journals Library; 2012 Aug. (Health Technology Assessment, No. 16.33.) 1, Introduction.

Goodpaster BH, Krishnaswami S, Harris TB, Katsiaras A, Kritchevsky SB, Simonsick EM, Nevitt M, Holvoet P, Newman AB. Obesity, regional body fat distribution, and the metabolic syndrome in older men and women. Arch Intern Med. 2005 Apr 11;165(7):777-83. doi: 10.1001/archinte.165.7.777.

Goodpaster BH, Krishnaswami S, Resnick H, Kelley DE, Haggerty C, Harris TB, Schwartz AV, Kritchevsky S, Newman AB. Association between regional adipose tissue distribution and both type 2 diabetes and impaired glucose tolerance in elderly men and women. Diabetes Care. 2003 Feb;26(2):372-9. doi: 10.2337/diacare.26.2.372.

Gorgoulis V, Adams PD, Alimonti A, Bennett DC, Bischof O, Bishop C, Campisi J, Collado M, Evangelou K, Ferbeyre G, Gil J, Hara E, Krizhanovsky V, Jurk D, Maier AB, Narita M, Niedernhofer L, Passos JF, Robbins PD, Schmitt CA, Sedivy J, Vougas K, von Zglinicki T, Zhou D, Serrano M,

Demaria M. Cellular Senescence: Defining a Path Forward. Cell. 2019 Oct 31;179(4):813-827. doi: 10.1016/j.cell.2019.10.005.

Guo W, Pirtskhalava T, Tchkonia T, Xie W, Thomou T, Han J, Wang T, Wong S, Cartwright A, Hegardt FG, Corkey BE, Kirkland JL. Aging results in paradoxical susceptibility of fat cell progenitors to lipotoxicity. Am J Physiol Endocrinol Metab. 2007 Apr;292(4):E1041-51. doi: 10.1152/ajpendo.00557.2006.

Gustafson B, Gogg S, Hedjazifar S, Jenndahl L, Hammarstedt A, Smith U. Inflammation and impaired adipogenesis in hypertrophic obesity in man. Am J Physiol Endocrinol Metab. 2009 Nov;297(5):E999-E1003. doi: 10.1152/ajpendo.00377.2009.

Gustafson B, Nerstedt A, Smith U. Reduced subcutaneous adipogenesis in human hypertrophic obesity is linked to senescent precursor cells. Nat Commun. 2019 Jun 21;10(1):2757. doi: 10.1038/s41467-019-10688-x.

Hadad N, Masser DR, Blanco-Berdugo L, Stanford DR, Freeman WM. Early-life DNA methylation profiles are indicative of age-related transcriptome changes. Epigenetics Chromatin. 2019 Oct 8;12(1):58. doi: 10.1186/s13072-019-0306-5.

Hammarstedt A, Gogg S, Hedjazifar S, Nerstedt A, Smith U. Impaired Adipogenesis and Dysfunctional Adipose Tissue in Human Hypertrophic Obesity. Physiol Rev. 2018 Oct 1;98(4):1911-1941. doi: 10.1152/physrev.00034.2017.

Handbook of Epigenetics (Second edition) The New Molecular and Medical Genetics2017, Pages 1-6Handbook of EpigeneticsChapter 1 - An Overview of Epigenetics

Hannou SA, Wouters K, Paumelle R, Staels B. Functional genomics of the CDKN2A/B locus in cardiovascular and metabolic disease: what have we learned from GWASs? Trends Endocrinol Metab. 2015 Apr;26(4):176-84. doi: 10.1016/j.tem.2015.01.008.

Hannum G, Guinney J, Zhao L, Zhang L, Hughes G, Sadda S, Klotzle B, Bibikova M, Fan JB, Gao Y, Deconde R, Chen M, Rajapakse I, Friend S, Ideker T, Zhang K. Genome-wide methylation profiles reveal quantitative views of human aging rates. Mol Cell. 2013 Jan 24;49(2):359-367. doi: 10.1016/j.molcel.2012.10.016.

Hellborg F, Qian W, Mendez-Vidal C, Asker C, Kost-Alimova M, Wilhelm M, Imreh S, Wiman KG. Human wig-1, a p53 target gene that encodes a growth inhibitory zinc finger protein. Oncogene. 2001 Sep 6;20(39):5466-74. doi: 10.1038/sj.onc.1204722.

Henninger AM, Eliasson B, Jenndahl LE, Hammarstedt A. Adipocyte hypertrophy, inflammation and fibrosis characterize subcutaneous adipose tissue of healthy, non-obese subjects predisposed to type 2 diabetes. PLoS One. 2014 Aug 22;9(8):e105262. doi: 10.1371/journal.pone.0105262.

Hernandez-Segura A, de Jong TV, Melov S, Guryev V, Campisi J, Demaria M. Unmasking Transcriptional Heterogeneity in Senescent Cells. Curr Biol. 2017 Sep 11;27(17):2652-2660.e4. doi: 10.1016/j.cub.2017.07.033.

Hernandez-Segura A, Nehme J, Demaria M. Hallmarks of Cellular Senescence. Trends Cell Biol. 2018 Jun;28(6):436-453. doi: 10.1016/j.tcb.2018.02.001.

Hickson LJ, Langhi Prata LGP, Bobart SA, Evans TK, Giorgadze N, Hashmi SK, Herrmann SM, Jensen MD, Jia Q, Jordan KL, Kellogg TA, Khosla S, Koerber DM, Lagnado AB, Lawson DK, LeBrasseur NK, Lerman LO, McDonald KM, McKenzie TJ, Passos JF, Pignolo RJ, Pirtskhalava T, Saadiq IM, Schaefer KK, Textor SC, Victorelli SG, Volkman TL, Xue A, Wentworth MA, Wissler Gerdes EO, Allison DB, Dickinson SL, Ejima K, Atkinson EJ, Lenburg M, Zhu Y, Tchkonia T, Kirkland JL. Corrigendum to 'Senolytics decrease senescent cells in humans: Preliminary report from a clinical trial of Dasatinib plus Quercetin in individuals with diabetic kidney disease' EBioMedicine 47 (2019) 446-456. EBioMedicine. 2020 Feb;52:102595. doi: 10.1016/j.ebiom.2019.12.004.

Höhn A, Weber D, Jung T, Ott C, Hugo M, Kochlik B, Kehm R, König J, Grune T, Castro JP. Happily (n)ever after: Aging in the context of oxidative stress, proteostasis loss and cellular senescence. Redox Biol. 2017 Apr;11:482-501. doi: 10.1016/j.redox.2016.12.001.

Horvath S, Erhart W, Brosch M, Ammerpohl O, von Schönfels W, Ahrens M, Heits N, Bell JT, Tsai PC, Spector TD, Deloukas P, Siebert R, Sipos B, Becker T, Röcken C, Schafmayer C, Hampe J. Obesity accelerates epigenetic aging of human liver. Proc Natl Acad Sci U S A. 2014 Oct 28;111(43):15538-43. doi: 10.1073/pnas.1412759111.

Horvath S. DNA methylation age of human tissues and cell types. Genome Biol. 2013;14(10):R115. doi: 10.1186/gb-2013-14-10-r115. Erratum in: Genome Biol. 2015;16:96.

Huang Y, Yan J, Hou J, Fu X, Li L, Hou Y. Developing a DNA methylation assay for human age prediction in blood and bloodstain. Forensic Sci Int Genet. 2015 Jul;17:129-136. doi: 10.1016/j.fsigen.2015.05.007.

Huh JY, Park YJ, Ham M, Kim JB. Crosstalk between adipocytes and immune cells in adipose tissue inflammation and metabolic dysregulation in obesity. Mol Cells. 2014 May; 37(5):365-71. doi: 10.14348/molcells.2014.0074.

Huynh FK, Hershberger KA, Hirschey MD. Targeting sirtuins for the treatment of diabetes. Diabetes Manag (Lond). 2013 May 1;3(3):245-257. doi: 10.2217/dmt.13.6.

InterAct Consortium, Scott RA, Langenberg C, Sharp SJ, Franks PW, Rolandsson O, Drogan D, van der Schouw YT, Ekelund U, Kerrison ND, Ardanaz E, Arriola L, Balkau B, Barricarte A, Barroso I, Bendinelli B, Beulens JW, Boeing H, de Lauzon-Guillain B, Deloukas P, Fagherazzi G, Gonzalez C, Griffin SJ, Groop LC, Halkjaer J, Huerta JM, Kaaks R, Khaw KT, Krogh V, Nilsson PM, Norat T, Overvad K, Panico S, Rodriguez-Suarez L, Romaguera D, Romieu I, Sacerdote C, Sánchez MJ, Spijkerman AM, Teucher B, Tjonneland A, Tumino R, van der A DL, Wark PA, McCarthy MI, Riboli E, Wareham NJ. The link between family history and risk of type 2 diabetes is not explained by anthropometric, lifestyle or genetic risk factors: the EPIC-InterAct study. Diabetologia. 2013 Jan;56(1):60-9. doi: 10.1007/s00125-012-2715-x.

Isakson P, Hammarstedt A, Gustafson B, Smith U. Impaired preadipocyte differentiation in human abdominal obesity: role of Wnt, tumor necrosis factor-alpha, and inflammation. Diabetes. 2009 Jul;58(7):1550-7. doi: 10.2337/db08-1770.

Issa JP. Aging and epigenetic drift: a vicious cycle. J Clin Invest. 2014 Jan;124(1):24-9. doi: 10.1172/JCI69735.

Ivanov A, Pawlikowski J, Manoharan I, van Tuyn J, Nelson DM, Rai TS, Shah PP, Hewitt G, Korolchuk VI, Passos JF, Wu H, Berger SL, Adams PD. Lysosome-mediated processing of chromatin in senescence. J Cell Biol. 2013 Jul 8;202(1):129-43. doi: 10.1083/jcb.201212110.

Janic A, Valente LJ, Wakefield MJ, Di Stefano L, Milla L, Wilcox S, Yang H, Tai L, Vandenberg CJ, Kueh AJ, Mizutani S, Brennan MS, Schenk RL, Lindqvist LM, Papenfuss AT, O'Connor L, Strasser A, Herold MJ. DNA repair processes are critical mediators of p53-dependent tumor suppression. Nat Med. 2018 Jul;24(7):947-953. doi: 10.1038/s41591-018-0043-5.

Jin B, Li Y, Robertson KD. DNA methylation: superior or subordinate in the epigenetic hierarchy? Genes Cancer. 2011 Jun;2(6):607-17. doi: 10.1177/1947601910393957.

Jones MJ, Goodman SJ, Kobor MS. DNA methylation and healthy human aging. Aging Cell. 2015 Dec;14(6):924-32. doi: 10.1111/acel.12349.

Justice JN, Gregory H, Tchkonia T, LeBrasseur NK, Kirkland JL, Kritchevsky SB, Nicklas BJ. Cellular Senescence Biomarker p16INK4a+ Cell Burden in Thigh Adipose is Associated With Poor Physical Function in Older Women. J Gerontol A Biol Sci Med Sci. 2018 Jun 14;73(7):939-945. doi: 10.1093/gerona/glx134.

Kaeser MD, Iggo RD. Promoter-specific p53-dependent histone acetylation following DNA damage. Oncogene. 2004 May 13;23(22):4007-13. doi: 10.1038/sj.onc.1207536.

Karagiannides I, Tchkonia T, Dobson DE, Steppan CM, Cummins P, Chan G, Salvatori K, Hadzopoulou-Cladaras M, Kirkland JL. Altered expression of C/EBP family members results in decreased adipogenesis with aging. Am J Physiol Regul Integr Comp Physiol. 2001 Jun;280(6):R1772-80. doi: 10.1152/ajpregu.2001.280.6.R1772.

Karakelides H, Irving BA, Short KR, O'Brien P, Nair KS. Age, obesity, and sex effects on insulin sensitivity and skeletal muscle mitochondrial function. Diabetes. 2010 Jan;59(1):89-97. doi: 10.2337/db09-0591.

Keller M, Hopp L, Liu X, Wohland T, Rohde K, Cancello R, Klös M, Bacos K, Kern M, Eichelmann F, Dietrich A, Schön MR, Gärtner D, Lohmann T, Dreßler M, Stumvoll M, Kovacs P, DiBlasio AM, Ling C, Binder H, Blüher M, Böttcher Y. Genome-wide DNA promoter methylation and transcriptome analysis in human adipose tissue unravels novel candidate genes for obesity. Mol Metab. 2016 Nov 16;6(1):86-100. doi: 10.1016/j.molmet.2016.11.003.

Khan MAB, Hashim MJ, King JK, Govender RD, Mustafa H, Al Kaabi J. Epidemiology of Type 2 Diabetes - Global Burden of Disease and Forecasted Trends. J Epidemiol Glob Health. 2020 Mar;10(1):107-111. doi: 10.2991/jegh.k.191028.001.

Khosla S, Farr JN, Tchkonia T, Kirkland JL. The role of cellular senescence in ageing and endocrine disease. Nat Rev Endocrinol. 2020 May;16(5):263-275. doi: 10.1038/s41574-020-0335-y.

Kim C, Kang D, Lee EK, Lee JS. Long Noncoding RNAs and RNA-Binding Proteins in Oxidative Stress, Cellular Senescence, and Age-Related Diseases. Oxid Med Cell Longev. 2017;2017:2062384. doi: 10.1155/2017/2062384.

Kim SR, Jiang K, Ogrodnik M, Chen X, Zhu XY, Lohmeier H, Ahmed L, Tang H, Tchkonia T, Hickson LJ, Kirkland JL, Lerman LO. Increased renal cellular senescence in murine high-fat diet: effect of the senolytic drug quercetin. Transl Res. 2019 Nov;213:112-123. doi: 10.1016/j.trsl.2019.07.005.

Kintscher U, Law RE. PPARgamma-mediated insulin sensitization: the importance of fat versus muscle. Am J Physiol Endocrinol Metab. 2005 Feb;288(2):E287-91. doi: 10.1152/ajpendo.00440.2004.

Kirchner H, Sinha I, Gao H, Ruby MA, Schönke M, Lindvall JM, Barrès R, Krook A, Näslund E, Dahlman-Wright K, Zierath JR. Altered DNA methylation of glycolytic and lipogenic genes in liver from obese and type 2 diabetic patients. Mol Metab. 2016 Jan 2;5(3):171-183. doi: 10.1016/j.molmet.2015.12.004.

Kirkland JL, Hollenberg CH, Kindler S, Gillon WS. Effects of age and anatomic site on preadipocyte number in rat fat depots. J Gerontol. 1994 Jan;49(1):B31-5. doi: 10.1093/geronj/49.1.b31.

Kirkland JL, Khosla S. Targeting cellular senescence prevents age-related bone loss in mice. Nat Med. 2017 Sep;23(9):1072-1079. doi: 10.1038/nm.4385.

Kirkland JL, Tchkonia T, Pirtskhalava T, Han J, Karagiannides I. Adipogenesis and aging: does aging make fat go MAD? Exp Gerontol. 2002 Jun;37(6):757-67. doi: 10.1016/s0531-5565(02)00014-1.

Kirkland JL, Tchkonia T. Cellular Senescence: A Translational Perspective. EBioMedicine. 2017 Jul; 21:21-28. doi: 10.1016/j.ebiom.2017.04.013.

Kirkland JL, Tchkonia T. Senolytic drugs: from discovery to translation. J Intern Med. 2020 Nov;288(5):518-536. doi: 10.1111/joim.13141.

Krstic J, Reinisch I, Schupp M, Schulz TJ, Prokesch A. p53 Functions in Adipose Tissue Metabolism and Homeostasis. Int J Mol Sci. 2018 Sep 4;19(9):2622. doi: 10.3390/ijms19092622.

Kuk JL, Saunders TJ, Davidson LE, Ross R. Age-related changes in total and regional fat distribution. Ageing Res Rev. 2009 Oct;8(4):339-48. doi: 10.1016/j.arr.2009.06.001.

Kumari R, Jat P. Mechanisms of Cellular Senescence: Cell Cycle Arrest and Senescence Associated Secretory Phenotype. Front Cell Dev Biol. 2021 Mar 29;9:645593. doi: 10.3389/fcell.2021.645593.

Kyle UG, Genton L, Hans D, Karsegard VL, Michel JP, Slosman DO, Pichard C. Total body mass, fat mass, fat-free mass, and skeletal muscle in older people: cross-sectional differences in 60-year-old persons. J Am Geriatr Soc. 2001 Dec;49(12):1633-40. doi: 10.1046/j.1532-5415.2001.t01-1-49272.x.

Laakso M, Zilinskaite J, Hansen T, Boesgaard TW, Vänttinen M, Stancáková A, Jansson PA, Pellmé F, Holst JJ, Kuulasmaa T, Hribal ML, Sesti G, Stefan N, Fritsche A, Häring H, Pedersen O, Smith U; EUGENE2 Consortium. Insulin sensitivity, insulin release and glucagon-like peptide-1 levels in persons with impaired fasting glucose and/or impaired glucose tolerance in the EUGENE2 study. Diabetologia. 2008 Mar;51(3):502-11. doi: 10.1007/s00125-007-0899-2.

Lakowa N, Trieu N, Flehmig G, Lohmann T, Schön MR, Dietrich A, Zeplin PH, Langer S, Stumvoll M, Blüher M, Klöting N. Telomere length differences between subcutaneous and visceral adipose tissue in humans. Biochem Biophys Res Commun. 2015 Feb 13;457(3):426-32. doi: 10.1016/j.bbrc.2014.12.122.

Laptenko O, Beckerman R, Freulich E, Prives C. p53 binding to nucleosomes within the p21 promoter in vivo leads to nucleosome loss and transcriptional activation. Proc Natl Acad Sci U S A. 2011 Jun 28;108(26):10385-90. doi: 10.1073/pnas.1105680108.

Lee YK, Chung Y, Lee JH, Chun JM, Park JH. The Intricate Role of p53 in Adipocyte Differentiation and Function. Cells. 2020 Dec 7;9(12):2621. doi: 10.3390/cells9122621.

Lefterova MI, Zhang Y, Steger DJ, Schupp M, Schug J, Cristancho A, Feng D, Zhuo D, Stoeckert CJ Jr, Liu XS, Lazar MA. PPARgamma and C/EBP factors orchestrate adipocyte biology via adjacent binding on a genome-wide scale. Genes Dev. 2008 Nov 1;22(21):2941-52. doi: 10.1101/gad.1709008.

Lehrke M, Lazar MA. The many faces of PPARgamma. Cell. 2005 Dec 16;123(6):993-9. doi: 10.1016/j.cell.2005.11.026.

Lekka E, Hall J. Noncoding RNAs in disease. FEBS Lett. 2018 Sep;592(17):2884-2900. doi: 10.1002/1873-3468.13182.

Leslie R, O'Donnell CJ, Johnson AD. GRASP: analysis of genotype-phenotype results from 1390 genome-wide association studies and corresponding open access database. Bioinformatics. 2014 Jun 15;30(12):i185-94. doi: 10.1093/bioinformatics/btu273.

Lewis-McDougall FC, Ruchaya PJ, Domenjo-Vila E, Shin Teoh T, Prata L, Cottle BJ, Clark JE, Punjabi PP, Awad W, Torella D, Tchkonia T, Kirkland JL, Ellison-Hughes GM. Aged-senescent cells contribute to impaired heart regeneration. Aging Cell. 2019 Jun;18(3):e12931. doi: 10.1111/acel.12931.

Li Q, Xiao M, Shi Y, Hu J, Bi T, Wang C, Yan L, Li X. eIF5B regulates the expression of PD-L1 in prostate cancer cells by interacting with Wig1. BMC Cancer. 2021 Sep 15;21(1):1022. doi: 10.1186/s12885-021-08749-w.

Li Y, Yun K, Mu R. A review on the biology and properties of adipose tissue macrophages involved in adipose tissue physiological and pathophysiological processes. Lipids Health Dis. 2020 Jul 9;19(1):164. doi: 10.1186/s12944-020-01342-3.

Ling C, Groop L. Epigenetics: a molecular link between environmental factors and type 2 diabetes. Diabetes. 2009 Dec; 58(12):2718-25. doi: 10.2337/db09-1003.

Ling C, Rönn T. Epigenetics in Human Obesity and Type 2 Diabetes. Cell Metab. 2019 May 7;29(5):1028-1044. doi: 10.1016/j.cmet.2019.03.009.

Liu Z, Wu KKL, Jiang X, Xu A, Cheng KKY. The role of adipose tissue senescence in obesity- and ageing-related metabolic disorders. Clin Sci (Lond). 2020 Jan 31;134(2):315-330. doi: 10.1042/CS20190966.

Long MD, Smiraglia DJ, Campbell MJ. The Genomic Impact of DNA CpG Methylation on Gene Expression; Relationships in Prostate Cancer. Biomolecules. 2017 Feb 14;7(1):15. doi: 10.3390/biom7010015.

Longo M, Spinelli R, D'Esposito V, Zatterale F, Fiory F, Nigro C, Raciti GA, Miele C, Formisano P, Beguinot F, Di Jeso B. Pathologic endoplasmic reticulum stress induced by glucotoxic insults inhibits adipocyte differentiation and induces an inflammatory phenotype. Biochim Biophys Acta. 2016 Jun;1863(6 Pt A):1146-56. doi: 10.1016/j.bbamcr.2016.02.019.

Longo M, Zatterale F, Naderi J, Parrillo L, Formisano P, Raciti GA, Beguinot F, Miele C. Adipose Tissue Dysfunction as Determinant of Obesity-Associated Metabolic Complications. Int J Mol Sci. 2019 May 13;20(9):2358. doi: 10.3390/ijms20092358.

Lu B, Huang L, Cao J, Li L, Wu W, Chen X, Ding C. Adipose tissue macrophages in aging-associated adipose tissue function. J Physiol Sci. 2021 Dec 4;71(1):38. doi: 10.1186/s12576-021-00820-2.

Luczak MW, Zhitkovich A. Nickel-induced HIF-1α promotes growth arrest and senescence in normal human cells but lacks toxic effects in transformed cells. Toxicol Appl Pharmacol. 2017 Sep 15;331:94-100. doi: 10.1016/j.taap.2017.05.029.

Lujambio A, Calin GA, Villanueva A, Ropero S, Sánchez-Céspedes M, Blanco D, Montuenga LM, Rossi S, Nicoloso MS, Faller WJ, Gallagher WM, Eccles SA, Croce CM, Esteller M. A microRNA DNA methylation signature for human cancer metastasis. Proc Natl Acad Sci U S A. 2008 Sep 9;105(36):13556-61. doi: 10.1073/pnas.0803055105.

Madsen MS, Siersbæk R, Boergesen M, Nielsen R, Mandrup S. Peroxisome proliferator-activated receptor γ and C/EBPα synergistically activate key metabolic adipocyte genes by assisted loading. Mol Cell Biol. 2014 Mar;34(6):939-54. doi: 10.1128/MCB.01344-13.

Marthandan S, Baumgart M, Priebe S, Groth M, Schaer J, Kaether C, Guthke R, Cellerino A, Platzer M, Diekmann S, Hemmerich P. Conserved Senescence Associated Genes and Pathways in Primary Human Fibroblasts Detected by RNA-Seq. PLoS One. 2016 May 3;11(5):e0154531. doi: 10.1371/journal.pone.0154531.

Mattick JS, Makunin IV. Non-coding RNA. Hum Mol Genet. 2006 Apr 15;15 Spec No 1:R17-29. doi: 10.1093/hmg/ddl046.

Mau T, Yung R. Adipose tissue inflammation in aging. Exp Gerontol. 2018 May; 105:27-31. doi: 10.1016/j.exger.2017.10.014.

McHugh D, Gil J. Senescence and aging: Causes, consequences, and therapeutic avenues. J Cell Biol. 2018 Jan 2;217(1):65-77. doi: 10.1083/jcb.201708092.

Meigs JB, Cupples LA, Wilson PW. Parental transmission of type 2 diabetes: the Framingham Offspring Study. Diabetes. 2000 Dec;49(12):2201-7. doi: 10.2337/diabetes.49.12.2201.

Mendioroz M, Do C, Jiang X, Liu C, Darbary HK, Lang CF, Lin J, Thomas A, Abu-Amero S, Stanier P, Temkin A, Yale A, Liu MM, Li Y, Salas M, Kerkel K, Capone G, Silverman W, Yu YE, Moore G, Wegiel J, Tycko B. Erratum to: Trans effects of chromosome aneuploidies on DNA methylation patterns in human Down syndrome and mouse models. Genome Biol. 2016 Jun 9;17(1):123. doi: 10.1186/s13059-016-0949-5. Erratum for: Genome Biol. 2015 Nov 25;16:263. doi: 10.1186/s13059-015-0827-6.

Meng RD, EL-Deiry WS. CHAPTER 17 - Cancer Gene Therapy with Tumor Suppressor Genes Involved in Cell-Cycle Control. Gene Therapy of Cancer (Second Edition), Academic Press. 2002; Pages 279-297. doi: 10.1016/B978-012437551-2/50018-5.

Minamino T, Orimo M, Shimizu I, Kunieda T, Yokoyama M, Ito T, Nojima A, Nabetani A, Oike Y, Matsubara H, Ishikawa F, Komuro I. A crucial role for adipose tissue p53 in the regulation of insulin resistance. Nat Med. 2009 Sep;15(9):1082-7. doi: 10.1038/nm.2014.

Mirra P, Desiderio A, Spinelli R, Nigro C, Longo M, Parrillo L, D'Esposito V, Carissimo A, Hedjazifar S, Smith U, Formisano P, Miele C, Raciti GA, Beguinot F. Adipocyte precursor cells from first degree relatives of type 2 diabetic patients feature changes in hsa-mir-23a-5p, -193a-5p, and -193b-5p and insulin-like growth factor 2 expression. FASEB J. 2021 Apr;35(4):e21357. doi: 10.1096/fj.202002156RRR.

Mitterberger MC, Lechner S, Mattesich M, Zwerschke W. Adipogenic differentiation is impaired in replicative senescent human subcutaneous adipose-derived stromal/progenitor cells. J Gerontol A Biol Sci Med Sci. 2014 Jan;69(1):13-24. doi: 10.1093/gerona/glt043.

Monickaraj F, Gokulakrishnan K, Prabu P, Sathishkumar C, Anjana RM, Rajkumar JS, Mohan V, Balasubramanyam M. Convergence of adipocyte hypertrophy, telomere shortening and hypoadiponectinemia in obese subjects and in patients with type 2 diabetes. Clin Biochem. 2012 Nov;45(16-17):1432-8. doi: 10.1016/j.clinbiochem.2012.07.097.

Moore LD, Le T, Fan G. DNA methylation and its basic function. Neuropsychopharmacology. 2013 Jan;38(1):23-38. doi: 10.1038/npp.2012.112.

Most J, Tosti V, Redman LM, Fontana L. Calorie restriction in humans: An update. Ageing Res Rev. 2017 Oct;39:36-45. doi: 10.1016/j.arr.2016.08.005.

Muñoz-Espín D, Serrano M. Cellular senescence: from physiology to pathology. Nat Rev Mol Cell Biol. 2014 Jul;15(7):482-96. doi: 10.1038/nrm3823.

Nacarelli T, Liu P, Zhang R. Epigenetic Basis of Cellular Senescence and Its Implications in Aging. Genes (Basel). 2017 Nov 24;8(12):343. doi: 10.3390/genes8120343.

Nelson G, Wordsworth J, Wang C, Jurk D, Lawless C, Martin-Ruiz C, von Zglinicki T. A senescent cell bystander effect: senescence-induced senescence. Aging Cell. 2012 Apr;11(2):345-9. doi: 10.1111/j.1474-9726.2012.00795.x.

Nigita G, Marceca GP, Tomasello L, Distefano R, Calore F, Veneziano D, Romano G, Nana-Sinkam SP, Acunzo M, Croce CM. ncRNA Editing: Functional Characterization and Computational Resources. Methods Mol Biol. 2019;1912:133-174. doi: 10.1007/978-1-4939-8982-9_6.

Nigro C, Leone A, Longo M, Prevenzano I, Fleming TH, Nicolò A, Parrillo L, Spinelli R, Formisano P, Nawroth PP, Beguinot F, Miele C. Methylglyoxal accumulation de-regulates HoxA5 expression, thereby impairing angiogenesis in glyoxalase 1 knock-down mouse aortic endothelial cells. Biochim Biophys Acta Mol Basis Dis. 2019 Jan;1865(1):73-85. doi: 10.1016/j.bbadis.2018.10.014.

Nilsson E, Ling C. DNA methylation links genetics, fetal environment, and an unhealthy lifestyle to the development of type 2 diabetes. Clin Epigenetics. 2017 Oct 3;9:105. doi: 10.1186/s13148-017-0399-2.

Novais EJ, Tran VA, Johnston SN, Darris KR, Roupas AJ, Sessions GA, Shapiro IM, Diekman BO, Risbud MV. Long-term treatment with senolytic drugs Dasatinib and Quercetin ameliorates age-

dependent intervertebral disc degeneration in mice. Nat Commun. 2021 Sep 3;12(1):5213. doi: 10.1038/s41467-021-25453-2.

Ogrodnik M, Zhu Y, Langhi LGP, Tchkonia T, Krüger P, Fielder E, Victorelli S, Ruswhandi RA, Giorgadze N, Pirtskhalava T, Podgorni O, Enikolopov G, Johnson KO, Xu M, Inman C, Palmer AK, Schafer M, Weigl M, Ikeno Y, Burns TC, Passos JF, von Zglinicki T, Kirkland JL, Jurk D. Obesity-Induced Cellular Senescence Drives Anxiety and Impairs Neurogenesis. Cell Metab. 2019 May 7;29(5):1061-1077.e8. doi: 10.1016/j.cmet.2018.12.008.

Oñate B, Vilahur G, Ferrer-Lorente R, Ybarra J, Díez-Caballero A, Ballesta-López C, Moscatiello F, Herrero J, Badimon L. The subcutaneous adipose tissue reservoir of functionally active stem cells is reduced in obese patients. FASEB J. 2012 Oct;26(10):4327-36. doi: 10.1096/fj.12-207217.

Onyango EM, Onyango BM. The Rise of Noncommunicable Diseases in Kenya: An Examination of the Time Trends and Contribution of the Changes in Diet and Physical Inactivity. J Epidemiol Glob Health. 2018 Dec;8(1-2):1-7. doi: 10.2991/j.jegh.2017.11.004.

Ortega Martinez de Victoria E, Xu X, Koska J, Francisco AM, Scalise M, Ferrante AW Jr, Krakoff J. Macrophage content in subcutaneous adipose tissue: associations with adiposity, age, inflammatory markers, and whole-body insulin action in healthy Pima Indians. Diabetes. 2009 Feb;58(2):385-93. doi: 10.2337/db08-0536. Epub 2008 Nov 13.

Pal S, Tyler JK. Epigenetics and aging. Sci Adv. 2016 Jul 29;2(7):e1600584. doi: 10.1126/sciadv.1600584.

Palmer AK, Kirkland JL. Aging and adipose tissue: potential interventions for diabetes and regenerative medicine. Exp Gerontol. 2016 Dec 15;86:97-105. doi: 10.1016/j.exger.2016.02.013. Epub 2016 Feb 26.

Palmer AK, Tchkonia T, LeBrasseur NK, Chini EN, Xu M, Kirkland JL. Cellular Senescence in Type 2 Diabetes: A Therapeutic Opportunity. Diabetes. 2015 Jul;64(7):2289-98. doi: 10.2337/db14-1820.

Palmer AK, Xu M, Zhu Y, Pirtskhalava T, Weivoda MM, Hachfeld CM, Prata LG, van Dijk TH, Verkade E, Casaclang-Verzosa G, Johnson KO, Cubro H, Doornebal EJ, Ogrodnik M, Jurk D, Jensen MD, Chini EN, Miller JD, Matveyenko A, Stout MB, Schafer MJ, White TA, Hickson LJ, Demaria M, Garovic V, Grande J, Arriaga EA, Kuipers F, von Zglinicki T, LeBrasseur NK, Campisi J, Tchkonia T, Kirkland JL. Targeting senescent cells alleviates obesity-induced metabolic dysfunction. Aging Cell. 2019 Jun;18(3):e12950. doi: 10.1111/acel.12950.

Pararasa C, Bailey CJ, Griffiths HR. Ageing, adipose tissue, fatty acids and inflammation. Biogerontology. 2015 Apr;16(2):235-48. doi: 10.1007/s10522-014-9536-x.

Parikh N, Hilsenbeck S, Creighton CJ, Dayaram T, Shuck R, Shinbrot E, Xi L, Gibbs RA, Wheeler DA, Donehower LA. Effects of TP53 mutational status on gene expression patterns across 10 human cancer types. J Pathol. 2014 Apr;232(5):522-33. doi: 10.1002/path.4321.

Parrillo L, Costa V, Raciti GA, Longo M, Spinelli R, Esposito R, Nigro C, Vastolo V, Desiderio A, Zatterale F, Ciccodicola A, Formisano P, Miele C, Beguinot F. Hoxa5 undergoes dynamic DNA methylation and transcriptional repression in the adipose tissue of mice exposed to high-fat diet. Int J Obes (Lond). 2016 Jun;40(6):929-37. doi: 10.1038/ijo.2016.36.

Parrillo L, Spinelli R, Longo M, Desiderio A, Mirra P, Nigro C, Fiory F, Hedjazifar S, Mutarelli M, Carissimo A, Formisano P, Miele C, Smith U, Raciti GA, Beguinot F. Altered PTPRD DNA methylation associates with restricted adipogenesis in healthy first-degree relatives of Type 2 diabetes subjects. Epigenomics. 2020 May;12(10):873-888. doi: 10.2217/epi-2019-0267.

Parrillo L, Spinelli R, Nicolò A, Longo M, Mirra P, Raciti GA, Miele C, Beguinot F. Nutritional Factors, DNA Methylation, and Risk of Type 2 Diabetes and Obesity: Perspectives and Challenges. Int J Mol Sci. 2019 Jun 19;20(12):2983. doi: 10.3390/ijms20122983.

Peterson CL, Laniel MA. Histones and histone modifications. Curr Biol. 2004 Jul 27;14(14):R546-51. doi: 10.1016/j.cub.2004.07.007.

Pirone L, Smaldone G, Spinelli R, Barberisi M, Beguinot F, Vitagliano L, Miele C, Di Gaetano S, Raciti GA, Pedone E. KCTD1: A novel modulator of adipogenesis through the interaction with the transcription factor AP2α. Biochim Biophys Acta Mol Cell Biol Lipids. 2019 Dec;1864(12):158514. doi: 10.1016/j.bbalip.2019.08.010.

Poulain-Godefroy O, Le Bacquer O, Plancq P, Lecoeur C, Pattou F, Frühbeck G, Froguel P. Inflammatory role of Toll-like receptors in human and murine adipose tissue. Mediators Inflamm. 2010; 2010:823486. doi: 10.1155/2010/823486.

Raciti GA, Fiory F, Campitelli M, Desiderio A, Spinelli R, Longo M, Nigro C, Pepe G, Sommella E, Campiglia P, Formisano P, Beguinot F, Miele C. Citrus aurantium L. dry extracts promote C/ebpβ expression and improve adipocyte differentiation in 3T3-L1 cells. PLoS One. 2018 Mar 29;13(3):e0193704. doi: 10.1371/journal.pone.0193704.

Raciti GA, Spinelli R, Desiderio A, Longo M, Parrillo L, Nigro C, D'Esposito V, Mirra P, Fiory F, Pilone V, Forestieri P, Formisano P, Pastan I, Miele C, Beguinot F. Specific CpG hyper-methylation leads to Ankrd26 gene down-regulation in white adipose tissue of a mouse model of diet-induced obesity. Sci Rep. 2017 Mar 7;7:43526. doi: 10.1038/srep43526.

Raciti GA, Spinelli R, Desiderio A, Longo M, Parrillo L, Nigro C, D'Esposito V, Mirra P, Fiory F, Pilone V, Forestieri P, Formisano P, Pastan I, Miele C, Beguinot F. Specific CpG hyper-methylation leads to Ankrd26 gene down-regulation in white adipose tissue of a mouse model of diet-induced obesity. Sci Rep. 2017 Mar 7;7:43526. doi: 10.1038/srep43526.

Ramirez-Carrozzi VR, Braas D, Bhatt DM, Cheng CS, Hong C, Doty KR, Black JC, Hoffmann A, Carey M, Smale ST. A unifying model for the selective regulation of inducible transcription by CpG islands and nucleosome remodeling. Cell. 2009 Jul 10;138(1):114-28. doi: 10.1016/j.cell.2009.04.020.

Ramtahal R, Khan C, Maharaj-Khan K, Nallamothu S, Hinds A, Dhanoo A, Yeh HC, Hill-Briggs F, Lazo M. Prevalence of self-reported sleep duration and sleep habits in type 2 diabetes patients in South Trinidad. J Epidemiol Glob Health. 2015 Dec;5(4 Suppl 1): S35-43. doi: 10.1016/j.jegh.2015.05.003.

Ratushnyy A, Ezdakova M, Buravkova L. Secretome of Senescent Adipose-Derived Mesenchymal Stem Cells Negatively Regulates Angiogenesis. Int J Mol Sci. 2020 Mar 5;21(5):1802. doi: 10.3390/ijms21051802.

Reconstructive fat grafting Geoffrey C. Gurtner MD, FACS, in Plastic Surgery: Volume 1: Principles, 2018.

Richard AJ, White U, Elks CM, Stephens JM. Adipose Tissue: Physiology to Metabolic Dysfunction. 2020 Apr 4. In: Feingold KR, Anawalt B, Boyce A, Chrousos G, de Herder WW, Dhatariya K, Dungan K, Hershman JM, Hofland J, Kalra S, Kaltsas G, Koch C, Kopp P, Korbonits M, Kovacs CS, Kuohung W, Laferrère B, Levy M, McGee EA, McLachlan R, Morley JE, New M, Purnell J, Sahay R, Singer F, Sperling MA, Stratakis CA, Trence DL, Wilson DP, editors. Endotext [Internet]. South Dartmouth (MA): MDText.com, Inc.; 2000–.

Robbins PD, Jurk D, Khosla S, Kirkland JL, LeBrasseur NK, Miller JD, Passos JF, Pignolo RJ, Tchkonia T, Niedernhofer LJ. Senolytic Drugs: Reducing Senescent Cell Viability to Extend Health Span. Annu Rev Pharmacol Toxicol. 2021 Jan 6;61:779-803. doi: 10.1146/annurev-pharmtox-050120-105018

Rönn T, Volkov P, Gillberg L, Kokosar M, Perfilyev A, Jacobsen AL, Jørgensen SW, Brøns C, Jansson PA, Eriksson KF, Pedersen O, Hansen T, Groop L, Stener-Victorin E, Vaag A, Nilsson E, Ling C. Impact of age, BMI and HbA1c levels on the genome-wide DNA methylation and mRNA expression patterns in human adipose tissue and identification of epigenetic biomarkers in blood. Hum Mol Genet. 2015 Jul 1;24(13):3792-813. doi: 10.1093/hmg/ddv124.

Roos CM, Zhang B, Palmer AK, Ogrodnik MB, Pirtskhalava T, Thalji NM, Hagler M, Jurk D, Smith LA, Casaclang-Verzosa G, Zhu Y, Schafer MJ, Tchkonia T, Kirkland JL, Miller JD. Chronic senolytic treatment alleviates established vasomotor dysfunction in aged or atherosclerotic mice. Aging Cell. 2016 Oct;15(5):973-7. doi: 10.1111/acel.12458.

Rosen ED, Hsu CH, Wang X, Sakai S, Freeman MW, Gonzalez FJ, Spiegelman BM. C/EBPalpha induces adipogenesis through PPARgamma: a unified pathway. Genes Dev. 2002 Jan 1;16(1):22-6. doi: 10.1101/gad.948702.

Rosen ED, Walkey CJ, Puigserver P, Spiegelman BM. Transcriptional regulation of adipogenesis. Genes Dev. 2000 Jun 1;14(11):1293-307.

Rovillain E, Mansfield L, Caetano C, Alvarez-Fernandez M, Caballero OL, Medema RH, Hummerich H, Jat PS. Activation of nuclear factor-kappa B signalling promotes cellular senescence. Oncogene. 2011 May 19;30(20):2356-66. doi: 10.1038/onc.2010.611.

Rufini A, Tucci P, Celardo I, Melino G. Senescence and aging: the critical roles of p53. Oncogene. 2013 Oct 24;32(43):5129-43. doi: 10.1038/onc.2012.640.

Ruotsalainen E, Salmenniemi U, Vauhkonen I, Pihlajamäki J, Punnonen K, Kainulainen S, Laakso M. Changes in inflammatory cytokines are related to impaired glucose tolerance in offspring of type 2 diabetic subjects. Diabetes Care. 2006 Dec;29(12):2714-20. doi: 10.2337/dc06-0147.

Russell, P. J. (2010). iGenetics: A Molecular Approach. San Francisco, CA: Pearson Education, Inc.

Schafer MJ, White TA, Evans G, Tonne JM, Verzosa GC, Stout MB, Mazula DL, Palmer AK, Baker DJ, Jensen MD, Torbenson MS, Miller JD, Ikeda Y, Tchkonia T, van Deursen JM, Kirkland JL, LeBrasseur NK. Exercise Prevents Diet-Induced Cellular Senescence in Adipose Tissue. Diabetes. 2016 Jun;65(6):1606-15. doi: 10.2337/db15-0291.

Schafer MJ, White TA, Iijima K, Haak AJ, Ligresti G, Atkinson EJ, Oberg AL, Birch J, Salmonowicz H, Zhu Y, Mazula DL, Brooks RW, Fuhrmann-Stroissnigg H, Pirtskhalava T, Prakash YS, Tchkonia T, Robbins PD, Aubry MC, Passos JF, Kirkland JL, Tschumperlin DJ, Kita H, LeBrasseur NK.

Cellular senescence mediates fibrotic pulmonary disease. Nat Commun. 2017 Feb 23;8:14532. doi: 10.1038/ncomms14532.

Schipper BM, Marra KG, Zhang W, Donnenberg AD, Rubin JP. Regional anatomic and age effects on cell function of human adipose-derived stem cells. Ann Plast Surg. 2008 May;60(5):538-44. doi: 10.1097/SAP.0b013e3181723bbe.

Schosserer M, Grillari J, Wolfrum C, Scheideler M. Age-Induced Changes in White, Brite, and Brown Adipose Depots: A Mini-Review. Gerontology. 2018;64(3):229-236. doi: 10.1159/000485183

Scully T, Ettela A, LeRoith D, Gallagher EJ. Obesity, Type 2 Diabetes, and Cancer Risk. Front Oncol. 2021 Feb 2; 10:615375. doi: 10.3389/fonc.2020.615375.

Sepe A, Tchkonia T, Thomou T, Zamboni M, Kirkland JL. Aging and regional differences in fat cell progenitors - a mini-review. Gerontology. 2011;57(1):66-75. doi: 10.1159/000279755.

Seto E, Yoshida M. Erasers of histone acetylation: the histone deacetylase enzymes. Cold Spring Harb Perspect Biol. 2014 Apr 1;6(4):a018713. doi: 10.1101/cshperspect.a018713.

Seydoux G. Mechanisms of translational control in early development. Curr Opin Genet Dev. 1996 Oct; 6(5):555-61. doi: 10.1016/s0959-437x(96)80083-9.

Sidler C, Kovalchuk O, Kovalchuk I. Epigenetic Regulation of Cellular Senescence and Aging. Front Genet. 2017 Sep 26;8:138. doi: 10.3389/fgene.2017.00138.

Sierra F, Kohanski R. Advances in geroscience. Springer 2016. doi: 10.1007/978-3-319-23246-1

Skurk T, Alberti-Huber C, Herder C, Hauner H. Relationship between adipocyte size and adipokine expression and secretion. J Clin Endocrinol Metab. 2007 Mar;92(3):1023-33. doi: 10.1210/jc.2006-1055.

Smith U, Kahn BB. Adipose tissue regulates insulin sensitivity: role of adipogenesis, de novo lipogenesis and novel lipids. J Intern Med. 2016 Nov;280(5):465-475. doi: 10.1111/joim.12540.

So AY, Jung JW, Lee S, Kim HS, Kang KS. DNA methyltransferase controls stem cell aging by regulating BMI1 and EZH2 through microRNAs. PLoS One. 2011 May 10;6(5):e19503. doi: 10.1371/journal.pone.0019503.

Sohn D, Graupner V, Neise D, Essmann F, Schulze-Osthoff K, Jänicke RU. Pifithrin-alpha protects against DNA damage-induced apoptosis downstream of mitochondria independent of p53. Cell Death Differ. 2009 Jun;16(6):869-78. doi: 10.1038/cdd.2009.17.

Somnath P. Modifiable Risk Factors for Diabetes Complications. US Pharm. 2019 Oct; 44(10):15

Song S, Lam EW, Tchkonia T, Kirkland JL, Sun Y. Senescent Cells: Emerging Targets for Human Aging and Age-Related Diseases. Trends Biochem Sci. 2020 Jul;45(7):578-592. doi: 10.1016/j.tibs.2020.03.008.

Spinelli R, Florese P, Parrillo L, Zatterale F, Longo M, D'Esposito V, Desiderio A, Nerstedt A, Gustafson B, Formisano P, Miele C, Raciti GA, Napoli R, Smith U, Beguinot F. ZMAT3 hypomethylation contributes to early senescence of preadipocytes from healthy first-degree relatives of type 2 diabetics. Aging Cell. 2022 Mar;21(3): e13557. doi: 10.1111/acel.13557.

Spinelli R, Parrillo L, Longo M, Florese P, Desiderio A, Zatterale F, Miele C, Raciti GA, Beguinot F. Molecular basis of ageing in chronic metabolic diseases. J Endocrinol Invest. 2020 Oct;43(10):1373-1389. doi: 10.1007/s40618-020-01255-z.

Spranger J, Kroke A, Möhlig M, Hoffmann K, Bergmann MM, Ristow M, Boeing H, Pfeiffer AF. Inflammatory cytokines and the risk to develop type 2 diabetes: results of the prospective population-based European Prospective Investigation into Cancer and Nutrition (EPIC)-Potsdam Study. Diabetes. 2003 Mar;52(3):812-7. doi: 10.2337/diabetes.52.3.812.

Stančáková A, Laakso M. Genetics of Type 2 Diabetes. Endocr Dev. 2016;31:203-20. doi: 10.1159/000439418.

Stevenson AJ, McCartney DL, Harris SE, Taylor AM, Redmond P, Starr JM, Zhang Q, McRae AF, Wray NR, Spires-Jones TL, McColl BW, McIntosh AM, Deary IJ, Marioni RE. Trajectories of inflammatory biomarkers over the eighth decade and their associations with immune cell profiles and epigenetic ageing. Clin Epigenetics. 2018 Dec 20;10(1):159. doi: 10.1186/s13148-018-0585-x.

Stout MB, Justice JN, Nicklas BJ, Kirkland JL. Physiological Aging: Links Among Adipose Tissue Dysfunction, Diabetes, and Frailty. Physiology (Bethesda). 2017 Jan;32(1):9-19. doi: 10.1152/physiol.00012.2016.

Stout MB, Tchkonia T, Kirkland JL (2014) The aging adipose organ: lipid redistribution, inflammation, and cellular senescence. In: Fantuzzi G, Braunschweig C (eds) Adipose tissue and adipokines in health and disease. Nutrition and Health. Humana Press, Totowa

Stout MB, Tchkonia T, Kirkland JL (2014) The aging adipose organ: lipid redistribution, inflammation, and cellular senescence. In: Fantuzzi G, Braunschweig C (eds) Adipose tissue and adipokines in health and disease. Nutrition and Health. Humana Press, Totowa29. López-Otín C, Blasco MA, Partridge L, Serrano M, Kroemer G (2013) The hallmarks of aging. Cell 153:1194–1217. doi: 10.1016/j.cell.2013.05.039

Strazhesko I, Tkacheva O, Boytsov S, Akasheva D, Dudinskaya E, Vygodin V, Skvortsov D, Nilsson P. Association of Insulin Resistance, Arterial Stiffness and Telomere Length in Adults Free of Cardiovascular Diseases. PLoS One. 2015 Aug 26;10(8):e0136676. doi: 10.1371/journal.pone.0136676.

Strycharz J, Drzewoski J, Szemraj J, Sliwinska A. Erratum to "Is p53 Involved in Tissue-Specific Insulin Resistance Formation?". Oxid Med Cell Longev. 2017;2017:8036902. doi: 10.1155/2017/8036902

Stumvoll M, Goldstein BJ, van Haeften TW. Type 2 diabetes: principles of pathogenesis and therapy. Lancet. 2005 Apr; 365(9467):1333-46. doi: 10.1016/S0140-6736(05)61032-X.

Sturm G, Cardenas A, Bind MA, Horvath S, Wang S, Wang Y, Hägg S, Hirano M, Picard M. Human aging DNA methylation signatures are conserved but accelerated in cultured fibroblasts. Epigenetics. 2019 Oct;14(10):961-976. doi: 10.1080/15592294.2019.1626651.

Tchkonia T, Corkey BE, Kirkland JL (2006a) Current views of the fat cell as an endocrine cell: lipotoxicity. Endocr. Updates 26, 105– 118.

Tchkonia T, Giorgadze N, Pirtskhalava T, Tchoukalova Y, Karagiannides I, Forse RA, DePonte M, Stevenson M, Guo W, Han J, Waloga G, Lash TL, Jensen MD, Kirkland JL. Fat depot origin affects adipogenesis in primary cultured and cloned human preadipocytes. Am J Physiol Regul Integr Comp Physiol. 2002 May;282(5):R1286-96. doi: 10.1152/ajpregu.00653.2001.

Tchkonia T, Giorgadze N, Pirtskhalava T, Thomou T, DePonte M, Koo A, Forse RA, Chinnappan D, Martin-Ruiz C, von Zglinicki T, Kirkland JL. Fat depot-specific characteristics are retained in strains derived from single human preadipocytes. Diabetes. 2006 Sep;55(9):2571-8. doi: 10.2337/db06-0540.

Tchkonia T, Kirkland JL. Aging, Cell Senescence, and Chronic Disease: Emerging Therapeutic Strategies. JAMA. 2018 Oct 2;320(13):1319-1320. doi: 10.1001/jama.2018.12440.

Tchkonia T, Lenburg M, Thomou T, Giorgadze N, Frampton G, Pirtskhalava T, Cartwright A, Cartwright M, Flanagan J, Karagiannides I, Gerry N, Forse RA, Tchoukalova Y, Jensen MD, Pothoulakis C, Kirkland JL. Identification of depot-specific human fat cell progenitors through distinct expression profiles and developmental gene patterns. Am J Physiol Endocrinol Metab. 2007 Jan;292(1):E298-307. doi: 10.1152/ajpendo.00202.2006.

Tchkonia T, Morbeck DE, Von Zglinicki T, Van Deursen J, Lustgarten J, Scrable H, Khosla S, Jensen MD, Kirkland JL. Fat tissue, aging, and cellular senescence. Aging Cell. 2010 Oct;9(5):667-84. doi: 10.1111/j.1474-9726.2010.00608.x.

Tchkonia T, Pirtskhalava T, Thomou T, Cartwright MJ, Wise B, Karagiannides I, Shpilman A, Lash TL, Becherer JD, Kirkland JL. Increased TNFalpha and CCAAT/enhancer-binding protein homologous protein with aging predispose preadipocytes to resist adipogenesis. Am J Physiol Endocrinol Metab. 2007 Dec;293(6):E1810-9. doi: 10.1152/ajpendo.00295.2007.

Tchkonia T, Tchoukalova YD, Giorgadze N, Pirtskhalava T, Karagiannides I, Forse RA, Koo A, Stevenson M, Chinnappan D, Cartwright A, Jensen MD, Kirkland JL. Abundance of two human preadipocyte subtypes with distinct capacities for replication, adipogenesis, and apoptosis varies among fat depots. Am J Physiol Endocrinol Metab. 2005 Jan;288(1): E267-77. doi: 10.1152/ajpendo.00265.2004.

Tchkonia T, Thomou T, Zhu Y, Karagiannides I, Pothoulakis C, Jensen MD, Kirkland JL. Mechanisms and metabolic implications of regional differences among fat depots. Cell Metab. 2013 May 7;17(5):644-656. doi: 10.1016/j.cmet.2013.03.008.

Testa R, Olivieri F, Sirolla C, Spazzafumo L, Rippo MR, Marra M, Bonfigli AR, Ceriello A, Antonicelli R, Franceschi C, Castellucci C, Testa I, Procopio AD. Leukocyte telomere length is associated with complications of type 2 diabetes mellitus. Diabet Med. 2011 Nov;28(11):1388-94. doi: 10.1111/j.1464-5491.2011.03370.x.

Trabucco SE, Zhang H. Finding Shangri-La: Limiting the Impact of Senescence on Aging. Cell Stem Cell. 2016 Mar 3;18(3):305-6. doi: 10.1016/j.stem.2016.02.002.

Tran D, Bergholz J, Zhang H, He H, Wang Y, Zhang Y, Li Q, Kirkland JL, Xiao ZX. Insulin-like growth factor-1 regulates the SIRT1-p53 pathway in cellular senescence. Aging Cell. 2014 Aug;13(4):669-78. doi: 10.1111/acel.12219.

Trayssac M, Hannun YA, Obeid LM. Role of sphingolipids in senescence: implication in aging and age-related diseases. J Clin Invest. 2018 Jul 2;128(7):2702-2712. doi: 10.1172/JCI97949.

Ungaro P, Mirra P, Oriente F, Nigro C, Ciccarelli M, Vastolo V, Longo M, Perruolo G, Spinelli R, Formisano P, Miele C, Beguinot F. Peroxisome proliferator-activated receptor-γ activation enhances insulin-stimulated glucose disposal by reducing ped/pea-15 gene expression in skeletal muscle cells: evidence for involvement of activator protein-1. J Biol Chem. 2012 Dec 14;287(51):42951-61. doi: 10.1074/jbc.M112.406637.

van der Zijl NJ, Goossens GH, Moors CC, van Raalte DH, Muskiet MH, Pouwels PJ, Blaak EE, Diamant M. Ectopic fat storage in the pancreas, liver, and abdominal fat depots: impact on β-cell function in individuals with impaired glucose metabolism. J Clin Endocrinol Metab. 2011 Feb;96(2):459-67. doi: 10.1210/jc.2010-1722.

Vergoni B, Cornejo PJ, Gilleron J, Djedaini M, Ceppo F, Jacquel A, Bouget G, Ginet C, Gonzalez T, Maillet J, Dhennin V, Verbanck M, Auberger P, Froguel P, Tanti JF, Cormont M. DNA Damage and the Activation of the p53 Pathway Mediate Alterations in Metabolic and Secretory Functions of Adipocytes. Diabetes. 2016 Oct;65(10):3062-74. doi: 10.2337/db16-0014.

Verzola D, Gandolfo MT, Gaetani G, Ferraris A, Mangerini R, Ferrario F, Villaggio B, Gianiorio F, Tosetti F, Weiss U, Traverso P, Mji M, Deferrari G, Garibotto G. Accelerated senescence in the kidneys of patients with type 2 diabetic nephropathy. Am J Physiol Renal Physiol. 2008 Nov;295(5):F1563-73. doi: 10.1152/ajprenal.90302.2008.

Vilborg A, Bersani C, Wilhelm MT, Wiman KG. The p53 target Wig-1: a regulator of mRNA stability and stem cell fate? Cell Death Differ. 2011 Sep;18(9):1434-40. doi: 10.1038/cdd.2011.20.

Vilborg A, Glahder JA, Wilhelm MT, Bersani C, Corcoran M, Mahmoudi S, Rosenstierne M, Grandér D, Farnebo M, Norrild B, Wiman KG. The p53 target Wig-1 regulates p53 mRNA stability through an AU-rich element. Proc Natl Acad Sci U S A. 2009 Sep 15;106(37):15756-61. doi: 10.1073/pnas.0900862106.

Vitseva OI, Tanriverdi K, Tchkonia TT, Kirkland JL, McDonnell ME, Apovian CM, Freedman J, Gokce N. Inducible Toll-like receptor and NF-kappaB regulatory pathway expression in human adipose tissue. Obesity (Silver Spring). 2008 May;16(5):932-7. doi: 10.1038/oby.2008.25.

Wang Z, Wei D, Xiao H. Methods of cellular senescence induction using oxidative stress. Methods Mol Biol. 2013;1048:135-44. doi: 10.1007/978-1-62703-556-9_11

Weisberg SP, McCann D, Desai M, Rosenbaum M, Leibel RL, Ferrante AW Jr. Obesity is associated with macrophage accumulation in adipose tissue. J Clin Invest. 2003 Dec;112(12):1796-808. doi: 10.1172/JCI19246.

Weissgerber TL, Savic M, Winham SJ, Stanisavljevic D, Garovic VD, Milic NM. Data visualization, bar naked: A free tool for creating interactive graphics. J Biol Chem. 2017 Dec 15;292(50):20592-20598. doi: 10.1074/jbc.RA117.000147.

Wiley CD, Flynn JM, Morrissey C, Lebofsky R, Shuga J, Dong X, Unger MA, Vijg J, Melov S, Campisi J. Analysis of individual cells identifies cell-to-cell variability following induction of cellular senescence. Aging Cell. 2017 Oct;16(5):1043-1050. doi: 10.1111/acel.12632.

Wissler Gerdes EO, Zhu Y, Tchkonia T, Kirkland JL. Discovery, development, and future application of senolytics: theories and predictions. FEBS J. 2020 Jun;287(12):2418-2427. doi: 10.1111/febs.15264.

Wu Z, Rosen ED, Brun R, Hauser S, Adelmant G, Troy AE, McKeon C, Darlington GJ, Spiegelman BM. Cross-regulation of C/EBP alpha and PPAR gamma controls the transcriptional pathway of adipogenesis and insulin sensitivity. Mol Cell. 1999 Feb;3(2):151-8. doi: 10.1016/s1097-2765(00)80306-8.

Xu M, Palmer AK, Ding H, Weivoda MM, Pirtskhalava T, White TA, Sepe A, Johnson KO, Stout MB, Giorgadze N, Jensen MD, LeBrasseur NK, Tchkonia T, Kirkland JL. Targeting senescent cells enhances adipogenesis and metabolic function in old age. Elife. 2015 Dec 19;4:e12997. doi: 10.7554/eLife.12997.

Xu M, Palmer AK, Ding H, Weivoda MM, Pirtskhalava T, White TA, Sepe A, Johnson KO, Stout MB, Giorgadze N, Jensen MD, LeBrasseur NK, Tchkonia T, Kirkland JL. Targeting senescent cells enhances adipogenesis and metabolic function in old age. Elife. 2015 Dec 19;4:e12997. doi: 10.7554/eLife.12997.

Xu M, Pirtskhalava T, Farr JN, Weigand BM, Palmer AK, Weivoda MM, Inman CL, Ogrodnik MB, Hachfeld CM, Fraser DG, Onken JL, Johnson KO, Verzosa GC, Langhi LGP, Weigl M, Giorgadze N, LeBrasseur NK, Miller JD, Jurk D, Singh RJ, Allison DB, Ejima K, Hubbard GB, Ikeno Y, Cubro H, Garovic VD, Hou X, Weroha SJ, Robbins PD, Niedernhofer LJ, Khosla S, Tchkonia T, Kirkland JL. Senolytics improve physical function and increase lifespan in old age. Nat Med. 2018 Aug;24(8):1246-1256. doi: 10.1038/s41591-018-0092-9.

Xu M, Tchkonia T, Ding H, Ogrodnik M, Lubbers ER, Pirtskhalava T, White TA, Johnson KO, Stout MB, Mezera V, Giorgadze N, Jensen MD, LeBrasseur NK, Kirkland JL. JAK inhibition alleviates the cellular senescence-associated secretory phenotype and frailty in old age. Proc Natl Acad Sci U S A. 2015 Nov 17;112(46):E6301-10. doi: 10.1073/pnas.1515386112.

Yang J, Huang T, Petralia F, Long Q, Zhang B, Argmann C, Zhao Y, Mobbs CV, Schadt EE, Zhu J, Tu Z; GTEx Consortium. Corrigendum: Synchronized age-related gene expression changes across multiple tissues in human and the link to complex diseases. Sci Rep. 2016 Jan 21;6:19384. doi: 10.1038/srep19384.

Yang JX, Rastetter RH, Wilhelm D. Non-coding RNAs: An Introduction. Adv Exp Med Biol. 2016; 886:13-32. doi: 10.1007/978-94-017-7417-8_2.

Yang X, Jansson PA, Nagaev I, Jack MM, Carvalho E, Sunnerhagen KS, Cam MC, Cushman SW, Smith U. Evidence of impaired adipogenesis in insulin resistance. Biochem Biophys Res Commun. 2004 May 14;317(4):1045-51. doi: 10.1016/j.bbrc.2004.03.152

Zamboni M, Rossi AP, Fantin F, Zamboni G, Chirumbolo S, Zoico E, Mazzali G. Adipose tissue, diet and aging. Mech Ageing Dev. 2014 Mar-Apr;136-137:129-37. doi: 10.1016/j.mad.2013.11.008.

Zbieć-Piekarska R, Spólnicka M, Kupiec T, Parys-Proszek A, Makowska Ż, Pałeczka A, Kucharczyk K, Płoski R, Branicki W. Development of a forensically useful age prediction method based on DNA methylation analysis. Forensic Sci Int Genet. 2015 Jul;17:173-179. doi: 10.1016/j.fsigen.2015.05.001.

Zhang Y, Sun Z, Jia J, Du T, Zhang N, Tang Y, Fang Y, Fang D. Overview of Histone Modification. Adv Exp Med Biol. 2021;1283:1-16. doi: 10.1007/978-981-15-8104-5_1.

Zhu J, Singh M, Selivanova G, Peuget S. Pifithrin-α alters p53 post-translational modifications pattern and differentially inhibits p53 target genes. Sci Rep. 2020 Jan 23;10(1):1049. doi: 10.1038/s41598-020-58051-1.

Zhu Y, Tchkonia T, Pirtskhalava T, Gower AC, Ding H, Giorgadze N, Palmer AK, Ikeno Y, Hubbard GB, Lenburg M, O'Hara SP, LaRusso NF, Miller JD, Roos CM, Verzosa GC, LeBrasseur NK, Wren JD, Farr JN, Khosla S, Stout MB, McGowan SJ, Fuhrmann-Stroissnigg H, Gurkar AU, Zhao J, Colangelo D, Dorronsoro A, Ling YY, Barghouthy AS, Navarro DC, Sano T, Robbins PD, Niedernhofer LJ, Kirkland JL. The Achilles' heel of senescent cells: from transcriptome to senolytic drugs. Aging Cell. 2015 Aug;14(4):644-58. doi: 10.1111/acel.12344

LIST OF PUBLICATIONS

(Years 2019-2022)

1. Parrillo L, Spinelli R, Costanzo M, **Florese P**, Cabaro S, Desiderio A, Prevenzano I, Raciti GA, Smith U, Miele C, Formisano P, Napoli R, Beguinot F. Epigenetic Dysregulation of the *Homeobox A5* (*HOXA5*) Gene Associates with Subcutaneous Adipocyte Hypertrophy in Human Obesity. *Cells*. 2022 Feb 18;11(4):728. doi:10.3390/cells11040728.

2. Spinelli R*, **Florese P***, Parrillo L, Zatterale F, Longo M, D'Esposito V, Desiderio A, Nersted A, Gustafson B, Formisano P, Miele C, Raciti GA, Napoli R, Smith U, Beguinot F. *ZMAT3* hypomethylation contributes to early senescence of preadipocytes from healthy first-degree relatives of type 2 diabetics. *Aging Cell.* 2022 Feb 11: e13557. doi: 10.1111/acel.13557- ***Joint first authorship.**

3. Spinelli R, Parrillo L, Longo M, **Florese P**, Desiderio A, Zatterale F, Miele C, Raciti GA, Beguinot F.Molecular basis of ageing in chronic metabolic diseases [published online ahead of print, 2020 May 1]. *JEndocrinol Invest*. 2020;10.1007/s40618-020-01255-z. doi:10.1007/s40618-020-01255-z.